谨将此文献给我的父亲

Identification and Evaluation of Improved Drying Methods of New Zealand Beeches by Means of an Energy-efficient Kiln Process

A Thesis Submitted in Fulfilment of the Requirement for the Degree of Philosophy in Chemical and Process Engineering

By

Zheng Zhang

Department of Chemical and Process Engineering

University of Canterbury

2000

ACKNOWLEDGMENTS

I would like to express my gratitude to all those who have made this thesis possible.

In particular I would like to thank Professor R.B. Keey, my principal supervisor, for his expert guidance and invaluable help throughout the research and in obtaining the scholarship. My gratitude also goes to my co-supervisor Dr. J.F.C. Walker, whose willingness to discuss any problems in a very short notice has been greatly appreciated.

I thank Dr G. Carrington of University of Otago for providing the funding for the project as well as very his helpful comments, advice and encouragement. My special thanks are also due to Dr Z Sun for all the advice and information on dehumidifying systems and the energy efficiency issues.

I sincerely thank Dr T A G Langrish and Mr L Pordage of the Department of Chemical and Process Engineering, University of Sydney for the great effort and patience in helping me with the optimisation program which plays a very important part in this project.

I also want to thank Timberlands West Coast Ltd for its support in supplying red beech samples for this project.

I want to thank all staff and postgraduates of the Department of Chemical and Process Engineering for their inspiration and encouragement. In particular, the very practical assistance from W Earl, A Allen and other technicians in the Department and also from P Fuller, of the School of Forestry.

Finally, I sincerely thank my parents and my wife, Weiping, for their understanding and encouragement. There is also a special person I want to acknowledge, my ten-year-old son, Teng; his own achievement gave me inspirations throughout my study period.

Summary

New Zealand *Nothofagus* timbers, especially *N. fusca* (red beech) and *N. truncata* (hard beech) are among the most refractory timbers in the world to be dried in conventional kilns. The recommended drying method is to air dry these New Zealand beech timbers to about or below their fibre-saturation point before kiln-drying to required moisture contents for end use. Because the air-dry process is an uncontrollable process, due to the weather conditions which may vary from day to day, an alternative strategy is needed.

This thesis presents studies on establishing and optimising new drying schedules for New Zealand beech timbers for kiln-drying from green conditions at low temperatures and in dehumidifying drying systems. The studies include: (1) Establishing stepwise drying schedules for drying *Nothofagus* timbers from green conditions; (2) Using a strain-limited model to optimise the initial step-wise drying schedules into moisture-based schedules. The optimised drying schedules are verified with small-scale experimental drying trials. Work includes the determination of mechanical properties and the drying behaviour of drying *N. fagus* timbers in their transverse direction. Also the effect of various pre-treatments on the drying rate and the mechanical properties are also determined. Finally, an assessment is made of the energy efficiency of the optimised drying schedules under the proposed dehumidifying drying system.

Five principal conclusions are drawn from this work:

(1) The stepwise drying schedule, which has a low temperature and high relative humidity at the beginning of the drying stage, and relatively higher temperature and low relative humidity at later stages, is able to dry New Zealand red and hard beech timbers from fresh conditions. The dried sample boards using this schedule only have slight warping caused by the differential shrinkage in the three directions. The comparison with the air-dried sample (open air, office environment), which had surface checking at early stage that later disappeared because of the stress reversal, showed the importance of early low temperature and high relative humidities in maintaining the quality of red and hard beech boards on drying.

The stepwise drying schedule can also dry the hot-water soaked red and hard beech boards without significant deformation. However, an appropriate treatment method plays an important part in preventing excessive deformation, including surface checking and internal cracks.

(2) The drying model of the optimisation program predicts the moisture-content profile close to the measured one from the verifying drying trials, especially when its average moisture content is above its fibre-saturation point. But the diffusion-type of model requires the use of an accurate diffusion coefficient, and only the diffusion coefficient measured for the actual species timber can provide an accurate moisture profile.

The optimisation program that used reference parameters from Australian *Eucalyptus* species like ironbark predicts drying schedules that were proved to be too harsh for the red beech timber. Internal cracks occurred in the drying trial with this schedule. The results indicate that most of the parameters from refractory *Eucalyptus* timbers are not suitable to be used to describe New Zealand beech *fusca*-type timbers. It is necessary to measure the actual mechanical properties of New Zealand beech timbers and use these values in the optimisation program.

(3) The temperature and moisture content of the wood affect the value of the ultimate strength in the following ways. An increase of temperature generally reduces the ultimate strength. The extent of reduction increases significantly when temperature reaches 55 °C or over. There are also signs that there is a minimum value of the ultimate strength at the temperature around 29 °C. The ultimate strength of red beech is also moisture-content dependent, with a minimum value at about the fibre-saturation point. The test results also show that, as the moisture content of the timber is increased above fibre-saturation, the strength value takes an almost constant value till the moisture content reaches about 75% or over, where the strength begins to increase again.

The ultimate strain of *N. fusca* is also dependent on temperature and moisture content. The results show that when sample moisture content drops below the fibre-saturation

point (FSP), the sample becomes more brittle and the value of ultimate strain decreases, while when the moisture content is above the FSP the value of the ultimate strain does not change greatly.

(4) Hot-water soaking treatment (for 8 hour at 80 °C) increases the diffusion coefficient of the red beech timber by an average value of 27.5 %, which leads to an increase of the permeability of the timber boards.

The red beech boards hot-water soaked for 8 hours were weakened by this thermal treatment. The ultimate strength of the red beech board was reduced by 12.5% in its transverse direction.

Hot-water soaking treatment also affects the ultimate strain, which increases marginally as the result of the thermal treatment.

(5) The optimised drying schedules can be adapted to the operation of dehumidifying drying kilns, according to the study of Carrington and colleagues of Otago University.

The drying schedules for red beech timber suggested by this study were used in dehumidifying kiln drying system and proved to be energy-efficient and feasible for commercial operation.

Table of Contents

Section A

The research scope and objectives of the work

Section B

Background information

Chapter 3 Dehumidifier kiln systems

Section D

Experimental procedures and results

Chapter 4 Experimental methods and apparatus

Chapter 5 Drying of New Zealand red and hard beech timber

Chapter 6 Mechanical properties and drying behaviour of red beech timbers in the transverse direction

Chapter 7 The development of a strain-limited drying schedule

Section E

Overview

Chapter 10 Discussion

Chapter 11 Conclusion

Table of Figures

Symbols

c_p	specific heat capacity of moisture wood
D	temperature-dependent diffusion coefficient
D_E	activation energy
D_r	pre-expontial factor
E	Young's modulus
j	mass flux of water from the board
k_m	mass-transfer coefficient
Mi	*change* of moisture
Q	total rate of heat transfer
t	time
T	temperature
T_g	air temperature
T_s	surface temperature
x	distance of the evaporative plane from the surface
X	moisture content
X_{fsp}	fibre-saturation point
X_s	moisture content at the timber surface
Y_G	humidity in the bulk air stream
Y_s	gas humidity above the timber surface
z	distance from the surface

ε_c	creep strain
ε_i	instantaneous strain
ε_{MS}	mecano-sorptive strain
ε_T	thermal strain
ε_X	free-shrinkage strain
λ_w	latent heat of vaporisation
λ_s	heat of sorption
ρ	wood density
ρ_{air}	air density
σ	stress
ξ	shrinkage

Section A

The research scope and objectives of the work

New Zealand beeches, red beech *(Nothofagus fusca)* and hard beech *(Nothofagus truncata)* in particular, are among the most temperature-sensitive hardwoods. They frequently contain tension wood and drying causes collapse which cannot be removed by reconditioning. Therefore the drying processes of these timbers usually require comparatively long periods under mild conditions and, consequently, these drying processes are very energy-consuming because of potential losses over an extensive drying schedule.

Air-drying methods have been used for lumber drying especially for some of the slow drying of these temperature-sensitive hardwoods. One of the advantages of air drying for the commercial kiln operator is to save energy. However, unpredictable weather conditions in some cases can significantly affect the quality of the air-dried materials, sometimes disastrously. A controlled drying method therefore is required to minimise the influences of ever-changeable weather conditions and enhance the maintenance of the product quality.

Some of the recently developed pre-treatments used for drying these timbers, hot-water soaking for example, might help to reduce drying time by as much as half. On the other hand, such pre-treatments also produce surface and internal checking in the timber. To identify and evaluate those results of pre-treatments would be quite helpful to the commercial practice of these processes.

Heat-pump dehumidifiers have great potential to substantially improve the energy efficiency of the drying process through recycling the latent heat of the evaporated moisture from the product being dried, especially for low-temperature applications, Such conditions are appropriate for drying the heat-sensitive red and hard beech timbers.

In the dehumidifier, instead of venting the humid air, it is processed through a cold heat exchanger (evaporator) which condenses some of the water in the air. The heat absorbed from the water vapour is used to vaporise a refrigerant. Compressed to a higher pressure by a compressor, this refrigerant has then a boiling point higher than room temperature, thus, on condensation, it releases its energy to the hot coil (condenser). The air passing through this hot coil is rewarmed and is relatively drier than when it entered the unit.

Besides its lower power consumption, the dehumidifier does not have to heat the air to the same extent to lower its relative humidity, and it is possible to obtain dry air at much lower temperature than in a conventional kiln.

Dehumidifier drying kilns also have the potential to help to reduce the CO_2 emission from conventional kilns heated by reducing the combustion of primary fuels. Such systems have the potential to be friendly to the environment.

The overall aim of this project is to develop a comprehensive understanding to kiln drying heat-sensitive New Zealand beech timbers from green and using the application of an energy-efficient dehumidifier dryer.

The first objective of the project is to establish the possible advantages and disadvantages deriving from the use of controlled conditions to dry such temperature-sensitive timber which could replace traditional uncontrolled air-drying methods. This means that the controlled drying process starts with the green wood. requiring very moderate conditions to prevent degrade, particularly at the start of drying when tensile stresses build up at the surface and cell collapse might occur in the interior of the board. Therefore, drying above fibre-saturation may be a lengthy process. As a matter of saving energy, it is proposed to consider the use of a dehumidifier. However, because of intensive use of electricity to warm up the drying system and maintain it to a controlled level possibly for a long period, therefore, an outcome of this part of the project will be a comprehensive evaluation of the energy efficiency of the dehumidification-drying systems and a comparison with other types of dryer for the same application.

Intermittent drying will also be considered in this project for its possible relaxation of stressed materials. Besides, this strategy may be used to take advantage of different power tariffs between daytime and night-time.

The second objective is to evaluate the possible improvement of the drying rate by means of pre-treatments.

Previous work (Kininmonth 1971, Gunzerodt *et al.* 1986, Haslett *et al.* 1986) on pre-treatments, including compression rolling, pre-freezing, pre-steaming, hot-water soaking, methanol soaking and chemical pre-treatment, have suggested that pre-treatments affect the drying process in two ways: by (1) improving the drying rate and / or the permeability; (2) Producing some degrade of product quality in many cases.

In exploring both aspects of pre-treatments, the thesis focuses on finding the optimum conditions for drying New Zealand hard and red beech with a minimum of degrade.

Of the pre-treatments, compression rolling, pre-freezing and methanol soaking are all reported as having one or more of the following disadvantages: (1) little improvement in drying rate; (2) production of severe macroscopic damage to the wood and so degrade; (3) uneconomic for commercial practice. Therefore the potential pre-treatment(s) to be investigated in this project will be selected from the hot-water soaking, pre-steaming, and chemical pre-treatment methods.

The importance of evaluating these pre-treatments is to optimise the conditions used to gain the best drying rate, and at the same time minimise the drying defects which would be unacceptable in commerce, e.g. furniture manufacture. The quality requirements will be based on the New Zealand Standard NZS 3631:1981.

The intention is also to describe the drying behaviour through tests on the mechanical properties and observe the subsequent behaviour. The test results will be used not only for comparison with other heat-sensitive timbers, but also will be used to derive the parameters and boundary conditions for a drying schedule optimisation.

The third objective of the project is to determine how energy-efficient a dehumidifying kiln is when drying hard and red beech timber from the green condition. Conventional slow-drying methods will be used for comparative purposes. The most energy-efficient conditions for the drying of hard and red beech in a dehumidifying kiln will be calculated.

Section B

Background information

Chapter 1

Wood Properties

§1.1 Wood and trees

A tree is defined as a woody perennial plant, typically having single stem or trunk, growing to a considerable height bearing lateral braches at some distance from the ground (Brown 1993).

A tree is a plant, which like all growing organisms, consists of cells. In temperate regions, each year the wood cells grow fast early in the spring season, producing springwood or earlywood. Later in the season, as winter approaches, growth slows producing summerwood or latewood. In the depth of winter there may be no woody growth at all. This consistent pattern of fast growth followed by slow growth gives temperate trees their distinctive annual rings. The earlywood cells have thin walls and large central openings or lumens. The latewood cells have thicker walls and smaller-diameter lumens. More wall material is produced in the latter part of the growing season.

§1.1.1 Softwood and hardwood trees

Trees are divided into two groups: softwoods and hardwoods.

The terms softwood and hardwood do not refer to the hardness or density of the wood. Softwoods are not always soft, nor are hardwoods always hard. Mountain-grown Douglas-fir, for example, produces an extremely hard wood although it is classified as a "softwood," and balsa wood, so useful in making toy models, is classified a "hardwood" although it is very soft.

In biological terms, softwoods are called gymnosperms, which are trees that produce "naked seeds." The most important groups of softwoods are the conifers or cone-bearing trees, which have seeds that are usually visible inside opened cones. All

species of pine, spruce, hemlock, fir, cedar, redwood and larch are softwoods. Nearly all softwood trees have another common characteristic: their leaves are actually needles or scales and they remain on the tree throughout the winter, which is why they are also called evergreen trees. Exceptions include larch and swamp cypress whose needles drop in the fall, leaving the tree bare during winter.

Hardwoods are biologically called angiosperms, which are trees that produce seeds enclosed in a fruit or nut. The hardwood category includes the oaks, ashes, elms, maples, birches, beeches and cottonwoods. In contrast to softwoods, hardwood trees have broad leaves and nearly all North American hardwoods are deciduous, which means they drop their leaves in the fall. However, there are exceptions: for instance holly and live oak are hardwoods that retain their leaves year- round, and New Zealand *Nothofagus* trees only lose their leaves in spring when the new buds open. In New Zealand, 95% of commercial timber harvested is softwood of which 90% consists of a single species, *Pinus radiata.* However, the major indigenous hardwood trees, particularly in the maintain area of the South Island, are *Nothofagus* species, which represents a significant possible future wood resource.

§1.1.2 Hardwood cells

Hardwood trees are more highly developed than the softwoods and their cell structure is more complex and variable. They have evolved a special way of conducting water from the roots to the leaves. Large, hollow cells (called vessels) lie within a mass of fibre tracheids. In hardwoods, all vertical water conduction is done through these vessels. Each vessel is made up of short segments or "elements" joined end-to-end (like drain pipes). The vessels are much larger in diameter than the fibre tracheids and can often be seen as tiny holes on the end grain of wood in tree species like ash, oak or elm. In contrast to the longitudinal tracheids found in softwoods, which provide support and conduct liquids, the fibre tracheids in hardwoods primarily provide support.

The ray cells of hardwoods are not unlike those in softwoods, but hardwood ray cells often form much wider bands or ribbons. They can be so wide as to be visible to the

naked eye. In fact, the rays are responsible for much of the distinctive grain pattern or figure of our common hardwood species. Were it not for the different colours and structural features of exposed vessels and rays, most species of hardwood would look similar.

§1.1.3 Cell-wall structure

The wall of a typical wood cell is composed of several layers, which are formed as new cells are created at the cambium layer. The middle lamella, composed mainly of lignin, serves as the glue bonding adjacent cells. The wall itself is made up of a primary wall and a three-layered secondary wall, each of which has distinct alignments of microfibrils. Microfibrils are "filament-like" bundles of cellulose molecules, interspersed with and surrounded by hemicellulose molecules and lignin.

In the primary wall (P), the microfibrils form a loose, irregular net-like orientation. In the outer (S1) layer of the secondary wall, the microfibrils are more precisely oriented, but are nearly perpendicular to the long axis of the cell. In the S2 layer, the microfibrils run almost parallel to each other in a tight spiral around the cell, generally at an angle of 10°-30° to the cell axis. This layer is the thickest and has the greatest effect on how the cell, and therefore, how the wood behaves. The smaller the angle the microfibrils make with the long direction of the cell, the stronger the cell is. In the innermost (S3) layer of the cell wall, the microfibrils are once again oriented almost at right angles to the cell's long axis.

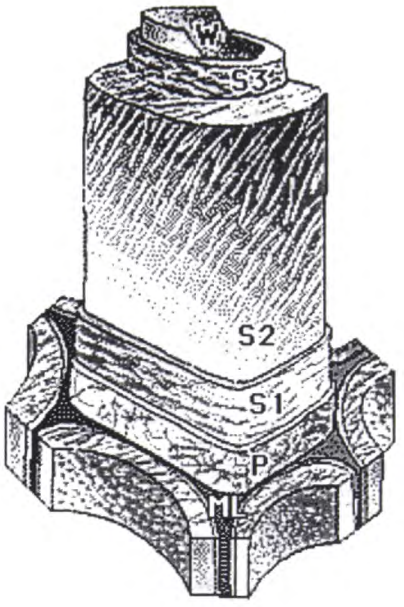

Fig. 1-1. Idealised model of typical wall structure of a fibre or tracheid. The cell wall consists of: P-primary wall; S1, S2, S3-layer of the secondary wall; W-warty layer (not always evident); ML-middle lamella, the amorphous, high-lignin-content material that binds cells together. Adapted from Koch, Peter. 1985.

§1.1.4 Chemical constituents of wood

Table 1-1 Chemical constituents of wood (Dinwoodie 1989)

Principal constituent	Percentage (mass)	
	Softwoods	Hardwoods
Cellulose	40-45	45-50
Hemicelluloses		
galactoglucomannans	15-20	-
arabinoglucuronoxylan	10	-
glucuronoxylan	-	20-30
glucomannan	-	1-5
Lignin	26-34	22-30
Extractives	0-5	0-10

§1.1.4.1 Cellulose

Cellulose $(C_6H_{10}O_5)_n$, one of the few natural polymers, occurs in the form of long straight filaments or chains which have been built up by linking glucose molecules end to end with each other within the cell wall from the glucose monomer ($C_6H_{10}O_6$). While the degree of polymerisation can vary from one species of wood to the next, it is considered that there are from 8000 to 10000 units on average (Goring and Timmell, 1962). Because so many glucose molecules will link together, cellulose is said to have a high degree of polymerisation. This means that even the longest cellulose molecules is only about 5 μm long (1 μm = .001 mm).

Cellulose, the main building substance of all plant cells, including trees, makes up about 50 percent of the dry weight of wood. Because bonding between and within glucose residues in the polymer is so strong, cellulose molecules are very strong and this is the reason as a material gets its strength. Lateral bonding between cellulose molecules is also quite strong, causing them to group together to form long crystalline structures called microfibrils. Microfibrils can be seen with an electron microscope.

All of the cellulose present in wood molecules (and all natural materials) is in a particular crystalline form Cellulose I, although cellulose may indeed crystallise in a number of different ways.

§1.1.4.2 Hemicelluloses

Hemicelluloses, the second chemical component of wood, make up 15 to 25 percent of the dry weight of wood. Unlike cellulose, which is made only from glucose, hemicelluloses consist of glucose and several other water-soluble sugars produced during photosynthesis. The degree of polymerization (that is, the number of sugar molecules connected together) is lower for hemicelluloses and they form linear polymer chains, which are lightly branched with single residue side chains rather than straight chains. Hemicelluloses surround microfibrils and are associated with them.

The hemicelluloses like cellulose, are carbohydrates which vary in composition between softwoods and hardwoods. They comprise mixtures of polysaccharides synthesised in wood from glucose, mannose, galactose, xylose, arabinose, 4-O-methylglucuronic acid and galacturonic acid residues; these mixtures are generally low in crystallinity and degree of polymerisation, the chain length averaging about 60-200 units (Tjerneld, 1998).

The major hemicellulose in hardwood is glucuronoxylan, which accounts for from 20-30% of the wood mass. A second hardwood hemicellulose is glucomannan which is present in amounts less than 5% of the total mass. Generally, the proportion of hemicelluloses is greater in hardwoods than in softwoods.

§1.1.4.3 Lignin

The third major chemical component of wood is lignin, a complex chemical, completely different from cellulose. Lignin makes up about 15 to 30 percent of the dry weight of wood. It occurs in the wood throughout the cell wall, forming a mixture around the microfibiles. However, it is also concentrated toward the outside of cells and between cells. Lignin is a three-dimensional polymer, though its exact structure is not fully understood. Lignified plants differ from those that do not have lignin, (for example, grasses). Wood would be similar to cotton (which is almost 100 percent cellulose) if it was not for lignin. Lignified woody plants have stiffness and are able to grow tall. Lignin is thermoplastic, which means it becomes pliable at high temperatures and hardens again when it cools.

The lignin molecule is large, comprising an irregular assembly of hydroxy- and methoxy-substituted phenylpropane units. The precursors of lignin biosynthesis are different in softwoods and hardwoods, thereby giving rise to two different types of lignin. In softwoods it is derived basically from the polymerisation of coniferyl alcohol and is known as guaiacyl lignin; it is present in amounts ranging from 24-34% of the mass of the wood. The lignin content of hardwoods is generally slightly lower and comprises both guauacyl and syrinyl units formed as a copolymer from coniferyl and sinapyl alcohols.

§1.1.4.4 Extractives

Cellulose, hemicelluloses, and lignin are the basic building blocks in wood. Other non-structural components found in the woody tissue includes the deposition of silica, sulphur salts, and calcium salts in a few hardwood species which are important for the point of view of their blunting action on machine tools; however, it is the presence in many softwoods and hardwoods of highly complex organic compounds which is of even greater technical interests. They are collectively known as gums (water soluble) and extractives (water insoluble). These organic compounds, when present, comprise 1-10% of the total mass of the wood. Most of them display at least some degree of toxicity, and many of them display a high degree of toxicity to biological predators. The compounds are specific to certain timbers, e.g. tannin in oak and pinosylrin in Scots pine. The type and amount of organic material present therefore accounts for the wide range in natural durability that occurs in different woods. *Fusca*-type *Nothofugas* timbers have particularly high amount of extractive material (up to 9-12%) (Uprichard 1975, Lloyd 1975).

§1.2 Wood

Throughout recorded history, the unique characteristics and relative abundance of wood have made it one of mankind's most valuable and useful natural resources. Today literally thousands of products that we take for granted come from solid wood, wood pulp and chemicals derived from wood. Wood is so important a building material because first, only wood is a renewable resource. No other building material-- steel, aluminium, brick, concrete, plastics, glass, ceramics--can be regenerated as can trees. Also trees provide wildlife habitat and recreational areas while they grow. New Zealand southern beeches provide protection forest cover in fragile high-country area, but the hardwood has limited high value end use. The future utilisation of this resource is matter of political debate.

§1.3 New Zealand beeches and their origin

§1.3.1 Origin and distribution:

The New Zealand beeches belong to the genus *Nothofagus* or "false beeches" named by Blume in 1850 to include the beech-like species of the Southern Hemisphere. However these beeches continued to be included with their Northern Hemisphere *Fagaceae* counterparts in the genus *Fagus* and it was not until sometime later that this new generic name become accepted. Four of the New Zealand *taxa* were transferred from *Fagus* to *Nothofagus* by the Swedish botanist Oersted in 1873, but again there was slow acceptance of the change. Even as late as 1906, Cheeseman still included the New Zealand species in the genus of *Fagus*. It was not until about 1910, after the adoption by Cockayne, that the transfer of the New Zealand beeches species to the genus *Nothofagus* was finally accepted within New Zealand botanical circles (Poole 1950b).

The genus now commonly known as the "Southern beeches", belongs to the *Fagaceae*, a family of woody shrubs and trees with alternative (rarely whorled), stipulate leaves: small unisexual flowers: and a fruit which is a nut enclosed in an often hardened cupule. *Nothofagus* trees are found in South America, New Zealand, some part of Australia and the highlands of New Guinea. These beeches are of ancient lineage, having originated in Gondwanaland, the vast southern continent which straddled the south pole between 250 and 360 million years ago.

There are five New Zealand beeches, *Nothofagus memziesii* (silver beech), *Nothofagus fusca* (red beech), *Nothofagus truncata* (hard beech), *Nothofagus solandri var. solandri* (black beech) and *Nothofagus solandri var. cliffortioides* (mountain beech). The five New Zealand beeches have a similar appearance. They are medium-density hardwoods with many small and evenly-spaced vessels and rays. Growth rings are moderately distinct, evenly distributed and often wavy or crenate. It is very difficult to distinguish the five *Nothofagus* species on microscopic wood characteristics alone. The wood structure is similar to maple *(Acer spp.)*. birch *(Betula*

spp.) and European beech. *(Fagus spp.)* (NZFS 1974). Indeed, early botanists placed *Nothofagus* variety in the genera, *Betula* and *Fagus* from their superficial likeness in these familiar families.(Poole 1987)

§1.3.2 Microstructural characteristics

The vessel elements of all the beeches are about 800μm in length. The vessels are relatively narrow, typically no larger than 80μm in tangential diameter, with a wall thickness of less than 4μm. Spacing is regular, 100±20 vessels per square millimetre. The vessels are often solitary, but may form radial groups of up to four vessels or more in the case of *N. solandri var. cliffortioides.* Tyloses are reasonably common in the *fusca* group. Vessel cells are joined longitudinally by simple perforation plates or occasionally in combinations of simple/scalariform plates. Vessel/vessel pits are numerous, but small, bordered and oval (approximately 6μm minor diameter). Vessel/ray pits are large, half-bordered and elongated (NZFS 1974).

The fibres have an average length of 900μm and are moderately thick-walled. Typically fibres are 25μm in diameter with a wall thickness of 6μm. If pits are present in the fibres, they are small, simple and slit-like. Fibres appear flattened immediately preceding the earlywood (NZFS 1974).

Rays are uniseriate or biseriate (always uniseriate in the *solandri* subgroup) and not more than 25 cells high except in *N. solandri*, which is characterised by tall rays usually one cell wide and up to 50 cells high. Ray / ray pits are small and simple, numerous on tangential walls, but fewer on radial walls. Ray cells often contain tannins and starches. (Grace, 1996).

Parham (1933) used the strong tendency to a ring-porous condition, and wood fibres with extremely thick mucilaginous walls and small lumina, as distinguishing features of *N. truncata*. A wide terminal zone of compressed fibres was also observed at the end of early growth rings. The tendency to ring-porous condition and development of mucilaginous walls in fibres are characteristics of *N. fusca*, while *N. menziesii* is

characterised by the abundant distribution of vessels. According to NZFS (1974) all species have a band of thick-walled fibres in the last formed latewood. Although *N. truncata* is considered to be slightly ring-porous, the wood can be variable in this respect. The arrangement of vessels in the wood shows some variation within species depending on location of the tree (Meylan *et al*. 1978). *N. truncata* tends to have a smaller number of vessels compared to the other species. These are usually solitary but sometimes in radial pairs. Vessels are smaller and rays narrower compared to *N. fusca.*

§1.3.3 Red and hard beech trees

§1.3.3.1 Appearance

Red beech (*N. fusca)* is a tall, frequently massive evergreen, averaging 24-30 m in height, with a trunk 1.5-2.0 m in diameter. Trees up to 42.7 m tall and 3.0 m in diameter have been measured. Heavy basal flanges and root buttresses often develop, particularly on trees which grow in deep soils on lower slopes and terraces, and on poorly drained sites. It occurs mainly from East Cape to Cook Strait in the North Island, and north of Arthur's Pass in the South Island. It is also found between Lakes Te Anau and Wakatipu and the broken country to the north of this. Red beech is mostly associated with lowland or high-country forests, occupying deep fertile soils on lower valley slopes and terraces. (Wardle, 1984)

Hard beech (*N. truncata)* is a tall, partly deciduous tree, mostly reaching 24-30 m in height. It has been known to reach diameters up to 1.8 m, but trees of this size are liable to be defective. The small amount of timber which is produced is sawn from submature to earlymature trees, 45 -75 cm in diameter. Old trees are commonly stag-headed. The trunk is more or less cylindrical, but flutings, branch swellings and irregularities are pronounced. There are usually heavy basal flanges and root buttresses, especially on trees growing on gentle slopes and in poorly drained soils. Hard beech occurs most commonly in north-west of the South Island, from sea level to 900 m. Of the New Zealand beeches of merchantable size, it is the one most likely to be found on steep country. It is therefore the one most likely to be troubled with tension wood.

§1.3.3.2 *Physical and mechanical properties:*

Most of the information available on the mechanical properties of New Zealand beeches are those in the grain direction: (see Table 1.2):

Table 1.2 Some Physical and Mechanical Properties of Red Beech (NZFA1974)

Source	Air-dry Density (kg/m3)	Modulus of Rupture (MPa)		Modulus of Elasticity (GPa)		Hardness (kN)		Percentage Shrinkage from Green to 12% Moisture Content	
-	-	G	D	G	D	G	D	R	T
Percentage Shrinkage from Green to 12% MC	743	70	122	9.9	12.5	4.5	5.2	3.3	7.1
Murchison-Reefton area	625	60	102	8.0	9.7	3.0	3.1	-	-

There is little information on the mechanical and drying behaviour of the NZ beech timbers. Data for the elasticity in the transverse directions for *Nothofagus* timber is just not available. Data collected by Kollmann *et al.* (1968) suggest tangential and radial elasticity are approximately 6% and 11% respectively of the longitudinal values based on the relative elasticities of one maple *(Acer)* species, two birch *(Betula)* species and one beech *(Fagus)* species. The following tabulated properties (Table 1.3) are derived from Entrican *et al.* (1951) and NZFS (1974).

Table 1.3: Mechanical properties along the grain of New Zealand *Nothofagus* species at 0.12kg/kg moisture content

	N. menziesii	*N. fusa*	*N. truncata*	*N. solandri*
Tensile strength (MPa)				
radial	5.5	3.9	7.1	5.1
tangential	8.1	8.0	5.8	5.9
Compressive strength (MPa) at proportional limit				
transverse	6.6	7.9	9.6	10.9
Shrinkage %				
radial	3.1	3.3	3.2	3.2
tangential	7.7	7.1	6.8	7.8
Modulus of elasticity (GPa)				
longitudinal	10.2	14.1	14.5	13.7

Relatively low strength or high shrinkage or elasticity might indicate; all other things being equal, a greater chance of degrade. There is no apparent difference in these mechanical properties between the different species which adequately explains differences in drying behaviour (Grace 1996).

§1.4 References

1. Boon, S. 1996 Personal communication West Coast Timberlands Ltd Greymouth.

2. Brown, L. 1993 The New short Oxford English dictionary, Oxford Clarendon Press.

3. Butterfield, B. G., 1993 The structure of wood: An overview. In Walker J. C. F. (ed): "Primary wood processing: principles and practice" Chapman and Hall, London.

4. Clifiton, N. C., 1990 New Zealand timbers: The complete guide to exotic and indigenous woods, GP Books.

1. Desch, H. E. and Dinwoodie, J. M., 1981 Timber structure, properties, conversion and use 6th edition. Food Products Press.

2. Dimwoodie, J. M., 1989 Wood: Natures cellar, polymeric, fibre-composition, Institute of Metals London.

3. Dimwoodie, J. M., 1981 Timber: Its nature and behaviour, Macmillan London.

4. Doe, P. D., Oliver, A. R., Booker, J. D., 1994, A non-linear Strain and Moisture Content Model of Variable Hardwood Drying Schedules, 4th IUFRO International Wood Drying Conference, Rutorua, New Zealand pp. 203-210.

5. Grace, C., 1996 Drying characteristics of *Nothofagus truncata* heartwood, University of Canterbury M.E. thesis.

6. Jamieson, R., 1996 Personal communication New Zealand Ministry of forestry, Christchurch Office.

7. Kollmann, F. F. P., Cote W. A., 1968 Principles of wood science and technology, Springer, Berlin.

8. Meylan, B. A., Butterfield, R. G., 1978 The structure of New Zealand woods, DSIR bulletin 222.

9. Miller, W.,1974 Vapour recompression drying ---A feasibility study, New Zealand Forest Research Report, Rutorua, New Zealand.

10. NZFS. 1974 Timber properties and uses of the New Zealand beeches. New Zealand Forest Service, Wellington.

11. Poole, A. L., 1987 Southern Beeches, SIPC Wellington.

12. Stamm, A.J., 1964 Wood and cellulose science. The Ronald Press Company. New York.

13. Thorneycroft, J., H., 1994 The market potential for sawn New Zealand beech, M.E. thesis, University of Canterbury.

14. Walker, J. C. F., 1993 The Primary Wood Processing, Chapman & Hall London, pp247-284.

15. Wardle, J. A., 1984 The New Zealand Beeches: ecology, utilisation and management, NZFS, Rotorua New Zealand.

Chapter 2

Seasoning of Wood

§2.1 How wood dries

Timber dries because moisture in wood moves from zones of high concentrations to zones of low concentrations when the wood is exposed to a non-saturated environment. Thus, wood will dry first on the surface. Moisture from inside the board then moves toward the surface and eventually evaporates either at the surface or within the material, depending on the amount of moisture percent and the mechanism of movement.

During the drying process, several forces may be acting simultaneously to move water. These forces include:

1. Capillary action, which causes free water to flow, for the most part, through cell cavities and small openings in the cell wall (pits).

2. Differences in relative humidity in the wood which cause water vapour to move across voids by diffusion.

3. Differences in moisture activity which cause the bound water to move through the cell wall by diffusion, or diffusion through the adsorbate.

When green wood starts to dry, evaporation of water from the surface sets up capillary forces which exert a pull on the free water in the zones of wood beneath the surface, resulting in a flow if the wood is permeable. This process is similar to the movement of water in a wick. Much of the free water in the sapwood of softwood moves in this manner.

The sequence of the drying process is as follows:

- Moisture is evaporated from the wood surface.

- The evaporated moisture is replaced then by moisture from within the wood, thereby producing a moisture gradient across the cross section of the timber (drier at the surface and than the core).

- The moisture in the cell cavities is removed first; this moisture is called "free water".

- Once the free water has gone, the water from the cell wall (the bound water) is removed. The point at which all free water is lost is called the "fibre-saturation point". This is roughly the equivalent to the "shrinkage intersection point", when wood starts to shrink owing to the loss of moisture from the cell walls.

- When a timber board dries, stresses are set up within the wood. In the early stage, when moisture is above the fibre-saturation-point in the core, tensile stresses develop in the outer zones of the timber. These are balanced by the compressive stresses in the core of the piece. The stresses reverse when 30 - 50 percent of the initial moisture has evaporated, depending on the species.

§2.2 Important terms which are used in timber-drying process and their values

§2.2.1 Diffusion and Fick's first law:

Diffusion describes the movement of the molecules from places of high concentration to places of lower concentration (this agrees with everyday experience). The rate of movement of molecules is measured as the number of molecules passing through a unit area of interface plane per unit time.

Fick's first law of diffusion expresses that rate as a function of the difference in concentration, and a diffusion coefficient that depends on the molecular species present the structure, and the temperature and pressure in gaseous systems.

For one-dimensional diffusion in the x-direction, the diffusion flux is given by

$$J = -D\,(\partial C/\partial x) \qquad (2\text{-}1)$$

Where

J = net flux (moles per unit area per second)

D = diffusion coefficient (cm^2 /s)

$\partial C/\partial x$= concentration gradient ($moles.cm^{-2}$)

The coefficient D can be calculated from the equation

$$D = D_0 \exp(-Q/RT)$$

Where

Q = activation energy (J/mol)

R = gas constant (8.314 J/mol K)

T = absolute temperature (K)

D_0 = constant for the given diffusion system (molecule and structure)

The activation energy depends upon the availability of "space" for the molecule to move into and the bonding of the molecules: it would be much harder to move around in a room crowded with football players holding hands, than it would be to move through a room with the same number of small children each sitting quietly on the floor. In the same way, close-packed structures with strong chemical bonds have very high activation energy.

§2.2.2 *Fick's second law of diffusion*

Fick's second law describes the transient (time-variant or non-steady-state) diffusion of molecules in a material.

Fick's second law may be written as (for one-dimensional material)

$$\frac{\partial C}{\partial t} = \frac{\partial J}{\partial x} = -D\frac{\partial^2 C}{\partial x^2} \qquad (2\text{-}2)$$

Fick's second law describes time varying (non-steady-state) diffusion. One solution for this is:

$$\frac{C_S - C_z}{C_S - C_0} = erf\left[\frac{Z^2}{4Dt}\right]^{\frac{1}{2}} \qquad (2\text{-}3)$$

Where

C_S is the concentration of the diffusing molecules at the surface.

C_o is the initial concentration in the material

C_z is the concentration at location z beneath the surface after time t.

D is the diffusion coefficient

§2.2.3 *Diffusion model for timber*

Wood is an anisotropic material, which means there will be differences in the diffusion rate in different directions. Hence there is a different diffusion coefficient for each of the longitudinal, tangential and radial directions. Diffusion coefficient in an anisotropic material is not necessarily in the direction normal to the surface of

constant concentration, as is borne out by considering the following equation for diffusion in an anisotropic media (in rectangular coordinates) (Barnes 1988):

$$\frac{\partial C}{\partial t} = D_1 \frac{\partial^2 C}{\partial x^2} + D_2 \frac{\partial^2 C}{\partial y^2} + D_3 \frac{\partial^2 C}{\partial z^2} \qquad (2\text{-}4)$$

Where the x, y, z -directions are called the principal axes of diffusion, and D_1, D_2 and D_3 are the principal diffusion coefficients. Crank (1956) gives an equation which describes the relation between directions and diffusion coefficients:

$$D_n = l^2 D_1 + m^2 D_2 + n^2 D_3 \qquad (2\text{-}5)$$

where D_1, D_2, D_3 are diffusion coefficients along the principal axes and D_n is the diffusion coefficient " at right angles to the surface whose direction cosines relative to the principal axes are l, m and n".

Grace (1996) was able to determine the diffusion coefficient using the moisture content profile for the drying of *Nothofagus truncata* from the measured moisture when boards are long and wide, or when the ends and edges are effectively end-sealed, and the moisture movement is essentially one-dimensional. In isothermal conditions, the moisture flux is given by Fick's first law of diffusion in the following way:

$$J = -D \frac{\partial (\rho X)}{\partial z} \qquad (2\text{-}6)$$

where:		
	J = moisture flux	[kg/m^{2}s]
	ρ = basic density	[kg/m^3]
	D = diffusion coefficient	[m^2/s]
	X = (fractional) moisture content	[kg/kg]
	z = distance	[m]

Fick's second law of diffusion then becomes (for a variable diffusion coefficient)

$$\frac{\partial X}{\partial t} = \frac{\partial}{\partial z}\left(D\frac{\partial X}{\partial z}\right) \qquad (2\text{-}7)$$

where t = time [s]

The gradient $\partial X/\partial z$ can be thought of as a potential causing moisture transport, the antecedent of which is a more fundamental (and realistic) potential. Below fibre saturation such a potential may be the water-potential gradient (Siau, 1984). At this stage, no assumption need be made about the nature of the potential causing moisture movement, although the diffusion coefficient, D, is likely to be dependent upon the moisture content.

The diffusion coefficient may be obtained as a function of moisture content from measured moisture profiles. The integration of the above equation from some position $z=\varsigma$ to the centre of the wood, z=0, gives:

$$\int_{z=0}^{z=\varsigma}\frac{\partial X}{\partial t}dz = D_{z=\varsigma}\left[\frac{\partial X}{\partial z}\right]_{z=\varsigma} - D_{z=0}\left[\frac{\partial X}{\partial z}\right]_{z=0} \qquad (2\text{-}8)$$

For drying from two sides of a board, the moisture gradient at the centre of the board is assumed to be zero. If moisture profiles have been measured at times t and $t+\Delta t$, then Equation (2-8) simplifies to the partially discrete expression:

$$\frac{1}{\Delta t}\int_{z=0}^{z=\varsigma}(X_{t+\Delta t} - X_t)dz = D_{z=\varsigma,t=\upsilon}\left[\frac{\partial X}{\partial z}\right]_{z=\varsigma,t=\upsilon} \qquad (2\text{-}9)$$

where $\upsilon = (2t+\Delta t)/2$

The various terms in Equation (2-9) can be measured from actual moisture profiles to give the diffusion coefficient at position $z=\varsigma$. The moisture content at $z=\varsigma$ and time $t=\upsilon$ is also known, and therefore the diffusion coefficient can be expressed as a

function of moisture content. Successive use of Equation (2-9) yields this function. Figure 2-1 illustrates the method.

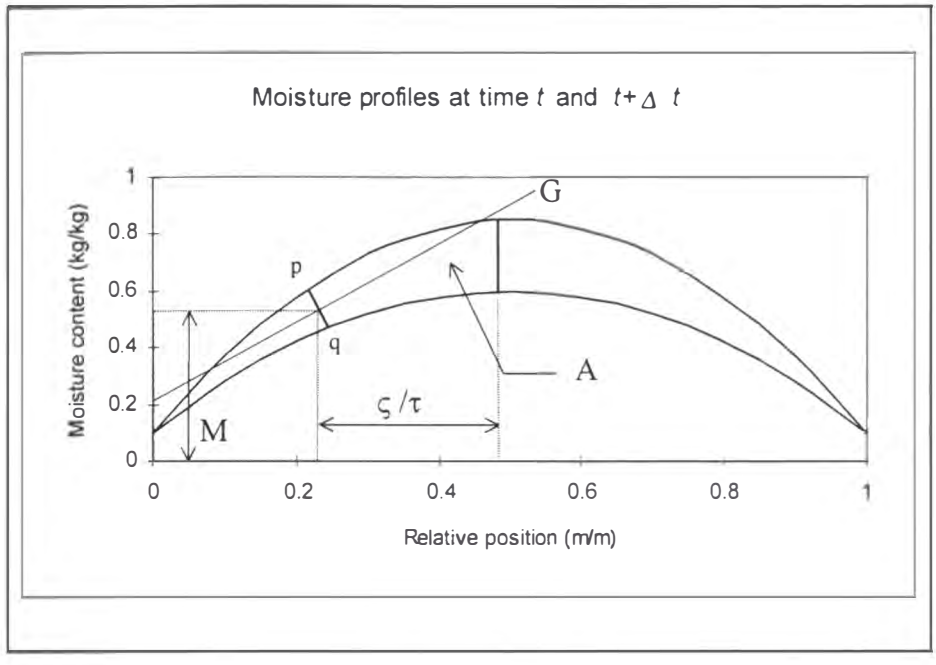

Fig 2-1 Calculation of diffusion coefficient

Referring to Figure2-1, if:

M = average moisture content across line *pq*.

G = average gradient of the moisture profile across line *pq*.

A = area bounded by the moisture profiles, line *pq*, and the line z=0.

τ = thickness of the board in which moisture profiles were measured;

then:

$$M = X_{z=\varsigma,t=0} \tag{2-10}$$

$$\tau G = \left[\frac{\partial X}{\partial z}\right]_{z=\varsigma,t=0} \tag{2-11}$$

$$\tau A = \int_{z=0}^{z=\varsigma} (X_{t+\Delta t} - X_t)dz \tag{2-12}$$

The two moisture profiles are joined by the line *pq*. This need not be a line of constant relative position, as implied by Equation 2-9. A more accurate estimation of *M* and *G* is often possible if *pq* is not vertical.

The axes in Figure 2-1are in terms of the dimensionless quantities, [X] and [z/τ-0.5]. Therefore *M*, *G* and *A* are all dimensionless. If τ is the thickness of the board in metres and Δt is the time in seconds between measuring the two moisture profiles, then Equations 2-9 to 1-12 can be combined to give the diffusion coefficient, D:

$$D_{X=M} = \frac{A}{G} \times \frac{\tau^2}{(\Delta t)} \qquad (2\text{-}13)$$

Values of the diffusion coefficient for control and pre-steamed wood are derived from Grace (1996) using the above analysis.

§2.2.4 *Diffusion coefficients for New Zealand red and hard beech timbers:*

The following table lists some of previous work on diffusion coefficients for New Zealand red beech.

Table 2-1 Diffusion coefficients for moisture movement in *Nothofugas fusca* (m^2/s)

source:	Ross (1986)	Barnes (1988)	Crawshaw (1988)
tangential:	$6.9\pm0.8 \times 10^{-11}$	$3.3\pm0.8 \times 10^{-11}$	N/A
radial:	$1.2\pm0.2 \times 10^{-10}$	$1.4\pm0.3 \times 10^{-10}$	$2.2\pm0.2 \times 10^{-10}$
temperature:	45°C	35°C	36°C

Grace (1996) has obtained the transverse diffusion coefficient of pre-treated and untreated hard beech timber at 20 °C. Average values of 3×10^{-11} (m^2/s) and 5×10^{-11} (m^2/s) were calculated for control sample and pre-steamed samples respectively. Barnes (1988) reported that diffusion coefficient of New Zealand red beech is slightly higher than these values.

§2.2.5 *Fibre-saturation point (FSP)*

FSP is the moisture content when all the free water from the cell cavities has been evaporated, but the cell walls remain saturated (Ministry of Forestry, 1996). Typically it is considered to be around 30 % dry basis (net). Shubin (1990) gives the following data:

Table 2-2 The relationship between basic density and fibre-saturation point of different species:

Species	Basic density /kgm^{-3}	FSP / %
Oak, *Quervs, sp.*	656	33
Birch, *Betula sp.*	513	26
Spruce, *Picea sp.*	370	25
European Beech *Fagus sp.*	533	24
Pine, *Pinus sp.*	457	22.5

The European beech (*Fagus sp.*) is closely related to the southern beeches (*Nothofagus spp*) and thus a fibre-saturation point of 25% may be considered to be typical for southern beech timber thought to be due to small difference in the of the composition of the cell-wall structure and the presence of water-soluble substance.

§2.2.6 *Relative humidity:*

The relative humidity of a damp gas is a measure of its fractional saturation with moisture. Almost always the relative humidity is defined as the ratio of the partial pressure of moisture p_w to the saturated-vapour pressure p_w^o, although some reference works such as the Smithsonian Meteorological Table (Keey 1978) use a ratio of humidities instead. In this item, the former, and the commoner, definition is adopted (Keey 1978). The relative humidity ψ is thus given by

$$\psi = p_w / p_w^0 \qquad (2\text{-}14)$$

Clearly Equation (2-14) for the humidity Y may be written as

$$Y = (\frac{M_w}{M_G}) \frac{\psi P_w^0}{P - \psi P_w^0} \tag{2-15}$$

Re-arrangement of Equation (2-15) yields an explicit expression for ψ :

$$\psi = \frac{YP}{(Y)M_W / M_G)P_W^0} \tag{2-16}$$

The EMC and RH temperature relationships can be expressed in equation form, which is sometimes more convenient to use than tabular data. Useful equations can be derived from theories for the adsorption of water on hygroscopic materials. One such equation that works particularly well is the modified Hailwood-Horrobin model based on the sorption of water onto polymer hydrates. Simpson (1973) gives the following expression:

$$M = \frac{1800}{W}\left[\frac{k\psi P_w^0}{1 - k\psi P_w^0} + \frac{k_1 k \psi P_w^0 + 2k_1 k_2 k^2 \psi P_w^{0\,2}}{1 + k_1 k \psi P_w^0 + k_1 k_2 k^2 \psi P_w^{0\,2}}\right] \tag{2-17}$$

where

M is moisture content,

ψP_w^0 is relative vapour pressure, and

$$W = 330 + 0.452T_{db} + 0.00415T_{db}^2 \tag{2-18}$$

$$k = 0.791 + 0.000463T_{db} - 0.000000844T_{db}^2 \tag{2-19}$$

$$k_1 = 6.34 + 0.000775T_{db} - 0.0000935T_{db}^2 \tag{2-20}$$

$$k_2 = 1.09 + 0.0284T_{db} - 0.0000904T_{db}^2 \tag{2-21}$$

§2.2.7 Moisture content

The standard method of determining moisture content is by oven-drying, and the moisture content of wood is expressed as a percentage of the oven-dry weight. The oven-dry weight is determined by heating wood at 103±2 °C until a constant weight is reached. The formula used to determine moisture content is:

$$MC = \frac{IW - OD}{OD} x100 \qquad (2\text{-}22)$$

where

MC = moisture content in percent

IW = initial weight of the wood

OD = oven-dry weight of the wood.

This assumes that the equilibrium moisture content under oven conditions is essentially zero.

§2.2.8 Equilibrium moisture content

Wood is generally dried to a specified moisture content depending upon its end use. However, wood is a hygroscopic material. Therefore, it constantly picks up or looses moisture to maintain equilibrium with the environment. Thus, wood is constantly shrinking or swelling. The amount of moisture which wood will gain or lose depends upon the temperature of the air and the relative humidity. At a constantly maintained temperature and relative humidity, wood will reach an equilibrium when it neither loses nor gains moisture. At this point, wood is said to have reached its equilibrium moisture content (EMC). The sorption of moisture on wood shows hysteresis: the equilibrium moisture content of never-dried wood on drying is different from that for wetting from previously-dried material. Movement of moisture by diffusion results from differences in the relative humidity and moisture content between the surface and the interior or between any two zones of the wood. Moisture in wood moves to

the surface by simultaneous diffusion of vapour and bound water as well as other mechanism. In comparison with capillary movement, diffusion is a slow process.

§2.3 Methods for drying New Zealand beech timbers

The *fusca*-type New Zealand beeches, red beech *(Nothofagus fusca)* and hard beech *(Nothofagus truncata)* in particular, are among the most temperature-sensitive hardwoods. They frequently contain tension wood and drying causes collapse which cannot be removed by reconditioning. Therefore the drying processes for these timbers usually require comparatively long periods under mild conditions, and consequently, these drying processes are very energy consuming because of potential thermal losses over an extensive drying schedule.

Kinimonth and Williams (1974) of New Zealand Forest Research Institute described New Zealand red and hard beech in these terms: "heart grades collapse and warp excessively if kiln-dried from green and takes 4-5 weeks for 1 in (25 mm) to dry. " They recommended a four- stage drying cycle:

a. Air-dry under covered stack until 40% moisture content.
b. Steam at 100 °C for 2 hours to hasten drying
c. Pre-dry down until highest moisture content is 25%.
d. Kiln-dry using the schedule in table 2-3. Alternatively, air dry and finish on the schedule given.

Table 2-3. Recommended drying schedule for New Zealand red and hard beech timbers (after Kininmonth and Williams 1974).

Moisture content %	Dry-bulb temperature, °C	Wet-bulb,°C temperature
30	54.5	49.0
25	60.0	51.5
20	65.5	54.5
16	65.5	49.0
Conditioning	76.5	75.5 C

The schedule requires the conditioning for at least 10 hours. If boards contain sapwood they should be separated and dried rapidly to minimise staining.

Air-drying methods have been used for lumber drying especially for some of the slow drying of these temperature-sensitive hardwoods. One of the advantages of air drying for the commercial kiln operator is to save energy. However, unpredictable weather conditions in some cases could significantly affect the quality of the air-dried materials, sometimes disastrously. The long term air-drying of several months means that valuable timber has to be held for lengthy periods, representing a considerable cost, even if the material does not deteriorate. A controlled drying method therefore is required to minimise the influences of ever-changeable weather conditions and enhance any guarantee of the product quality. At the same time it should be energy-efficient.

§2.4 Drying schedules for heat-sensitive or collapse-prone timbers:

A kiln schedule can be defined as "a series of temperatures and humidity and air velocity settings used to produce stress-free timber of a pre-determined moisture content range, in as short time as possible" (Ministry of Forestry, 1996).

There are a few types of drying schedules developed for heat-sensitive or collapse-prone timbers:

1. Air-dry to a moisture content below under fibre saturation prior to conventional kiln schedules.

The traditional New Zealand beech timber-drying schedules adopted this strategy, as the timbers are very refractory when the moisture contents are above fibre saturation due to low mechanical strength and high stiffness value.

2. Intermittent drying technique

Its potential to relax stressed samples might help to reverse what is believed to be unavoidable collapse and degrade. However, the cost of handling and the prolonged period of occupying the kiln space will be the major concerns in evaluating the economics of the technique.

3. Continuous drying schedules:

A continuous drying schedule maintains a small temperature gradient between the air in the kiln and the surface of the wood, so that the drying force is more constantly restrained to avoid the development of excessive moisture-content gradients and with unspectacular degrade.

There are two types of continuous drying schedules: continuously rising schedule and continuously varying schedule.

Continuous rising drying schedule

Continuously rising drying schedule is an accelerating drying process, starting with the dry-bulb temperature inside the kiln as near as practical to the ambient temperature and a constantly increasing temperature gradient rate is maintained throughout the drying process (Nassif 1983).

Continuously varying schedule

Different from the continuous rising schedule, both the dry-bulb temperature and the wet-bulb depression are controlled in the continuously varying schedule, and the each of them increase at a small rate according to the level of the moisture contents. Generally speaking, the continuously varying schedule is divided into two stages. In the first stage, a very slow rate of temperature rise is applied, then when boards are dried to the fibre-saturation point, a higher rate of temperature rise is used. The two stage-strategy aims to reduce the risk of excessive defects in the early stage of the drying (Nassif 1983).

§2.5 Wood drying behaviour:

As a piece of wood dries, a moisture profile will develop within the wood, with the highest moisture content at the centre of the board. Shrinkage occurs whenever the moisture content in the board falls below the fibre-saturation point. The condition occurs when essentially all the free water has been removed from the free space within the fibre and from inside the vessels (hollow fibre) and the remaining moisture is bound to the cell walls themselves.

The shrinkage that tries to occur will be restrained by the wetter central part of the board, thus creating a tensile stress at the surface. This tensile stress is balanced by a compressive stress in the core (Salin 1992). Later in the drying process, the region where the shrinkage is inhibited will move towards the centre of the board, and therefore the tensile forces move inwards too. If these tensile stresses set up during drying exceed the tensile strength of the wood perpendicular to the grain, the fibres will separate, creating a check. Checks can be observed easily on the surface and the ends of the timber, but internal checks are harder to detect (Svennson 1996). It must also be noted that checking will occur in earlywood above fibre saturation, due to the tension increasing as the moisture evaporates; these checks may subsequently close up since moist wood behaviour is plastic at the higher kiln temperatures.

Another form of drying degrade is collapse. Collapse is cell failure due to excessive capillary tension: heat-weakened walls collapse locally reducing the thickness of the board and giving rise to a wavy washboard surface. It occurs mainly at the start of the drying when capillary forces dominate. Collapse is caused by a tensile force (hydrostatic force) in the water which fills the cell cavities (free water), so collapse only occurs above FSP. It is possible to reduce the severity of collapse by using lower temperature kiln schedules.

Warp is a general term meaning the distortion of timber caused by differential shrinkage. The amount of warp is influenced by the type of timber being dried (eg. intrinsic wood properties, growth-ring orientation and thickness variation) and the

stacking procedure. It can be minimised by high standards of kiln-charge preparation and to use of kiln stack weights. Honeycombing is internal checking that is not always visible on lumber surfaces; sometimes it is associated with collapse.

There is also another phenomenon associated with drying process, stress reversal which is a condition that occurs in drying after the moisture content of the core of the piece falls below the fibre saturation point. The surface is in compression and the core is in tension.

§2.5.1 Theory on cell collapse

Kauman (1958) investigated the causes of collapse during drying of *Eucalyptus regnans*. He found that the drying stresses were a significant factor, since the shell of a board undergoing drying shrinks more than the core initially, exerting a compressive stress upon it which can contribute to collapse. Capillary tension, however, was recognised as the principal cause of collapse.

It is clear that the capillary tension resulting from the drying of wood can be reduced by the displacement of the water in wood by a liquid with lower surface tension. Ellwood *et al.* (1959) demonstrated that collapse can be eliminated in the drying of susceptible hardwoods by exchanging the water with methanol and ethanol, but it is not feasible on a commercial scale.

Collapse occurs in wood when the capillary tension exceeds the compressive strength perpendicular to the grain. In the case of a susceptible species such as *Sequoia sempervirens*, the Wood Handbook (USAD 1955) gives a value of 520lb/in^2 (35.4 atm) for the compressive strength of green material.

Lower temperatures must often be used during the early stages of drying because of the hazards associated with too rapid removal of capillary water at high temperatures. The key to the future progress in speeding up drying process appreciably is probably to be found in discovering new methods of removing capillary water more effectively than is possible with present drying methods. Therefore it is important to understand

the movement of capillary water during drying process as it relates to the onset of capillary tension within the wood.

The factors responsible for collapse of wood during drying are listed below:

1. Small pit-membrane openings increase the susceptibility of the wood to collapse due to the resulting high capillary tension.

2. A high surface tension of the liquid evaporated from the wood promotes collapse. When free water is replaced by a low-surface-tension organic liquid, collapse may sometimes be prevented.

3. A low-density wood has thin cell walls which collapse easily due to low compressive strength.

4. Elevated temperatures decrease cell-wall strength and therefore render the wood more susceptible to collapse.

§2.6 Mechanical behaviour of timber under drying

§2.6.1 Strength and Modulus of Elasticity

There are two key mechanical properties, failure strength (strength) and stiffness (modulus of elasticity). Thus, the strength of a material such as wood refers to its ability to resist applied forces that could lead to its failure. Elasticity represents the amount of deformation that occurs under an applied force assuming the material behaves as an elastic body.

The application of a small load to a piece of wood will cause the sample to deform elastically. If the material is a linear elastic solid, then the increments in deflection are proportional to the increments in load which can be expressed as

Applied load α deformation, or $\frac{applied \cdot load}{deformatiom} = a\ constant$ (2-23)

Some of the terms involved are:

$$Stress = \frac{Load(N)}{Cross - Sectional\_area(mm^2)} \quad (N/m^2, \text{or } Pa) \qquad (2\text{-}24)$$

and

$$Strain = \frac{deformation(mm)}{original \cdot length(mm)} \quad (1) \qquad (2\text{-}25)$$

and

$$Modulus\ of\ elasticity = \frac{stress(\sigma)}{strain(\varepsilon)} = a\ constant \quad (N/m^2 \text{ or } Pa) \qquad (2\text{-}26)$$

(Modulus of elasticity is denoted by E, which is often referred as the stiffness and is generally quoted in GPa for timber).

The limit of proportionality: If the applied force is above a certain level of loading, known as the limit of proportionality, departure from linearity occurs such that, for each further increment in stress, there is a more than a proportional increment in deformation i.e. the strain is non-linearly elastic. If an applied load above the limit of proportionality is removed, the sample will not return to zero deformation, but the stress-strain line will follow a line lying parallel to the initial linear region, terminating on the strain axis at some finite deformation. This explanation assumes the recovering material is behaving as a linear elastic solid and the permanent residual deformation is due to structural change in the cell wall. Thus, permanent deformation has been induced in the sample which will take the form of cell crushing, if the load has been applied in longitudinal compression; or cell-wall micro-failures, if a longitudinally applied tensile load has been applied.

The moisture content effect on timber strength, strain and stiffness:

The fibre-saturation point is an arbitrary condition to describe the supposed situation where cell cavities are empty but the cell walls are still saturated with water, which is called bound water. This bound water is only associated with the matrix constituents of this fibre-composite, in the other words those substances that contain hydroxyl groups to which the bound water is thought to bond. X-ray diffraction analysis clearly indicates water does not enter the core of the microfibrils. The amount of bound water is limited by the number of accessible sorption sites available and by the number of water molecules that can be held at each one, as well as any possibility of water molecule clusters attracting themselves to the cell wall. When this reaches a maximum value the wood is at the fibre-saturation point. This sorption is temperature-dependent and decreases by about 0.1% per 1 °C rise in temperature; it also decreases with increasing density (Dinwoodie 1989).

Removal of the water from the matrix layer results in the microfibrils moving into closer proximity, thereby increasing the inter-microfibrillar bonding. Therefore as the wood shrinks, there is a corresponding increase in many of the mechanical properties (Dinwoodie 1989).

The variations of longitudinal compressive strength against moisture content is given in many textbooks (e.g. Dinwoodie 1989). The strength of the wood begins to rise with diminishing moisture content below fibre saturation.

Dinwoodie (1989) reports that the moisture content - modulus of elasticity (longitudinal) relationship also has similar pattern as the moisture content-compressive strength relationship. Above the fibre-saturation point, the maximum longitudinal compressive strength is independent of moisture content (Fig. 2-2), but the modulus of rigidity and the modulus of elasticity appear to rise with moisture content above 50% (Fig. 2-3, Fig 2-4), but this effect is not discussed in Dinwoodie (1989).

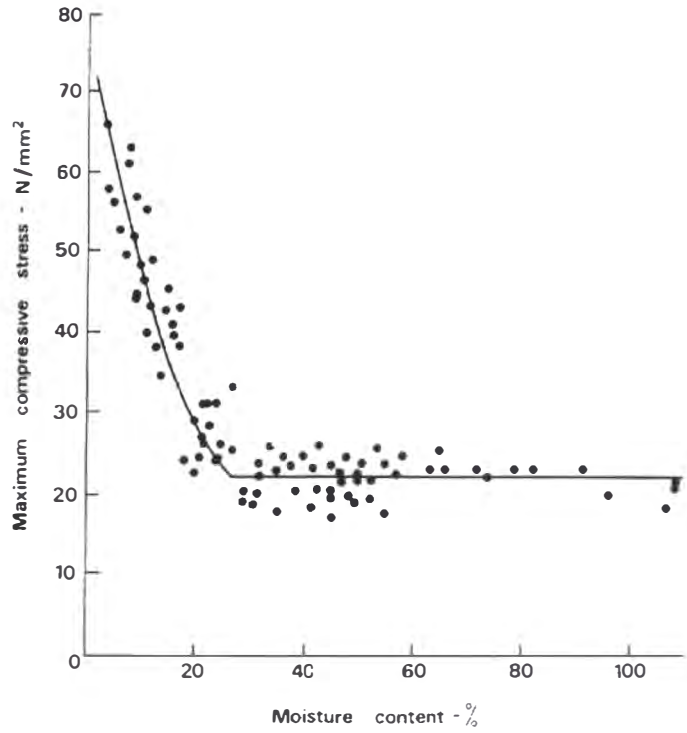

Fig 2-2 Relationship of longitudinal compression strength to moisture content of the wood (Dinwoodie, 1989).

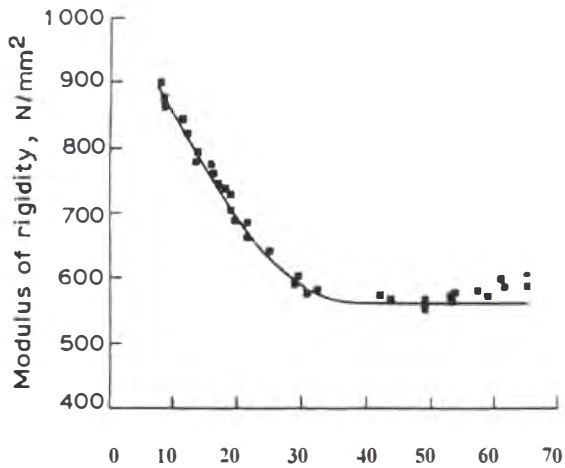

Fig 2-3 Relationship of longitudinal modulus of rigidity vs moisture content of the wood (Dinwoodie, 1989).

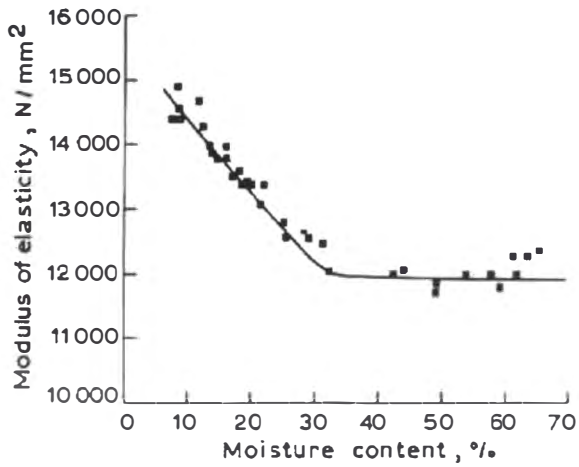

Fig 2-4 Relationship of longitudinal modulus of elasticity vs moisture content of the wood (Dinwoodie, 1989).

Total strains in drying timbers

The strains that the drying timber may experience can be expressed by the following additive equation (Keey *et al.* 2000):

$$\varepsilon_{Tot} = \varepsilon_I + \varepsilon_C + \varepsilon_S + \varepsilon_M + \varepsilon_T \qquad (2\text{-}27)$$

where ε_I = instantaneous elastic strain, ε_C = creep strain, ε_S =free shrinkage strain, ε_M = mechano-sorptive strain and ε_T is the thermal strain. These strains are measured as relative change in length (in terms of the initial length).

An instantaneous strain is produced in a specimen immediately on application of a load. An elastic strain is totally recoverable if the stress is removed before it exceeds the proportional limit (Figure 2-5). The magnitude of the instantaneous strain for a given load is dependent on the temperature and the moisture content of the wood sample.

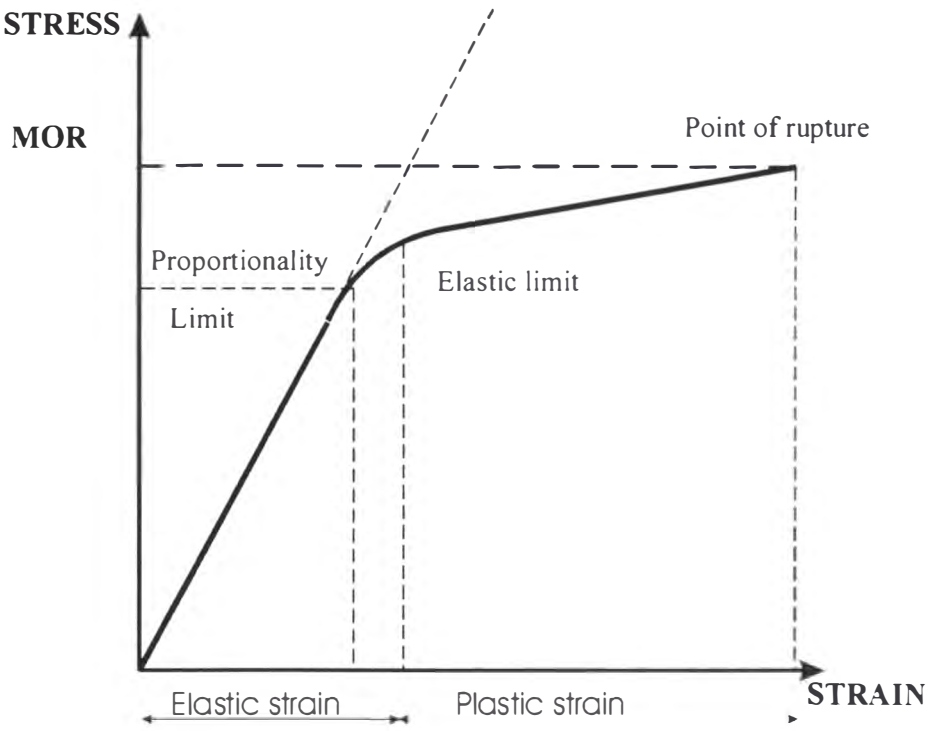

Figure 2-5 Stress-strain diagram for a wood sample at constant moisture content with progressive loading

Creep strain is a time-dependent component of the strain, and relates to plastic flow of the material.

The mechano-sorptive strain is due to the interaction between stress and the rate of moisture-content change. It does not occur during steady-state moisture movement.

Thermal strain:

Thermal expansion of wood refers to the increase in the dimensions of the material with an increase in temperature provided the moisture content of the wood does not also change. Experiments have demonstrated that the resultant change in the dimension of a material due to heating is proportional to the initial dimension and to the change in temperature. The proportionality constant is called the coefficient of thermal expansion (α).

Thermal expansion is described mathematically by the relationship:

$$\Delta D = \alpha D_i(\Delta T) \qquad (2\text{-}28)$$

where:

ΔD = increase in the dimension

D_i = initial dimension

ΔT = increase in temperature

To calculate the final dimension of the material, the equation above may be written as follows:

$$D_f = D_i[1 + (\alpha)(\Delta T)] \qquad (2\text{-}29)$$

The coefficient of thermal expansion of oven-dry wood in the longitudinal direction (α_{OL}) is independent of both species and specific gravity and ranges from 3 x 10^{-6} to 5 x 10^{-6} per ° C.

On the other hand, the coefficient of thermal expansion of oven-dry wood in the radial and tangential directions increase directly with specific gravity. Over the specific gravity range of $0.1 < 0 < 0.8$, the coefficients can be approximated by the following equations (Desch and Dinwoodie, 1996):

$$\alpha_{OR} = (9.9 + 32.4G_0)x10^{-6}/^oC \qquad (2\text{-}30)$$

$$\alpha_{OT} = (18.4 + 32.4G_0)x10^{-6}/^oC \qquad (2\text{-}31)$$

The coefficients of thermal expansion can be considered independent of temperature over the range of –50° C to 55° C.

The thermal expansion of moist wood is more difficult to characterise because it becomes overshadowed by shrinkage and swelling due to moisture interaction. When moist wood is heated, it tends to expand due to thermal expansion but at the same time it tends to shrink because of the reduction in bond moisture content, the fibre-

saturation point being about 24 % at 100 ° C compared with a value of about 32% at 20° C.

In the table2-4, thermal expansion coefficients of different materials have been derived by artificially maintaining the same moisture content at different temperatures, an occurrence unlikely to happen in practice.

Table 2-4 Thermal properties of selected woods (Desch and Dinwoodie,1996)

Material	Density (kg/m^3)	Thermal conductivity (W/mK)		Specific heat capacity (J/kgK)	Linear thermal expansion ($x10^{-6}$ per K)		
		R	L		R	T	L
Balsa	176	0.06	-		16	24	--
Spruce	340	0.10	0.21		24	35	3.5
Douglas-fir	512	0.11	-	1360	27	45	3.5
Yellow birch	660	-	-		32	39	3.6
European oak	673	0.16	0.28		--	--	--

§2.6.2 *Previous studies on viscoelastic strains:*

According to Schaffer (1972), wood behaves non--linearly over the whole stress-level range, with linear behaviour being a good approximation at low stresses, and Boltzmann's superposition principle appling to stress-strain behaviour for stress up for to 40% of the short-time behaviour.

a) Effect of temperature

An increase in temperature will generally reduce the stiffness of timber in bending, tension or compression (Davidson 1962; Bach and McNatt 1990: Kingston and Budgen 1972), especially above 55 °C. This is known to be the temperature at which lignin alters its conformation and hemicelluloses begin to soften (Morlier 1994).

The interaction of creep with variable temperature results in a complex behaviour that may be difficult to predict from constant-temperature creep tests (Schniewind 1968).

For example, an increase in temperature in the range 20 - 90 °C during a bending test results in a creep that was larger than the creep observed at the highest temperature (Jouve and Sales 1986).

b) Effect of moisture

Moisture in wood acts as a plasticiser. Therefore, creep increases with moisture content (Bodig and Jayne 1982, Schniewind 1968), Bach (1965) deduced from tensile tests that an increase of 0.04 kg/kg in moisture content had about the same effect as an increase in temperature of about 6 °C within the moisture content (0.04-0.12 kg/kg) and temperature limits of his experiment.

The effect of the interaction of moisture movement (drying and wetting) with the mechanical behaviour of wood, is called the mechano-sorptive effect (Grossman 1976 1978), and is reviewed by Schniewind (1968), Bodig and Jayne (1982), Hunt (1990 1991), and Gril (1988). The mechanosorptive effect has been related to the possible rearrangement of hydrogen bonds in the sorptive layer below fibre saturation, and thus depends upon the rate of moisture loss.

c) Residual stresses and long-term strength of wood

Drying of wood and the consequent moisture changes generate cause stresses perpendicular to the grain, which may cause checking of the initially stress-free wood

During drying of timber, stresses perpendicular to the grain appear due to the moisture gradient and shrinkage of the material. In the past, the drying stresses were first calculated by the use of purely elastic methods (Dinwoodie 1989). This predicted stresses several times higher than the strength of wood in the tangential direction. More realistic values were obtained by plastic analysis (Dinwoodie 1989). This is, however, an inappropriate method for wood under tension, when the behaviour is far

from being plastic (Dinwoodie 1989), the plastic behaviour, which relaxes the stress in some extent, should be considered in calculation.

The molecular organisation of wood is a complex system composed of a large number of chemical substances with molecules of a wide range of sizes and shapes distributed unevenly throughout the fibre walls. Basically, however, three main polymers may be distinguished in wood:

- Cellulose, a long-chain crystalline polymer;
- Hemicelluloses, medium-length and semi-crystalline polymers;
- Lignin, consisting of completely amorphous polymers.

Polymers are known for having well-defined plastic behaviour. Temperature has a great influence on the deformations either elastic or time-dependent, which are described by the so-called time-temperature superposition principle (which can be extended to a time-pressure-temperature superposition).

As far as the influence of a variation in the steady-state humidity value is concerned, it is justifiable to consider, according to Back and Salmen (1982), that adsorbed water in the polymers produce a variation of the transition temperature of these polymers.

Altogether it has been established that the following variables are involved in wood plastic behaviour:

- Wood characteristics (density, microfibril angle, elastic modulus, shrinkage rate, etc.)
- Stress
- Stress history
- Time
- Moisture content
- Moisture content change
- Moisture content history
- Temperature

- Temperature history (possible)

§2.6.3 *Characteristics of mechano-sorptive creep (Morlier 1994)*

a. During moisture desorption below FSP, the creep increases faster than it would at constant moisture content, regardless of the rate of desorption.

b. During any first sorption at a given moisture level after loading, the creep increases faster than it would at constant moisture content, regardless of the rate of sorption.

c. During any subsequent moisture sorption at the same moisture level, the creep deflection usually decreases, although it may remain constant or even slightly increase. This apparent recovery of bending deflection during sorption has been ascribed to differential dimensional changes on the tension and compression faces. This conclusion was supported quantitatively by measurements (Morlier 1994).

d. As a general rule, the effect of moisture content change on total creep deflection is much greater than the effect of time.

e. During moisture cycling there is an "exhaustion" process, the creep increment per cycle slowly decreases and tends towards a limiting value. At this limit the effect of the following still applies, i.e. the creep increases during desorption but decreases again during sorption.

f. Mechano-sorptive creep is linear at low stresses (about 10% of the breaking load). This applies to tensile, compressive and bending modes. Linearity with stress means that Boltzmann's superposition principle can be applied, so that a single stress independent compliance function j can be used. Thus, with constant stress and moisture content, the strain can be calculated as:

$$\varepsilon(t) = \sigma j(u,t) \qquad (2\text{-}32)$$

With changing stress, but constant moisture content, the strain is

$$\varepsilon(t) = \int_0^t j(X, t-\tau)\frac{\partial \sigma}{\partial \tau}.\partial\tau \qquad (2\text{-}33)$$

With constant stress, but changing moisture content, the strain is

$$\varepsilon(t) = \int_0^t j(X, \partial X, t-\tau)\frac{\partial X}{\partial \tau}.\partial\tau \qquad (2\text{-}34)$$

With both stress and moisture content changing, the strain is

$$\varepsilon(t) = \int_0^t \int_0^t j(X, \partial X, t-\tau)\frac{\partial X}{\partial \tau}.\partial\tau \frac{\partial \sigma}{\partial \tau}\partial\tau \qquad (2\text{-}35)$$

Stress linearity allows sign changes of stress including tension, compression and recovery to be incorporated. It also makes the calculation relatively simple for automatic computation since the strain for each new stress increment can be added to those already present.

Mechano-sorptive creep is not symmetrical in tension and compression, although the final magnitudes appear to be similar. At higher stress levels, it is non-linear. The strain increases rapidly and irrecoverably in the compression zones due to cell-wall buckling damage. The extent of cell-wall damage is especially sensitive to stress level and to high moisture contents.

On removal of a load, the wood 'recovers' in a similar manner to that for normal creep, approximately according to the usual expectations of a material that is linearly elastic with stress. The elastic modulus on unloading is not measurably different from that on loading, unless the compression is high enough to cause compression damage. In the latter case, the elastic modulus is decreased and the zero--load dimensional change coefficient is increased. Recovery is speeded up by moisture changes or cycling, especially during wetting i.e. there is a "memory" of the original dimensions (Fig. 2-6).

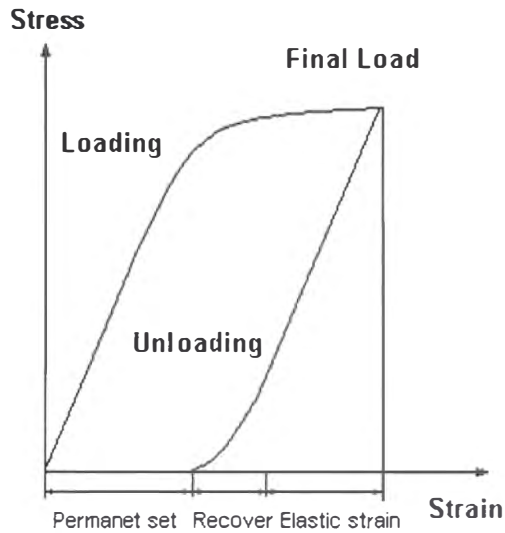

Figure 2-6 Stress-strain diagram for loading and unloading wood

Mechano-sorptive creep effect is also observed on loading perpendicular to the grain (Ugolev 1976), both in creep and stress relaxation (Perkitny and Kinston 1972), and always involves at least two-dimensional changes. In the case of bending, it is the difference between the dimensional changes of the tensile and compressive faces; in the case of direct tension or compression it is the difference between the measured dimensional changes and those estimated to take place for the same moisture change under zero load.

Mechano-sorptive effect is strongly reduced by chemical treatments of wood, such as acetylation and formaldehyde cross-linking (Norimoto *et al.* 1987). This supports the theory that MS creep is associated with the making or breaking of hydrogen bonds under an imposed stress.

However, the breaking of hydrogen bonds and remaking hydrogen bonds resulting from a constant moisture gradient through a piece of wood, does not result in mechano-sorptive creep (Armstrong 1972). This behaviour suggests that mechano-sorptive creep in wood depend on the anatomical structure of wood, in addition to the effect of stress bias of hydrogen bonds. However, it always is the moisture content change that generates the MS strain.

Mechano-sorptive creep, although it mainly applies to moisture changes below the fibre saturation point, has occasionally been observed above this moisture level, mainly in species that are prone to collapse during drying, which show an abnormal shrinkage above fibre saturation, thereby emphasising the link between dimensional changes and mechano-sorptive creep (Armstrong 1972).

§2.7 Methods of Seasoning Wood

§2.7.1 Objectives of Seasoning

Regardless of the method used, the objectives of any seasoning process are to dry the material to a low, specified uniform moisture content with a minimum amount of degrade in a minimum amount of time with a minimum cost for operating expenses and equipment. These objectives are not all compatible with one another, and one must often be sacrificed to satisfy another. The conditions for each situation must necessarily determine the relative emphasis placed on each objective. Thus the rate of drying must often be retarded to allow the wood to dry with a minimum of degrade. If beech is being dried for furniture-grade timber, this is certainly true. If cordwood were being dried for firewood, however, drying defects would make little difference, and drying the wood in a minimum of time at a minimum cost would be the only considerations.

§2.7.2 Air Drying

Of the methods available for seasoning wood, air drying is the oldest and simplest. Air-dried lumber is suitable for exterior use. However, green timber is also frequently allowed to partially air dry prior to kiln drying. Since the effectiveness of the drying process depends upon weather conditions which control the drying rate and the final moisture content that can be reached, air drying has been replaced by kiln drying in many areas, but is still an important process. Most air-seasoned material is dried in flat piles with stickers placed between layers, but when it is essential to have rapid

drying to prevent sap stain, end piling may be used. In humid areas, this may be necessary if a dry kiln is not available. Such end racking promotes good air circulation and consequent rapid drying, which eliminates the staining problem, but often causes end-surface checking and warping of the material. Another method of piling once used to promote rapid drying was edge piling (Tiemann 1938). Although it is generally thought that air drying is a gentle method of seasoning timber, it can be severe, depending on the time of the year and the species involved. Material cut from the oaks, sycamore, beech, maple, and other hardwoods which have large rays will surface check readily and, consequently, thick material cut from these trees is given special treatment. To eliminate rapid end drying, the ends are frequently coated with a material such as paraffin or tar to retard evaporation, but often this is not enough protection, and it is necessary to place the material in what are known as semi-kilns in which the drying rate is still more retarded. Semi-kilns are often nothing more than covered sheds in which the material is piled, but they may often be large enclosed buildings in which low heat and controlled humidity are used to slowly dry the wood. In semi-kilns where the temperature is maintained at 110 °F to 120 °F (37.8 °C to 48.9 °C) and fans are used to circulate the air, green stock may be dried to 8 to 12 percent moisture content in 3 months (Henderson,1951).

Air seasoning has been extensively treated in the literature. Fullaway and Hill (1928), Mathewson (1930), Peck (1956), and Rietz and Page (1971).

§2.7.3 Kiln Drying

Kiln drying of lumber is perhaps the most effective and economical method available. Drying rates in a kiln can be carefully controlled and defect losses reduced to a minimum. The length of drying time is also greatly reduced and is predictable so that dry lumber inventories can often be reduced. Where staining is a problem, kiln drying is often the only reasonable method that can be used unless chemical dips are employed.

Kilns may be divided into two classes, progressive and compartment kiln (Thelen, 1923). In the progressive kiln, timber enters at one end and moves progressively

through the kiln much as a car moves through a tunnel. Temperature and humidity differentials are maintained at different settings along the lumber charge is progressively dried as it moves from one end to the other. In both kilns, the charge is static . Box kilns are universal in New Zealand.

§2.7.4 Special Methods

There are many other methods available for drying wood, but for various reasons, chiefly economic, none of these has ever achieved the popularity of air seasoning or kiln drying. Among these "special" methods are: chemical seasoning (McMillen, 1960); high-frequency dielectric heating (McMillen and James, 1961); resistance heating; emersion in hot liquid metal; boiling in oily liquids (McMillen, 1956a); infra-red radiation (Anon. 2, 1965); vacuum drying (Anon. 3, 1956); vapour drying (Anon. 1964), solvent seasoning (McMillen, 1956b); high-temperature drying by solar radiation (Peck, 1962) and forced-air drying with unheated (Stevens, 1965) and heated air (Kimbal and Torgeson, 1959). A few of these methods are of marginal commercial importance; some are apparently impractical; others at present are uneconomical. Whether these methods are impractical and uneconomical today should not eliminate them from our thinking, however. Many improvements in wood seasoning are yet to be made, and it is only by inquisitive thinking into newer and less perfected ways of drying that improvements in the drying process can be achieved.

§2.8 References

Amburgey, T. L., 1994 Colour, stain, and the drying process, Profitable solutions for quality drying of softwoods and hardwoods, Forest products research society. pp 66-68.

Armstrong J. P., Patterson, D. W., 1995 Variation of final moisture content of 4/4 yellow-poplar lumber dried in a small dehumidification kiln, Forest Prod. J. **45** (5) pp51-52.

ATDG (Australia timber drying group), 1997 Timber drying quality standard, CSIRO Forest Products Laboratory, Victoria Australia.

Barnes, P.C.I., 1988. Moisture diffusion in Red and Hard Beech during drying. Bachelor of Engineering Report, Department of Chemical and Process Engineering, University of Canterbury

Campbell, G. S., 1980 Index of kiln drying schedules for timber dried in Australia, Commonwealth Scientific and Industrial Research Organisation Building Research Division.

Chawshaw, A.J., 1988. Pretreatments to hasten the drying of Hard Beech. Bachelor of Engineering Report, Department of Chemical and Process Engineering, University of Canterbury.

Chen, G., Keey, R. B., Walker, J. C. F., 1997, Stress relief for sapwood *Pinus radiata* Boards by cooling and steam-conditioning processes, Holz als Roh- und Werkstoss, Vol **55** pp 351-360

Choong, E. T., Chen, Y., Mamit, J. D. Ilic J., Smith, W. R., 1994, Moisture transport properties in hardwoods, 4th IUFRO International wood drying conference, Rotarua, New Zealand.

Choong, E., T., Chen, Y., Shupe, T., 1996 Effect of steaming and hot-water soaking on movement of moisture in hardwood during drying, 5th IUFRO International wood drying conference.

Innes T. C., 1995 Collapse and internal checking in the latewood *of Eucalyptus regnans* F Mull. Wood science and technology **30** (1995) pp 373-383.

Innes T. C., 1996 Collapse during seasoning of *eucalypt* timbers, 5th IUFRO International wood drying conference.

Innes T. C., 1995 Stress model of a wood fibre in relation to collapse, Wood science and technology **29** (1995) pp 363-376.

Isherwood, D.H., 1979. Investigation into the behaviour of Hard Beech during drying and as a result of pre-treatment. Bachelor of Engineering Report, Department of Chemical and Process Engineering, University of Canterbury

Kass, A. J., 1969 Inelastic mechanical behaviour in wood stresses perpendiculat to the grain radially. Ph.d these, The University of Machigan, USA.

Karlekar, B.F., 1983. Thermodynamics for engineers. Prentice-Hall, N.J.

Kaylhan, F., 1982 Simultaneous heat and mass transfer with local three-phrase equilibria in wood drying, Weyerhaeuser Company, Tacoma, WA. 98477,USA.

Keep, L.-B., 1998 The Determination of time-dependent strain in *Pinus radiata* under kiln-drying conditions, M.E. thesis, Department of Chemical & Process Eng. Univ. of Canterbury.

Keey, R. B., 1994 Heat and mass transfer in kiln drying: a review, Proc. 4th IUFRO International wood drying conference, Rotorua, New Zealand.

Keey, R. B., 1990 Introduction to industrial drying operations, Pergamon Press.

Keey, R. B., Langrish, T. A. G., Walker, J. C. F., 2000 Kiln-drying of lumber, Springer-Verlag, Berlin.

Milota, M., R., Wengert, E., M., 1995 Applied drying technology, 1988 to 1993, Forest product journal, Vol **45,** P. 33-41.

Ministry of Forestry, 1996 Producing quality kiln-dried timber in New Zealand.

Morlier, P., 1997 Micro-mechanical aspects of oak drying, International conference of COST action E8.

Nassif, N. M., 1983, Continuously Varying Schedules (CVS) – A New Technique in Wood drying, Wood Science and Technology **17** (2) pp. 139-144.

Pang, S, 1994 High-temperature drying of *Pinus radiata* in a batch kiln. Ph.D thesis University of Canterbury New Zealand.

Quarles, S. L., Wengert E. M., 1989 Applied drying technology, 1978-1988, Forest Prod. J. **39** (6) 25-38.

Ranta-Maunus, A., 1989 Analysis of drying stresses in timber, Paper and timber 10/1989 pp 1120-1122.

Rice, W. W., Gatchell, C. J., 1983 Kiln drying procedures for system 6 northern red oak, Proceedings 34th annual meeting western drying kiln clubs, pp. 79-88.

Ross, D.A., 1986. Investigating the moisture movement of Hard Beech during drying. Bachelor of Engineering Report, Department of Chemical and Process Engineering, University of Canterbury.

Siau, J.F., 1984. Transport processes in wood. Springer-Verlag, Berlin.

Simpsom, W. T., 1973 Predicting equilibrium moisture content of wood by mathematical models, Wood and Fibre **5**(1) pp 40-49.

Ward, C. J., Simpson, W. T., 1987 Comparison of four methods for drying bacterially infected normal thick red oak, Forest Prod. J. **37** (11/12) 15-22.

Chapter 3

Dehumidifier kiln systems

§3.1 Dehumidifier kilns

Although dehumidification drying is relatively new compared to conventional kiln drying, it is now used by significant numbers of kiln operators. Reasons for its popularity include low capital investment compared with high-temperature operation and simplicity of operation. The process is based on refrigeration technology, which is both reliable and cost-efficient.

A refrigeration-based dehumidifier is used to remove water from the kiln chamber. Heat generated by the dehumidifier is returned to the kiln to provide the energy needed for evaporation of moisture from the wood. Since refrigeration units will not operate efficiently at high temperatures, maximum temperatures are limited to about 160 °F / 70 °C. although most units operate at still lower temperatures. Electric strip heaters or small-capacity electric or gas-fired steam boilers are essentially supplemental heating units to bring the kiln quickly to operating temperatures. Drying conditions are normally milder than those used in conventional steam kilns, so that drying times are somewhat longer in consequence. Because of the milder conditions, there is less tendency for drying degrade, and warping is reduced. Inspection during the course of drying is enhanced since operators are able to move freely in and out of the kiln at the temperatures commonly used. There is no provision for relieving drying stresses, however, unless steam can be introduced into the kiln.

Dehumidifiers have great potential to substantially improve the energy efficiency of drying process through recycling the latent heat of the moisture from the product being dried, especially for low-temperature applications, Such mild conditions are needed for drying the heat-sensitive red and hard beech timbers.

In the dehumidifier, instead of venting the humid air, it is processed through a cold heat exchanger (evaporator), which condenses some of the water in the air. The heat

absorbed from the water vapour is used to vaporise a refrigerant. Compressed to a higher pressure by a compressor, this refrigerant has then a boiling point higher than room temperature; thus, on condensation, the refrigerant releases its energy to the hot coil (condenser). The air passing through this hot coil is rewarmed and is relatively drier then when it entered the unit. Besides its lower power consumption, the dehumidifier does not have to heat the air to lower its relative humidity, and it is possible to obtain dry air at much lower temperatures than in a conventional kiln.

Dehumidifier drying kilns also have the potential to help to reduce the CO_2 emissions in comparison to conventional kilns, by reducing the combustion of primary fuels. Such systems thus have the potential to be more friendly to the environment (Carrington *et al* 1995).

Not all the heat-pump dryers are dehumidifiers, there are other types of heat-pump dryers which suit different drying conditions. The Figs 3-1 to 3-5 are schematic diagrams of other types of heat-pump driers. The arrows indicate the directions of the movement of the air.

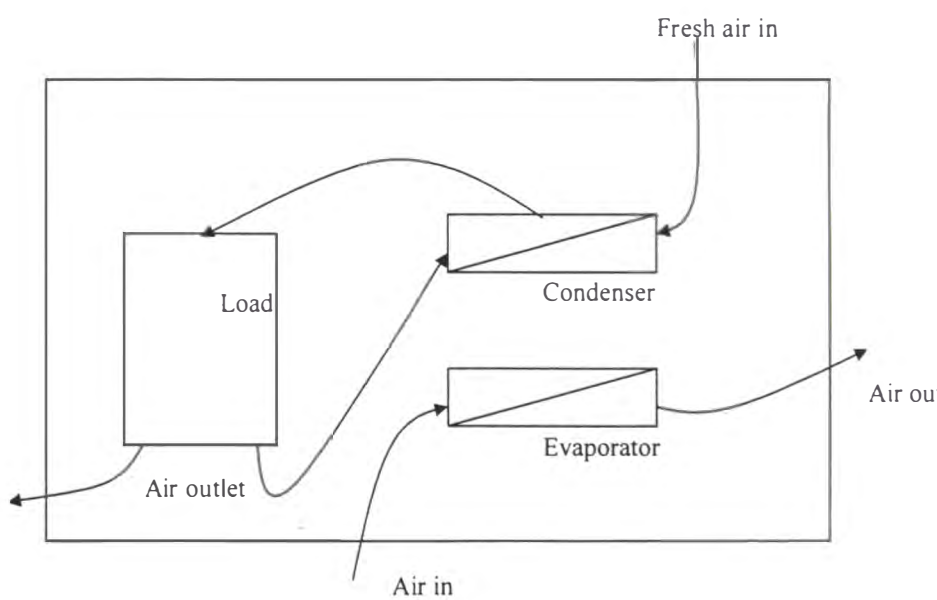

Figure 3-1 An atmospheric energy source heat-pump dryer, is basically a heat-and-vent dryer, employing a heat-pump source. It is suited to low-temperature drying when the atmospheric temperature is already warm and humidity low.

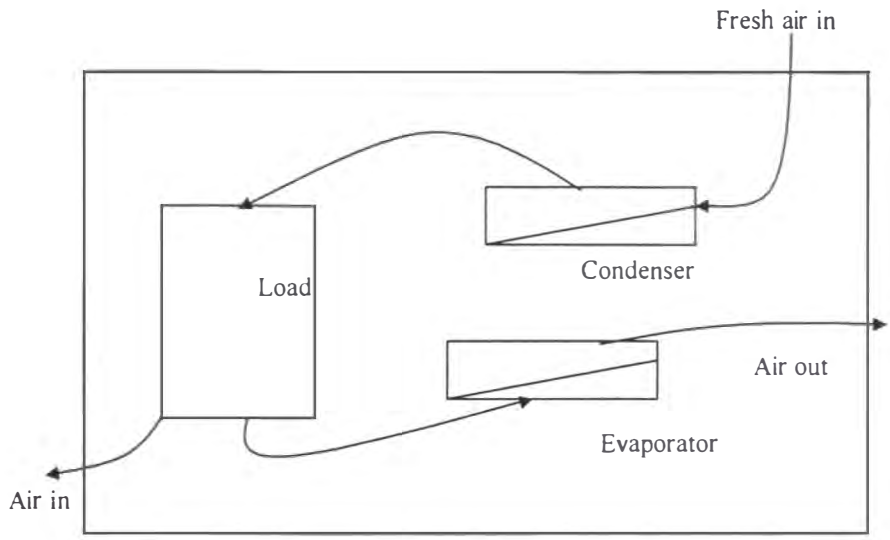

Figure 3-2 An open-cycle heat pump, in which the kiln air is ultimately exhausted to atmosphere and replaced by fresh air from the outside. This system is most suitable when the atmospheric temperature is already warm and the humidity low. It utilises the existing drying capacity of the atmosphere.

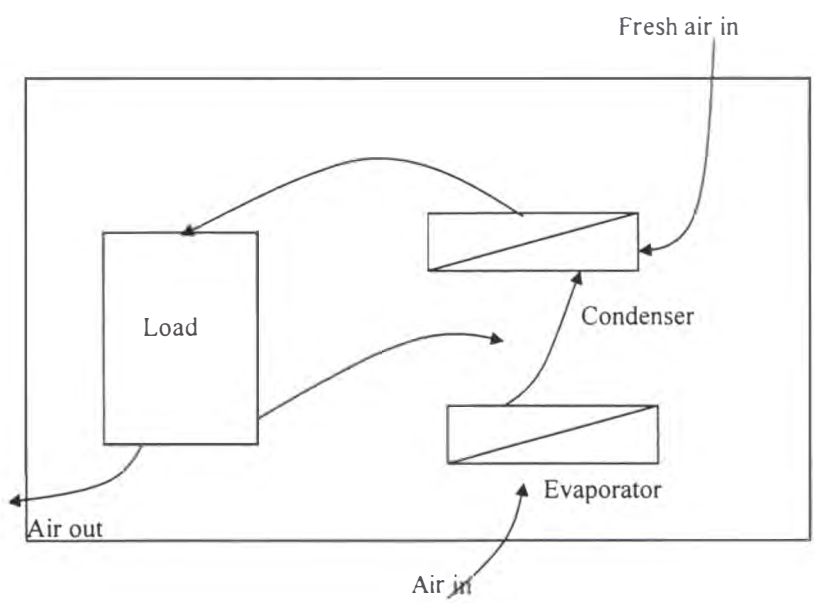

Figure 3-3 An open-system heat pump, in which the kiln air is ultimately exhausted to atmosphere and replaced by fresh air from the outside. This system is most suitable for low-temperature drying with low humidity air.

Dehumidifier dryers have to be designed to suit particular drying conditions:

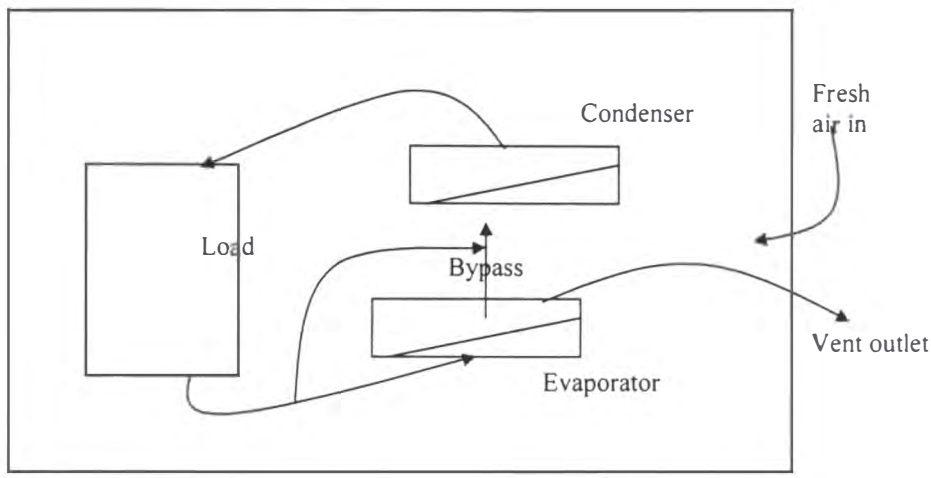

Figure 3-4 A dehumidifier system suitable for application when the kiln temperature is much higher than atmospheric temperature.

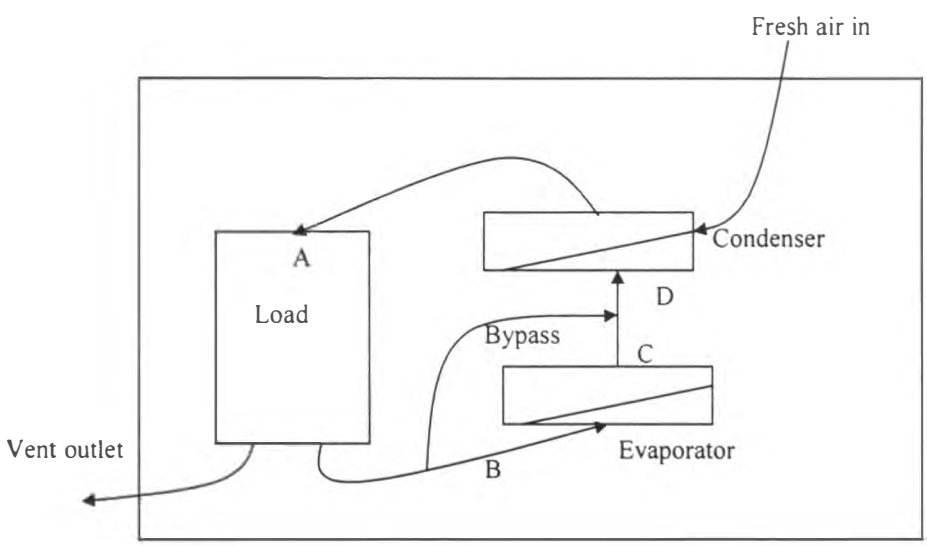

Figure 3-5 A dehumidifier system suitable for application when temperature is close to the atmospheric temperature

An enthalpy-humidity diagram of such a heat pump dehumidifier:

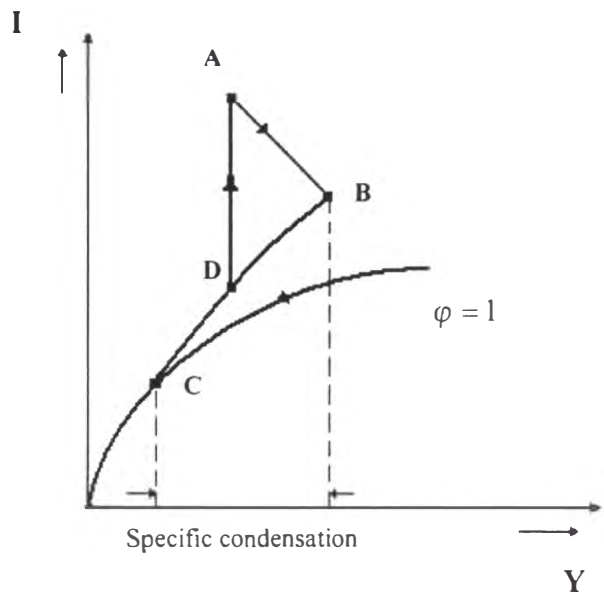

Figure 3-6 An enthalpy-humidity diagram of a heat pump dehumidifier shown in Fig 3-5.

The exhaust air leaving the product being dried (state B) is passed over the evaporator coil of the heat pump, where it is cooled to C. As a result of this cooling, some of the moisture contained in the exhaust air condenses out and is drained away. The recirculated air which has been cooled has to be raised in temperature to state A before re-contracting the product. This is done by passing the air over the condenser, where it picks up both latent and sensible heat recovered from the evaporator, and the heat associated with the work of compression. Air at condition C mixes with bypass air at condition B to yield the mixture at state D, which is then heated to state A.

Carrington *et al.* (1995) reported the results of performance tests examining the energy efficiency of a medium-temperature dehumidifier employing a passive economiser and staged liquid subcooling, using the refrigerant HFC134a. Figures 3-7 a ,b show that the data for specific moisture extraction rate and absolute moisture extraction rate. The former is a measure of the energy efficiency, the latter the drying rate.

The measured specific moisture extraction rate (Carrington *et al.* 1995) was 7.91 kg/ kwh, representing the performance of a specific dehumidifier, and excludes heat losses and fan energy. However, by combining a good design of dehumidifier with good drying schedules, the efficiency of the drying system as a whole certainly has the potential to be improved from the current level.

Even though the heat-pump dryers are, in theory, high-efficiency devices for drying, in practice their use is relatively uncommon. The reasons for this are: (1) there are no accepted norms for the performance of dehumidifiers; (2) the industry supplying the technology is fragmented; (3) the performance of existing dehumidifier products is uneven in terms of both reliability and efficiency; (4) current dehumidifier operating practices are normally on an *ad hoc* basis; (5) there is no consensus on the use of dehumidifiers relative to other drying methods; (6) they lack economies of scale being limited by the mechanical equipment available, eg. high-temperature drying of 120 m^3 loads which can be completed in 24 hours. Future effort is therefore needed to improve the potential of a dehumidifier wood-drying system. The requirements include improved drying schedules and improved designs of heat pumps to operate over a wider temperature range.

The records from Belfast Timber Kilns Ltd (unpublished) show that the six 50 m^3 kilns equipped with 2-3 closed-loop dehumidifying system have an average specific moisture extraction rate of 0.77- 0.83 kg/kWh when drying hardwood or softwood timber, as well as mixed species timber. According to the manager, this is competitive with the conventional drying kilns on the market. However, this competitiveness is based on no pre-treatments, no reconditioning, which means no extra handling costs.

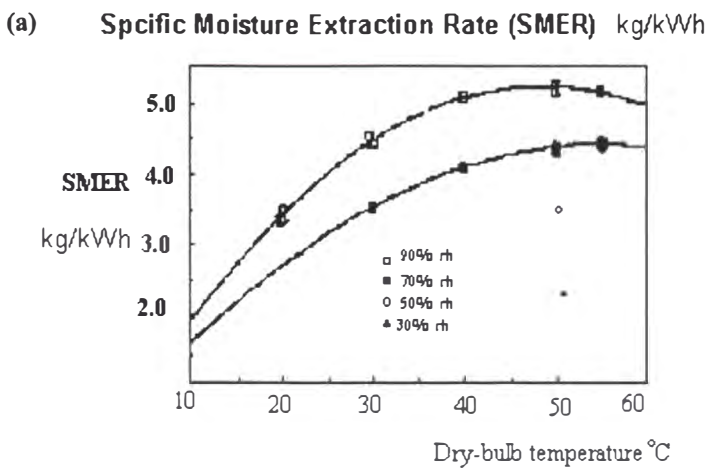

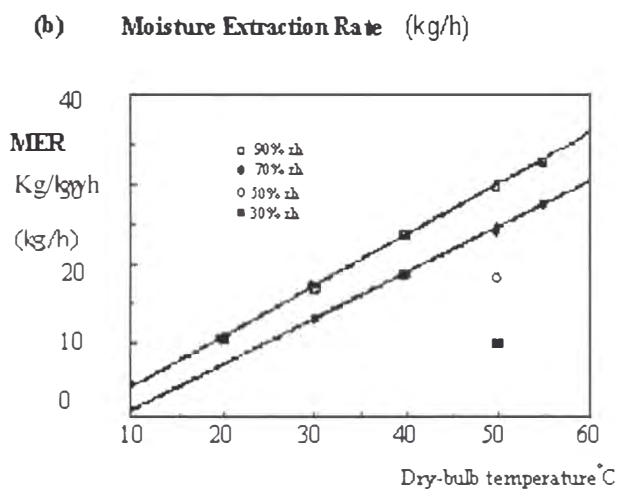

Figure 3-7a, b Performance of dehumidifying kilns drying *Pinus radiata* boards (Carrington *et al.* 1995)

§3.2 The Advantages and Limitations of Using Dehumidifying Kilns

Kininmonth and Haslett (1981) have analysed some of the advantages of using dehumidifying systems for timber drying. They state:

Dehumidifiers offer the best opportunity to install a self-contained, low-temperature dryer, and have superseded the oil-fired, recirculating dryer which is no longer economic because of greatly increased fuel costs. Under these circumstances, the major advantages of dehumidifiers are:

- For annual production of about 3500 m^3 or less, the capital cost is lower than conventional kilns and steam-raising plant. As production increases above this figure, the conventional kilns become progressively more favourable, because the capital cost of the steam-raising plant is spread over more kilns.

- Unit running costs of commercial dehumidification dryers do not change greatly with the size of the plant because the heat input is directly from mains electricity. Costs of \$6-8 (per m^3) have been obtained for a range of units (based on 1980 power cost in areas with special rates of 3-4 cents/kWh). These costs were low and were favoured by economy of scale. The current power rate is about 10 cents/kWh, the translated cost therefore is \$ 20-30 (per m^3).

- The dryer is easy to operate. The operator can enter the dryer to inspect the load and operating procedures and instrumentation are simple.

- They are extremely energy-efficient. It has been shown that about 65% of the energy used in a conventional kiln is for evaporation of moisture. In a dehumidifier, the latent heat of vaporisation is recovered because the evaporated moisture is condensed within the chamber. A study at Forest Research Institute (FRI unpublished report 1981) showed that drying of 50-mm untreated radiata pine in a dehumidifier consumes 700-800 MJ/m^3, against 1500 MJ/m^3 in a

conventional steam-heated kiln. The lower energy consumption compensates for the higher unit cost of the electrical energy used in the dehumidifier.

- Because of the slower drying rates, dehumidifier kilns can cope with mixtures of species and thickness better than a conventional kiln although it is preferable to avoid mixed charges.

- Maintenance costs are lower than in dryers operating at higher temperatures.

§3.3 Limitations of the process

Kininmounth and Haslett (1981) also described some of the limitations of the dehumidifier drying kilns:

- There is no provision for the relief of the drying stresses. This is a limiting factor only if thick timber is being ripped into thinner boards - the two halves will cup towards each other and the severity of this stress-related movement will increase if the dryer has rapid air flow and uses a schedule allowing for rapid reduction of relative humidity. Research at FRI has shown that stress in dehumidificational drying is general less than in conventional kilns. But in the latter there is a opportunity to remove stresses by conditioning.

- Drying times are much longer than in conventional kilns. The drying time for 50-mm untreated radiata pine is 5-7 days in a conventional kiln if the timber is green-off-the-saw; in a dehumidifying dryer the time is 21 days for the same moisture loss. Some owners have quoted much shorter times, 10-14 days, but these apply to material that has had preliminary air-drying. The drying time will be a function of a number of factors such as rate of air flow, the humidity cycle used, the operating temperature, and the initial moisture content, so the time cannot be predicted without this knowledge.

- The dehumidifying operating conditions are not enough to sterilise the wood. Australian quarantine regulations specify 74 ℃ for six hours for materials up to 50 mm thick.

In the conventional kiln drying of sawn timber, the following are the components of energy consumption (Kininmonth *et al.* 1980)

1. Heat is required to evaporate moisture from the timber, i.e., the latent heat of the vaporisation plus the energy need to remove bound water from wood substance.

2. Heat is lost from the kiln because of the venting or exhausting moist air at the kiln operating temperature and the inlet cold air requires heating to the operating temperature. Heat is also required to raise the evaporated moisture from the temperature of the board surface to the dry-bulb temperature of the kiln air.

3. Heat is required to bring the dry timber to the final dry-bulb temperature and to raise the moisture that is evaporated to the evaporation temperature.

4. Heat is required to raise the temperature of the kiln body to the final dry-bulb temperature.

5. There are heat loses by conduction, convection, and radiation from the kiln structure to the surroundings.

6. There are miscellaneous heat losses caused by leakage of air, over-venting, and incidents such as opening the kiln to inspect boards.

Since the thermal energy plays an important part of the timber-drying process, it is useful to assess heat efficiency as well as the total energy efficiency of the drying kiln.

Kininmonth (1980) defined the heat efficiency η_H and the total energy efficiency η as follows:

η_H = heat required to evaporate moisture/ total heat supplied to the kiln

η_T = energy required to evaporated moisture/total energy supplied to the kiln

Therefore, it is possible to calculate the various amounts of heat as categorised above for kiln drying of sawn timber by using a method similar to that devised by Shottafer and Shuler (1974).

However, the energy efficiency of a dehumidifying kiln can be expressed by the efficiency of a dehumidifier and that of an individual kiln

The efficiency and drying speed of a dehumidifier depends on temperature and humidity. There are two key rates that are used to describe the performance of a dehumidifier:

- Drying rate: the drying rate is a measure of the capacity of the dehumidifier, and is also known as the dehumidifier is Moisture Extraction Rate MER_d (kg_{H2O}/h).

- Energy efficiency: the best measure of the efficiency for a dehumidifier is the Specific Moisture Extraction Rate, or $SMER_d$ (kg_{H2O}/kWh). This is the amount of water removed from the dehumidifier per unit of electricity.

The energy efficiency of a kiln can be characterised by the kiln is Specific Moisture Extraction Rate $SMER_k$. New Zealand Energygroup Ltd. indicates that an typical dehumidifying kiln should expect $SMER_k$ to be in the range of 2-3 kg/kWh, while superior performance would be greater than 3 kg/kWh. $SMER_k$ also depends on the size of the kiln (Energygroup Ltd 1998).

Traditionally hard-to-dry species like Australian eucalypts and New Zealand beeches,

which have low moisture permeability and a tendency to deform, were recommended to be air-dried to about their fibre-saturation points before being kiln-dried to the required moisture content. This saves energy and expensive kiln space besides maintaining quality.

The advantage of air-drying also includes the use of relatively milder conditions than those of the conventional kiln. However, the air-dry method, which depends totally on the uncontrollable weather conditions, is not always reliable, The quality of the air-dried boards may vary greatly and the drying time could take 12 to 24 months (Carrington *et al.* 1999).

An alternative method is needed to dry these hard-to-dry timbers at a low temperature and an initially high relatively humidity and yet be energy-efficient.

A dehumidifying kiln has the right operating temperature range and the controllability of the drying conditions to replace the air-dry process and to gain better quality in a controlled fashion. The commercial feasibility of drying New Zealand beech timber from green conditions depends on the energy efficiency of the process

§3.4 Reference

Bannister P., Carrington, C. G., 1994 Dehumidifier drying technology: New opportunities. 4th IUFRO international wood drying conference Rotorua New Zealand.

Bannister, P., Carrington, C. G., 1995 Dehumidification using heat pump driers, Proceedings IPENZ conference pp. 327-332.

Carrington, C. G. Bannister, P., Bansal, B., Sun Z. F., 1995 Design of medium temperature dehumidifier systems, Report submitted to 19th IIR Congress.

Carrington, C. G., Bannister, P., Liu, Q., 1995 Performance analysis of dehumidifier using HFC134a, Int. J. Refrig. Vol. 18 No. 7 pp. 477-485.

Carrington, C. G., 1994 Electric heat pumps for product drying / a report prepared for The Electricity Corporation of New Zealand Otago University.

Carrington, C. G. Sun, Z. F., 1999 Dehumidifier dryers for hard-to-dry timbers, 19th IIR Congress Sydney Australia.

Clarke, N., 1996 Personal Communication, Belfast Timber Kilns Ltd.

Energy Group Limited, 1998 Guidelines for operating dehumidifier timber kilns, Dunedin New Zealand.

Section C

Experimental procedures and results

Chapter 4

Experimental methods and apparatus

§4.1 Experimental material and preparation

§4.1.1 Sample preparations

The beech timber boards used for the project were kindly supplied by Timberlands West Coast New Zealand Ltd from freshly cut logs in the Grey Valley. To avoid any unnecessary complexity, only red beech samples were used in the initial drying tests. The original size of each of the six boards was 110mm x 58mm x 1200mm. The boards were sprinkled with water, sealed in a plastic bag and stored in a cold room at 4 °C until needed.

To fit the drying facilities, the boards used in the large drying tunnel were cut into 110mm (longitudinal) x 13mm (radial) x160mm (tangential direction) samples, while those for the small drying chamber into 80mm x 13mm x 110mm samples. The samples were selected randomly, which means they may have come from different positions (height, type of orientation and so on) in a tree. Before use, all the samples were completely sealed with the paint Altex Devoe.

§4.1.2 Determination of the initial moisture contents

Samples were taken to measure the initial moisture contents, which later were used as a reference for controlling the drying schedules.

Before the formal drying experiment was carried out on the red beech samples, A one-inch thick hard beech board already collected by School of Forestry was used for testing the drying tunnel system. Although the hard beech samples had been stored since being freshly sawn, the moisture content of the sample boards, which were sawn to the size of 160 mm x 150 mm x 13 mm cut from that board, was only about 55% when they were used for the drying tests.

§4.1.3 *Hot water soaking of red beech samples*

Samples were put into a water bath at room temperature and the temperature of the water was raised at such a rate that the temperature of the water reached 83 °C within 1 hour. The samples were soaked at this temperature for 8 hours and afterwards the water and the samples were allowed to cool by itself. The samples were then stored in the cold room for later use.

§4.2 Experimental system

§4.2.1 *The large drying tunnel*

Initially a large drying tunnel was available and so was used for this work.

The large drying tunnel can be either automatically or manually controlled with the view to providing constant environmental conditions. The main features of the drying tunnel arrangement are:

- A centrifugal fan and air bypass system giving tunnel air velocities ranging between 1.5 to 3.0 ms^{-1} in the test section.

- An LX5600 solid state temperature sensor connected to an automatic controller. The controller uses proportional integral action to maintain the tunnel temperature around a set point ± 0.5 °C. The heat is supplied through four 2 kW electric heaters.

- A humidifying column which consists of a reservoir of water which is pumped to the top of the unit where it is dispersed by a perforated plate and allowed to fall back to the reservoir. Air comes in contact with the water counter-currently before the air enters the heating section of the tunnel at 100% relative humidity.

- A 6 kW AC power controller delivers from 0-6 kW of heat from a scale of settings 0 to 99. The device offers both automatic and manual control. Automatic control is achieved by a sensor connected to a series parallel interface (SPI), which sends

the signal to the computer. There a control program calculates the desired heat output level. This level is the output of the power controller.

- An LM355 amplifier which amplifies the three sensor readings: wet-bulb temperature, air temperature in the inlet and tunnel air temperature.

- A steam line carrying steam at 2 bar indirectly transfers heat to the humidifier for humidifier temperature above 30 °C. The temperature of the saturated air leaving the humidifier is in effect the wet-bulb temperature, T_w, in the test section; hence steam is often required where a high T_w is specified.

- A flow straightening section of three meshes and honeycomb made from straws (5 mm diameter) to ensure an even flow distribution around the balance.

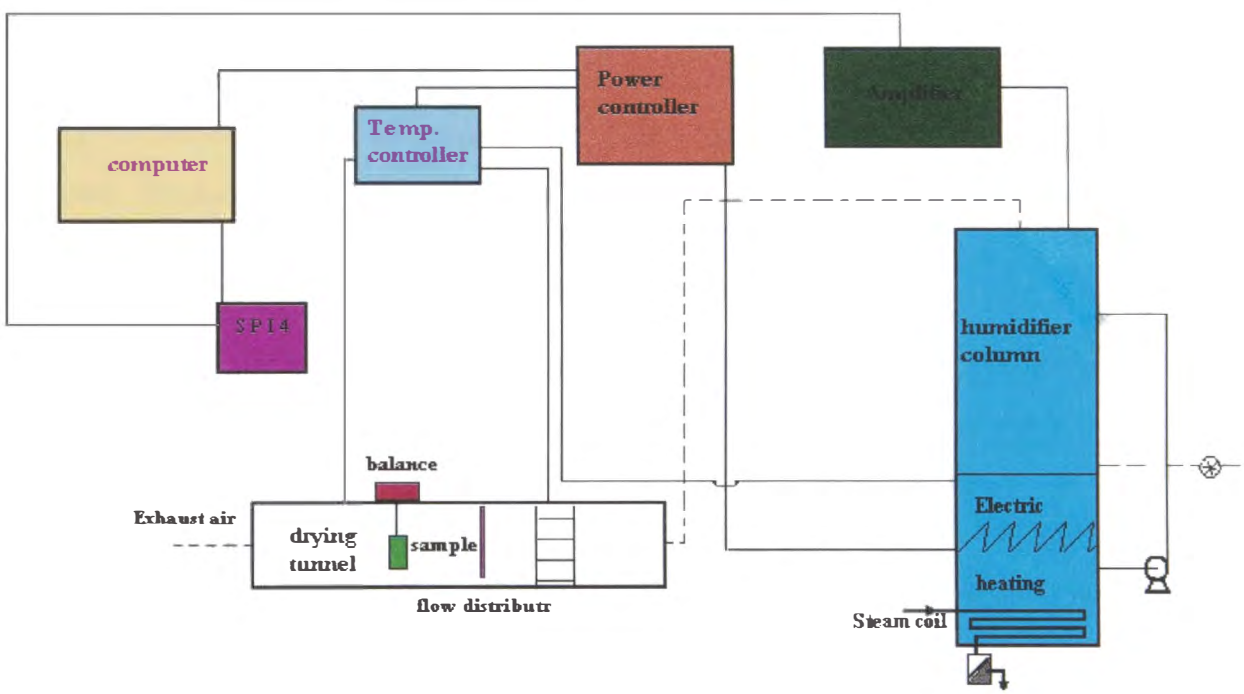

Fig 4-1 Large drying tunnel

- A Mettler PE360 electronic balance with a precision of ± 0.0001g for weighing the drying samples.

- A monitoring computer terminal. During tunnel operation, the terminal updates the dry and wet-bulb temperatures, running time of the experiment as well as the mass at a time determined by the operator.

§4.2.2 The small drying chamber

§4.2.2.1 The hardware

This apparatus was designed to simulate two different drying techniques, low temperature kiln drying and vacuum drying. It is also possible to simulate an oxygen-free atmosphere. The use of an oxygen-free atmosphere enables one to test theories regarding the oxidation of extractives from the timber during drying.

The system allows the following conditions: Air velocities of 1-3 ms^{-1} across the surface of the wood, wet-bulb temperatures of 60 °C and dry-bulb temperature of 70 °C max. The packed humidifying column was designed to produce saturated air up to 60 °C at an air flow rate of 40 litres per second.

The kiln section was designed to withstand external pressure, The design of the drying chamber jacket allows it to stop condensation of water vapour from the air inside the unit. The mass of the sample is measured by a loadcell which is placed on the top of the drying chamber. The drying chamber can be isolated by closing two ball valves located on the inlet and outlet pipework. The chamber materials are corrosion and temperature-resistant.

Vacuum or steam operation is available and is controlled manually. Low-temperature kiln conditions can be controlled automatically. However the air flow is controlled manually by changing the position of the inlet gate valve. The heat elements are controlled by on/off Omron controllers using a K-type thermocouple as the sensor element. The wet-bulb and the dry-bulb temperatures and the mass from the loadcell are logged to the computer. The wet-bulb and dry-bulb temperatures are measured using platinum-resistance thermometers (PRT), one located at the packed column outlet and the other inside the kiln section.

Cooling system: This project requires drying New Zealand red and hard beech timber from very low temperatures. The initial starting dry-bulb temperature is about 20 °C. However, during summer time, the temperature of the dry air supplied by the compressor and blower in the basement of the SRS building, exceeds this value. In order to ensure all year around operation, a bi-cooling system has been installed and could be controlled by the computer once the set point of the temperature is entered in to the computer.

§4.2.2.2 The software

The software used in the system-monitoring computer is the Advantech Genie. This data-acquisition and control software is used to log the wet-bulb and the dry-bulb temperatures recorded from the PRTs. It is also used to log the sample mass. The Genie software provides an icon-based, mouse-driven system for designing real automation and control strategies.

Two different types of operating strategies were written for this project. The first strategy converts the wet-bulb temperature depression into a relative humidity, which will also be displayed on the screen. The overview of this strategy, given in Genie software editor, is shown in the following diagram:

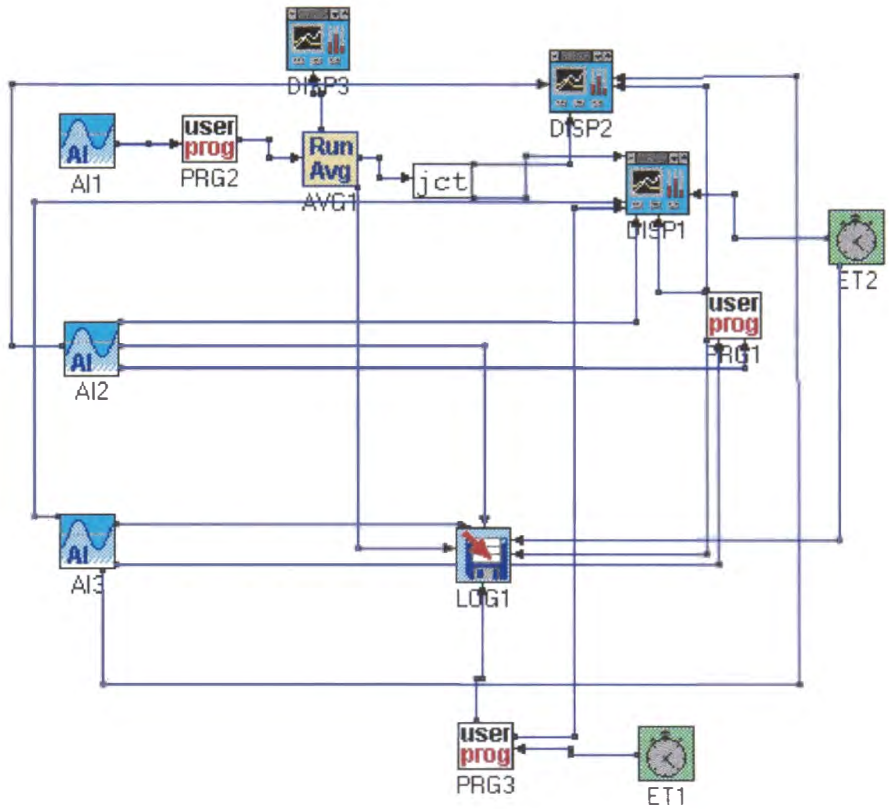

Figure 4.2 Strategy 1 for schedule development

The second strategy was developed for later stages of the research when a continuous drying schedule was needed for drying New Zealand red and hard beech timbers. These requires ramping up the temperature according to the status of the moisture content of the dried sample so that the drying conditions are changed as the moisture content is declining. This modification of the strategy required some hardware changes, which included replacing two temperature controllers and rearrangement of the related connections. The modified strategy is shown below:

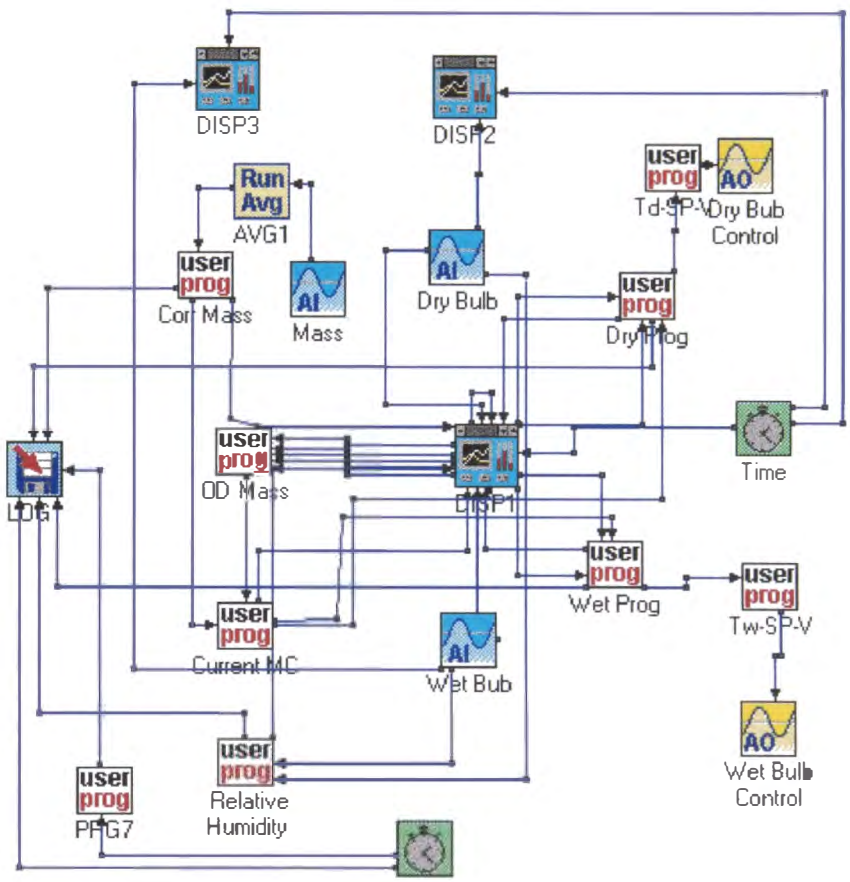

Figure 4.3 Strategy for schedule development in the modified drying system

§4.2.3 Mechanical test climate chamber

§4.2.3.1 Structure of the climate chamber

The original climate chamber was designed by Keep (1998), for her research project. The climate chamber consists of four main parts.

The first part is the climate chamber itself, which is a sealed cylindrical vessel containing moist air at a constant temperature and humidity. The cylinder has a height of 600 mm and a diameter of 450 mm. There is an inlet into the vessel that

allows humidified hot air into the chamber and an outlet that vents the exhaust air. Located outside the vessel is a balance to measure the weight of the moisture content control sample (III). The balance is a Sartorius BP110 with a maximum load of 110 grams and a sensitivity of 0.001gram. In the chamber, there is an attachment for the free shrinkage sample (II) and a frame for the sample (I) under tensile load. Sample I is kept under tensile load using hydraulic ram which is set at 550 kPa. The cylinder is trace-heated with silicon rubber-coated heating cable to maintain a constant elevated wall temperature to prevent condensation occurring.

The second part of the apparatus is the humidification column. The packed column is 100 mm in diameter and 1 metre high. Plastic mini-rings 15 mm diameter are used to fill the column. The airflow has a maximum rate of 5 L/min; and a minimum rate of 4 L/min. Water flows down the packed column, heating and humidifying the air that flows upwards. The outlet air leaves essentially at the adiabatic saturation temperature corresponding to the inlet water temperature.

The humidifying column cannot attain high relative humidity at high temperatures. There is a limit of around 80 °C for the wet-bulb temperature. To attain a full range of conditions, an alternative steam generator was designed. This part of the apparatus is basically a climbing-film evaporator. It is made up of an outside cylinder shell (diameter of 5 cm) that contains 48 tubes (diameter of 6.25 mm). The tubes are 22.86 cm long; this produces a heat transfer area of 0.23 m^2.

Air from the column then flows through the fourth part of the apparatus which is the air heating element, which raises the temperature of the humidified air to the desired dry-bulb temperature before entering the chamber. This heating unit consists of two elements from two paint stripper guns which are suitable for temperatures up to 140 °C. The output of the heating elements is monitored by a Shimaden controller. It senses the temperature being recorded downstream by the platinum resistance thermometer (PRT) and adjusts the output according to the set-point temperature value that has been entered into the controller. The humidity is measured using a temperature-compensated humidity transmitter, HY-CAL Engineering model CT-880-C. The sensor measures the temperature as well as the humidity and the humidity

output is automatically corrected for temperature over the full range of relative humidities (0-100%), and operating temperatures (-20-185 °C). Using this apparatus, the temperature variation is limited to ± 3 °C, and the relative humidity is able to be controlled to within a range of ± 3%.

§4.2.3.2 The modification of the climate chamber

The apparatus, as built by Keep (1998), was modified to improve the resolution of the data recording.

- The electronic cables were re-configurated to reduce the electronic interference, with less noise on the recorded load/strain curve data as a result.

- The direct current power for the four linear-position sensors has been increased from 1.5 Volts to 5 Volts. This increased the analog output of the strain by more than 3 times the original arrangement. It has significantly increased the accuracy of the strain, which is relatively small in value, only about 2 mm at the most. The resolution of the stress/strain curve as a result has improved to ± 0.001mm.

§4.2.3.3 Stress measurement

A tension/compression load cell was used to measure the force directly. It was placed between the hydraulic ram and wire that connected to the clamp. The output of the load cell was amplified and was measured using a digital voltmeter and recorded on a chart recorder. All the data in this experiment were logged on a personal computer using PC-LabDAS software which is an integrated, general-purpose software package for data acquisition, process control and data analysis.

§4.2.3.4 Strain measurement

A linear-position sensor (LPS) able to withstand temperatures up to 130 °C was used to measure the tensile strain. The LPS units were modified for this experiment to

increase the DC supplier from 1.5 to 5V so that the resolution of the output of the LPS increased twofold. An LPS was attached to each side of the sample to eliminate a possible bending effect by taking the average strain value. The LPS sat in a metal brace that was glued to the sample surface using Locktite 401 glue.

Chapter 5

Drying of New Zealand red and hard beech timber

§5.1 Introduction

The aim of this work is to achieve the first object of the project, ie. to establish a drying schedule that would allow the drying of New Zealand hard and red beech timber from the green condition without undue degrade.

Two types of drying schedules were used in the drying tests undertaken in two different drying facilities. The initial results show that, even though slight warping occurred under the very mild drying conditions used, these schedules might be suitable. There is evidence to show that warping is caused by the differences in the shrinkage rates in the tangential, radial and longitudinal directions in the samples.

§5.2 Drying Trials

Two types of drying schedules were adopted: a moisture-content control schedule and a fibre-saturation-point control schedule.

The moisture-content control schedule is a drying method in which the drying conditions (dry-bulb temperature and temperature depression) are changed at certain moisture contents. In practice, the sample weights, which were used to calculate the moisture contents of the sample while being dried, were used to determine the changeover points.

The moisture-content control schedule used in the trial is given in Table 5-1, and is designed to maintain a relatively uniform drying rate throughout the schedule. The moisture content steps are arbitrary and are based on those for red oak (*Quercus rubra L.*) (Rice and Gatchell 1983).

Table 5-1 Moisture-content (MC) control schedule

MC steps %	Kiln temperatures °C Dry-bulb	Depression	Wet-bulb	%RH	Equilibrium MC%
Green to 80	27	3	24	78	15.3
80 to 66	30	5	25	67	12.1
66 to 57	30	7	23	55	9.7
57 to 45	30	8	22	50	8.8
45 to 40	32	9	23	46	8.2
40 to 32	32	11	21	36	6.7
32 to 27	38	13	25	34	6.2
27 to 23	46	16	30	31	5.6
23 to 20	46	18	28	25	4.8

Trial 1:

Before this trial, hard beech samples of unknown origin were used in a few test runs with the drying tunnel, to gain experience in temperature-stability control, weighing /loading calibration, and computer-file transforming (MBF Basic to IBM format). This trial aimed to investigate how red beech timber behaves under a conservative drying schedule. Red beech and hot water-soaked red beech samples were dried under this moisture-content control schedule.

Trial 2

While moisture-content control was used in the large drying tunnel, while FSP-control drying was used in the small drying chamber, because the drying tunnel has a feed-

back computer-control system to adjust the changes of the temperatures when necessary. In the small chamber the temperatures are manually controlled, and it takes a period of time to stabilise them.

The FSP control schedule is a drying schedule in which one or two fixed dry-bulb and wet-bulb temperature combination(s) is/are used to dry the sample to (near) the sample fibre-saturation point (25% to 30% for red and hard beech), and then the sample is dried under a changing drying schedule to the final moisture content.

The FSP control schedule used is given in Table 5-2

Table 5-2 FSP control schedule

	Kiln temperatures (°C)				
MC steps(%)	Dry-bulb	Depression	Wet-bulb	RH %	Equilibrium MC %
Green to FSP	27	3	24	78	15.3
	30	7	23	55	9.3
30 to 23	45	15	30	31	5.6
23 to 20	45	17	28	5	4.8

§5.3 Trial results

Neither surface nor internal checks were found in any of the dried samples. Further analysis of the dried samples included measuring the profile of the shape of the dried samples and the finger-prong tests. These failed to show that any possible plastic stress causing collapse or other defects which might be related to the possible severeness of the drying schedules.

The moisture profiles were obtained by slicing the dried boards using a band saw. Sawdust was also collected to measure the moisture contents. The slices and the sawdust were dried in an oven at 103 ± 2 °C for at least 48 hours or until there was no more weight loss of the dried samples.

A finger-prong test was designed to measure and visually observe the deformation of the dried boards caused by the drying-induced stresses, the shrinkage or other deformation-created stresses within the dried boards. Cutting the boards in the fashion shown in Figure 5.1 allow the local stresses to reveal both their magnitudes and directions. For instance, straight fingers show the existence of neither compressive stress nor tensile stress (A), while fingers bending towards the core of the board show tensile stress (B) and fingers bending outwards reveal compressive stress (C) in the centre of the board.

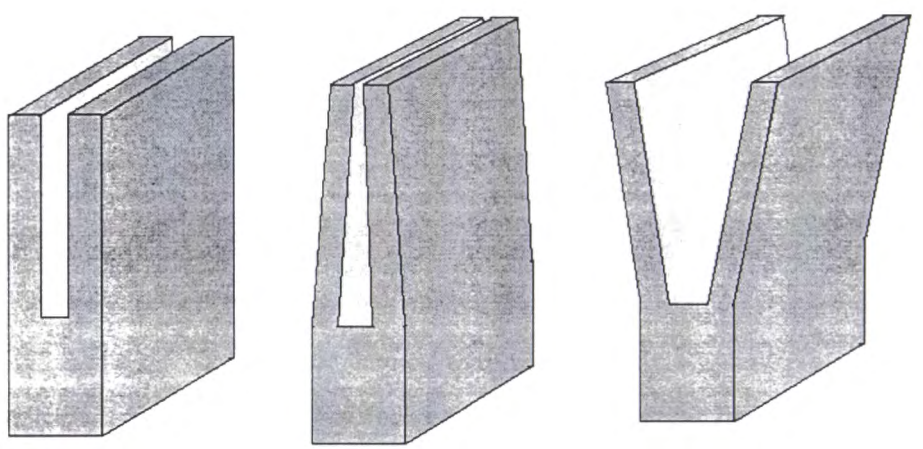

A: No stress.

B: Surface in compression; Core in tension.

C: Core in compression; Surface in tension.

Fig 5-1 Finger-prong test

Figs. 5-2 and 5-3 represent the these drying tests using the MC control schedule and a comparison of the drying of a hot-water-soaked red beech sample with a control sample. The latter results were consistent between those obtained under the same drying conditions.

Fig 5-2 shows the progress of drying unsoaked red beech timber. The length of time to dry the sample to the fibre-saturation point (30%) is about 70 hours, while it takes 330 hours to dry the sample close to the equilibrium moisture content under the final drying temperatures with moisture-content control schedule.

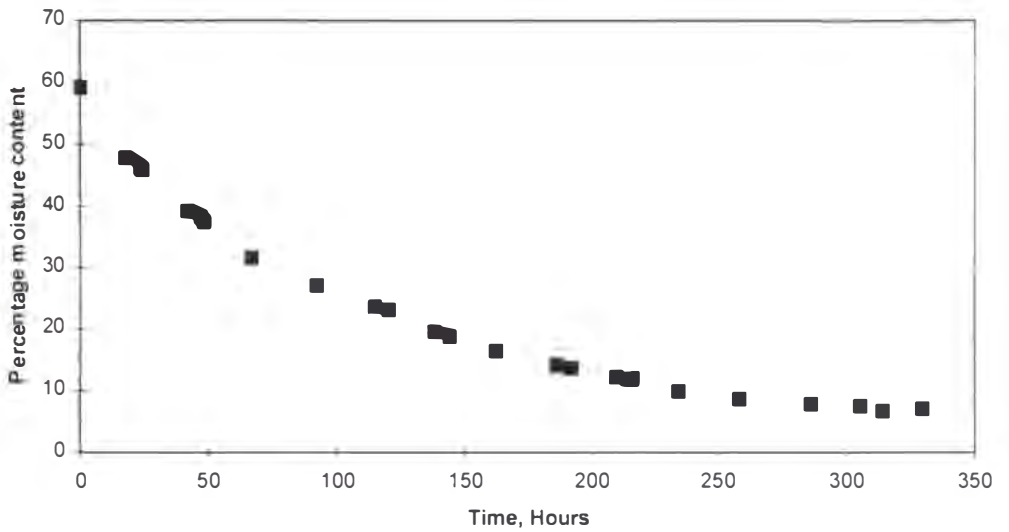

Figure 5-2 Moisture-loss curve for red beech timber dried with moisture-content control schedule

Part of the sample after drying was used to determine the final moisture content. Visual examination for surface checking and other defects was also done. The samples dried by the moisture-content control (MMC) schedule were found to have no defects, only displaying a slight warping. The deformation was determined by measuring and calculating the extent of curvature in the finger prong test. Of those tested, the curving movement was found to be less than 1% of the finger height. The growth rings were not entirely parallel to the sample drying surface, and this warping may be due to differences in directional shrinkage.

Figure 5-3 shows the progress of drying hot-water-soaked red beech timber under the same drying conditions. The length of time to dry the sample to the fibre-saturation point (30%) is only about 38 hours, while it only takes 220 hours to dry the sample close to the equilibrium moisture content under the final drying temperatures.

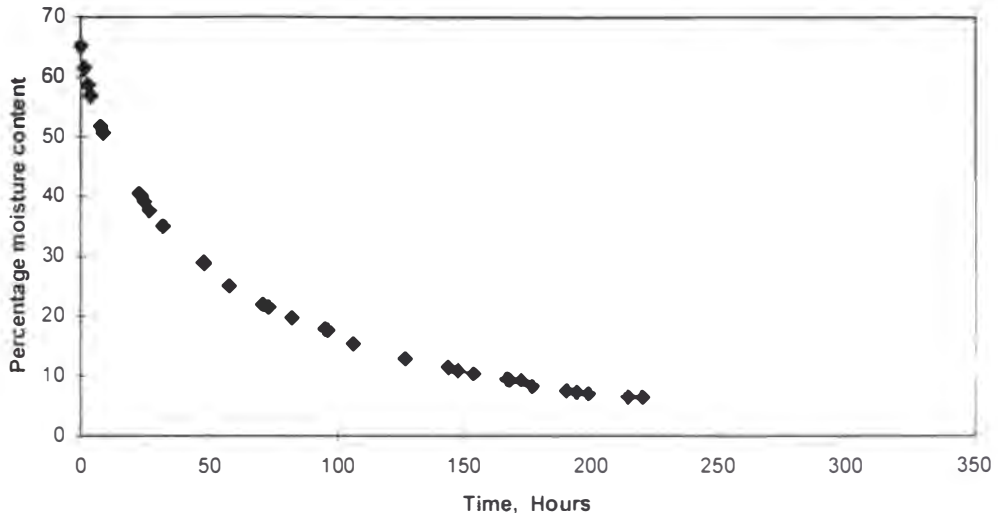

Figure 5-3 Moisture loss for hot water-soaked red beech timber dried with moisture-content control schedule

The final moisture content was also measured. Again, no defect was observed, just slight warp was found in the sample. However, the colour of the sample deepened as a result of the hot-water soaking.

The FSP-control schedule of the unsoaked red beech timber took up to 336-384 hours and the final moisture content was about 7%, Similar drying behaviour and very similar results for the quality of the final product of the drying were found in the small chamber as those in the large drying tunnel. and analysis was done on the samples dried by the small drying chamber to determine the causes of the slight warping.

There was no surface checking in the samples dried, no internal checks were found either from slicing the sample boards, but shrinkage was found in the transverse directions.

Thin boards and sawdust from the cuts were collected to measure the moisture contents of different slices from the sample's drying surfaces to the core of the dried board.

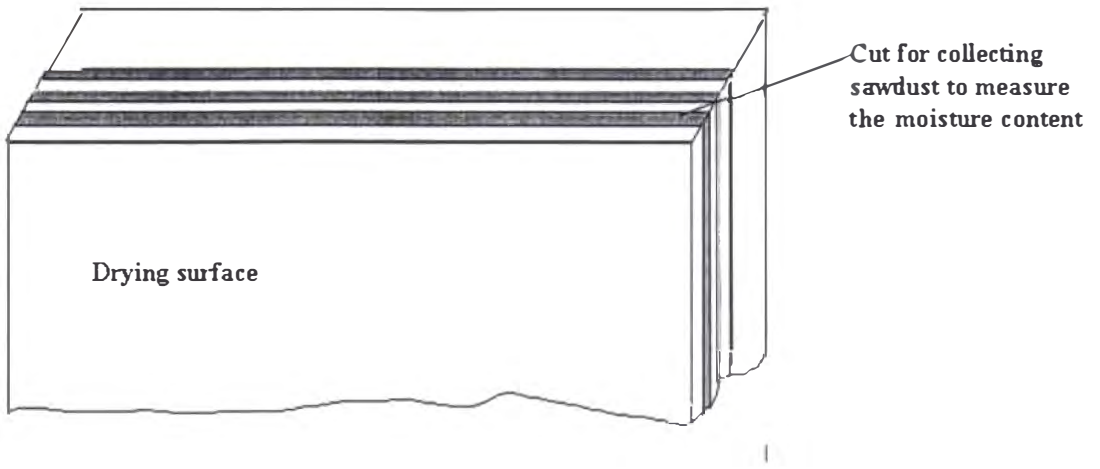

Figure 5-4 The method of measuring the moisture profile

The shape of the moisture profile being rather flat was unlike that from previous work (Grace 1996) in which thicker hard beech timber (50mm) samples were used and a "bell-shaped" moisture profile was found. Fig 5-5 illustrates a moisture profile of the dried sample from the small drying chamber by using the FSP-control schedule.

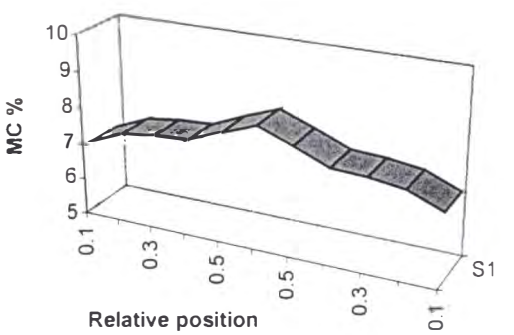

Figure 5-5 Moisture profile of dried sample in small drying chamber

The sample was cut as shown in Fig 5-4 to measure the moisture -content profile. The average shrinkages in radial tangential and longitudinal directions were measured by measuring the change of length two fixed points in each of the three directions. The average shrinkage of the sample which had the moisture content profile given in Fig 5-5 is as follows:

Tangential shrinkage:	6.65%
Radial shrinkage:	7.76%
Longitudinal shrinkage:	negligible

A test sample was sawn from a given dried samples, as shown in Fig 5-1. Any distortion of the prongs will show if there are residual drying stresses.

The actual result of the prong test showed that there were no visually obvious signs of degradation (case-hardening).

§5.4 Characteristic drying curves for red beech

Characteristic drying curves have been produced form the drying trials of the red beech boards as well as the simulation in the optimisation program. The experimental results were later used by Sun *et al.* (1998,1999) to evaluate the energy efficiency of the drying schedules presented in this thesis.

§5.4.1 Characteristic drying curve

Van Meel (1958) has suggested that a single characteristic drying curve can be drawn for a material being dried. At each volume-averaged, free moisture content, it is assumed that there is a corresponding specific drying rate to the unhindered rate in the first drying period that is independent of the external drying conditions. A characteristic drying curve theory was proposed by Keey and Suzuki (1974) based on the drying of a porous, non-hygroscopic slab of infinite extent, which was later extended to the drying of spherical particles (Keey, 1992).

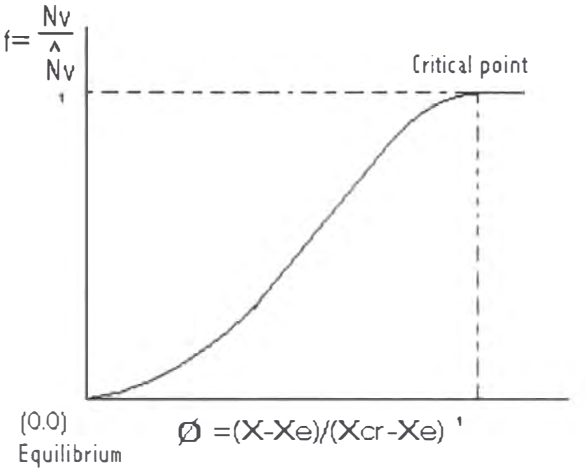

Fig 5-6 Characteristic drying curve. After Keey (1992)

The relative drying rate is defined as:

$$f = \frac{N_v}{\hat{N}_v} \tag{5-1}$$

where N_v is the rate in the first drying period, and the characteristic moisture content becomes:

$$\Phi = \frac{\overline{X} - X_E}{X_{cr} - X_E} \tag{5-2}$$

where $\overline{X}$ is the volume-averaged moisture content, X_{cr} is the moisture content at the critical point, and X_E that at equilibrium. Thus the drying curve is normalised to pass through the point (1,1) at the critical point of transition in drying behaviour and the point (0,0) at equilibrium.

§5.4.1 .1 The characteristic drying curves of timbers

The characteristic drying curves for timber, both hardwoods and softwoods, can reflect the difference in which drying rate changes with respect to the change of the moisture contents. Keey and Walker (1988) illustrated the difference of the characteristic drying curves between *Pinus radiata* and *Nothofagus truncata*, reflecting the difference in permeability of the two species.

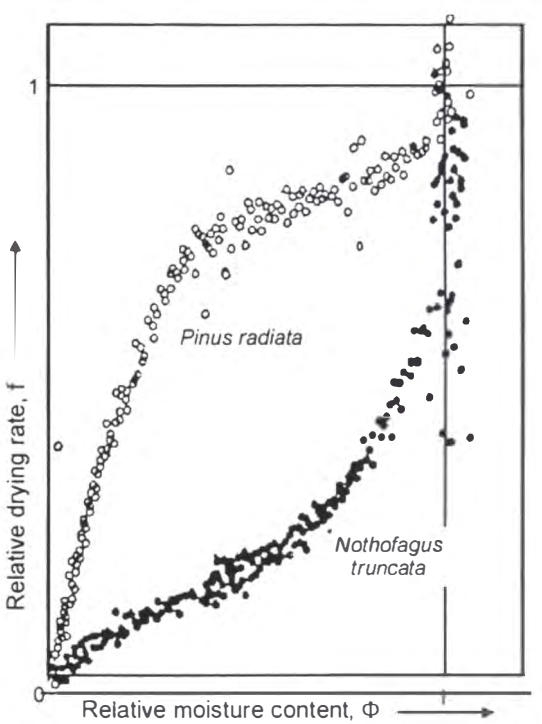

Fig. 5-7 Characteristic drying curves *for Nothofagus truncata* and *Pinus radiata* (sapwood)

The drying curve for the pine sapwood shows the characteristic profile for drying dominated by capillary-driven flows, with an initial fall at high moisture contents, and a subsequent period when the rates slowly dwindle while liquid continuity is maintained: whereas the curve of the hardwood is a typical of a process controlled by diffusional mechanism with progressive increase in resistivity.

§5.4.2 Normalised drying curves observed from drying of Nothofagus fusca

A normalised drying curve was obtained from the drying tests with small samples of New Zealand red beech in the small drying tunnel. Red beech samples were sawn and cut from the green boards. The samples used in the test were 110mm (longitudinal) x 13mm (radial) x160mm (tangential direction). The samples' ends were sealed with Altex Devoe paint. The samples were than dried with a stepwise drying schedule, which was described in section §5.2. Trials also included the drying of hot water-soaked samples and the control ones without pre-treatment.

The normalised drying curves are calculated from Fig 5-2 and Fig 5-3. The initial averaged moisture contents were used as the moisture contents at the critical point when evaluating the characteristic moisture content (Equation 5-2).

In normalising the drying curves, consideration was given to the change of the drying mechanism – the relative humidity change due to the change of drying conditions, and the consideration can be expressed in the following way:

The relative drying rate g in the apparent characteristic drying curve can be evaluated as the ratio of the humidity driving force (Y_S-Y_G) to the initial value $(Y_{W0}-Y_{G0})$:

$$g = \frac{(Y_s - Y_G)}{(Y_{W0} - Y_{G0})} \qquad (5\text{-}3)$$

While the fundamental characteristic drying curve, the change of the drying mechanism yields the relative drying rate f:

$$f = \frac{(Y_S - Y_G)}{(Y_W - Y_G)} \qquad (5\text{-}4)$$

Where (Y_W-Y_G) is the unhindered driving force at a particular time in the drying process. It can be rewritten as

$$f = \frac{(Y_S - Y_G)}{(Y_W - Y_G)} * \frac{(Y_{W0} - Y_{G0})}{(Y_{W0} - Y_{G0})} = \frac{(Y_S - Y_G)}{(Y_{W0} - Y_{G0})} * \frac{(Y_{W0} - Y_{G0})}{(Y_W - Y_G)} \tag{5-5}$$

$$= g.\frac{(Y_{W0} - Y_{W0})}{(Y_W - Y_G)} \tag{5-6}$$

In the limit when bulk humidities are small,

$$Y_{G0} \cong Y_G \to 0 \tag{5-7}$$

then

$$f = g.\frac{Y_{W0}}{Y_W} \tag{5-8}$$

The following diagrams are normalised drying curves for untreated and hot-water soaked red beech timbers on the basis of equation (5-8):

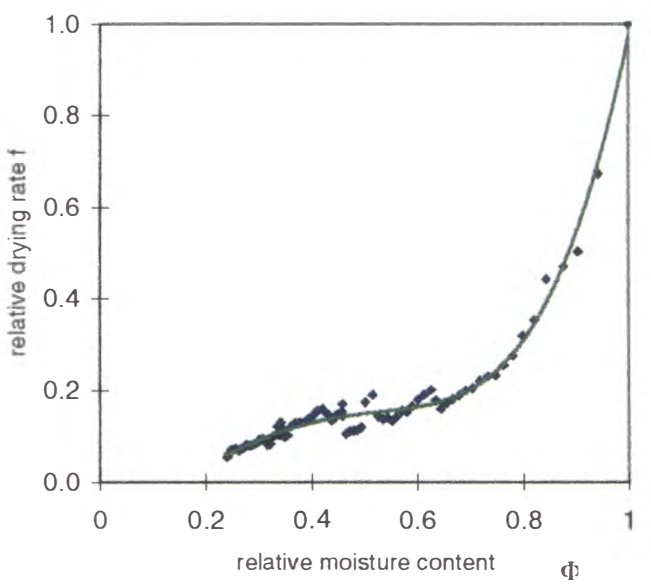

Fig.5-8 Normalised drying curve of untreated New Zealand red beech

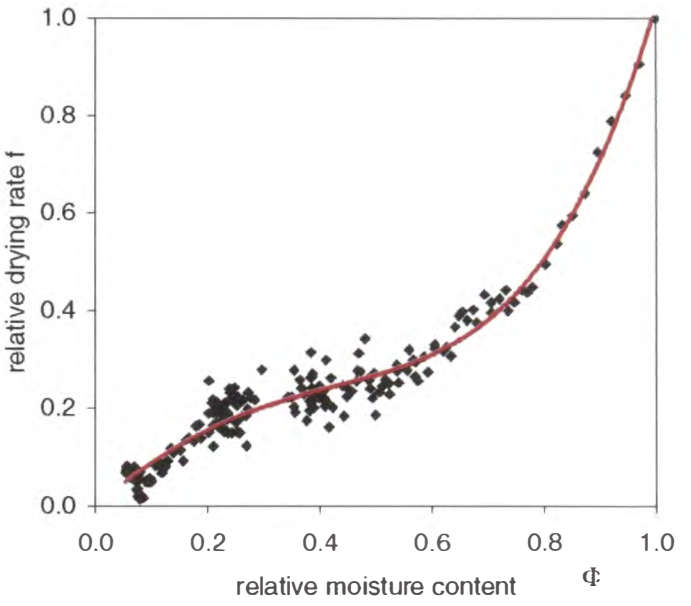

Fig. 5-9 Normalised drying curve of hot water-soaked New Zealand red beech

The comparison of the normalised drying curves shows that the hot-water soaking treatment enhances the relative drying rate at certain point of relative moisture content.

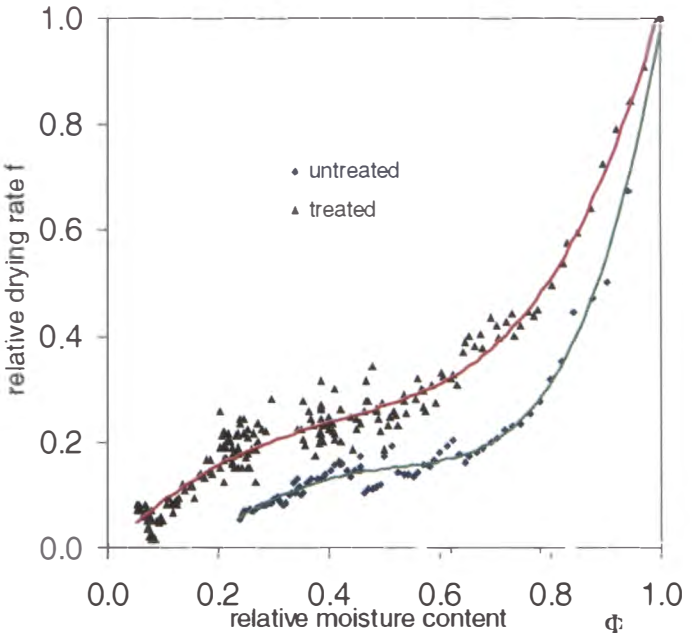

Fig. 5-10 Comparison of normalised drying curves of untreated and hot water-soaked New Zealand red beech timber

§5.5 Reference

Grace, C., 1996 Drying characteristics of *Nothofagus truncata* heartwood, University of Canterbury M.E. thesis.

Keey, R. B., Suzuki, M., 1974 On the characteristic curve, Int. J. Heat Mass Transfer **17** pp 1455-1464.

Keey, R. B., 1994 Heat and mass transfer in kiln drying: a review, 4th IUFRO International wood drying conference, Rotarua, New Zealand.

Keey, R. B., Langrish, T. A. G., Walker, J. C. F., 2000 Kiln-drying of lumber, Springer-Verlag, Berlin , pp315.

Kumar, M., 1991 Investigation into the behaviour of red beech during intermittent drying, University of Canterbury B.E. thesis.

Milota, M., R., Wengert, E., M., 1995 Applied drying technology, 1988 to 1993, Forest Product Journal, Vol **45,** pp. 33-41.

Ministry of Forestry, 1996 Producing quality kiln-dried timber in New Zealand Wellington.

NZFS. 1974. Timber properties and uses of the New Zealand beeches. New Zealand Forest Service, Wellington.

Pang, S. 1994 High-temperature drying of *Pinus radiata* in a batch kiln Ph.D thesis University of Canterbury New Zealand.

Quarles, S. L., Wengert E. M., 1989 Applied drying technology, 1978-1988, Forest Prod. J. **39** (6) 25-38.

Rice, W. W., Gatchell, C. J., 1983 Kiln drying procedures for system 6 northern red oak, Proceedings 34th annual meeting western drying kiln clubs, pp. 79-88. Madison, Wis. USA.

Ross, D.A., 1986. Investigating the moisture movement of Hard Beech during drying. Bachelor of Engineering Report, Department of Chemical and Process Engineering, University of Canterbury.

Shang, D., Rasmuson, A., Zhang, X-D., 1995 Design of solar-dehumidification wood drying kiln characterised by high capacity and temperature, Drying technology, **13**(5-7), pp. 1431-1445.

Siau, J.F., 1984. Transport processes in wood. Springer-Verlag, Berlin.

Simpson, W. T., Verrill, S. P., 1997 Estimating kiln schedules for tropical and temperate hardwoods using specific gravity, Forest Prod. J. **47**(7/8) pp.64-68.

Skaar, C., 1988. Wood water relations. Springer-Verlag, Berlin.

Stamm, A.J., 1964. Wood and cellulose science. The Ronald Press Company, New York.

Walker, J. C. F., 1993 The Primary Wood Processing, Chapman & Hall London, 247-284.

Ward, C. J., Simpson, W. T., 1987 Comparison of four methods for drying bacterially infected normal thick red oak, Forest Prod. J. **37** (11/12) 15-22.

Chapter 6

Mechanical properties and drying behaviour of red beech timbers in the transverse direction

§6.1 Introduction

As noted previously, New Zealand beeches, red beech *(Nothofagus fusca)* and hard beech *(Nothofagus truncata)* in particular, are among the most temperature-sensitive hardwoods. They frequently contain tension wood and conventional kiln drying causes collapse, which cannot be removed by reconditioning. Therefore the drying processes of these timbers usually require comparatively long periods under mild conditions and, consequently, these drying processes are very energy-consuming because of potential thermal losses over an extensive drying schedule.

Understanding the stress-strain relationships in the direction perpendicular to the grain is essential to optimise a drying schedule which would not only minimise the degrading of the drying products, but would also be energy efficient.

The transverse tensile strength and its load-deformation relationship have been studied through tests with small specimens of red beech *(Nothofagus fusca)*. This is very important information for the drying process of New Zealand beech timbers. not only because it is scarcely available at the moment but also the close look at the load-deformation relationship could provide crucial information for the simulation of the drying of these degrade-prone hardwood species from their fresh conditions.

§6.2 Material and experimental preparation

§6.2.1 Specimens:

Samples used in the experiment were cut from three boards sized 1.2m x 150mm x 50 mm, which came from one of the logging sites of Timberlands West Coast Ltd. The wood was wrapped with a plastic film and bagged to minimise moisture loss from evaporation and stored in its fresh condition in a cold room at 4 °C.

Samples for mechanical tests were cut from selected timber boards which were re-sawn to give samples sized 150 x 50 x 5mm. They were either kept in fresh conditions or air-dried to various moisture contents. Later they were reconditioned to their equilibrium moisture content by sealing in a plastic bag at ambient temperature for sufficient time for the release of most of the drying stress, in other words, with no visible warping. The boards were planed to a thickness of 5 mm before small samples were cut from them such that the tensile stress could be applied in the direction perpendicular to the grain (Figure 6-1). The samples then were loaded in a climate chamber, where temperature and relative humidity were well-controlled, with tensile stress in the direction perpendicular to the grain. The strain or the elongation of the sample as a result of the tensile stress was measured by two linear position sensors (LPS) attached on each side of the sample. Thermal strain was also measured in the climate chamber without any stress applied. For comparative purposes, some of the samples were pre-treated by hot-water soaking for as long as 8 hours at temperatures raised to 80°C so that the possible affects of pre-treatment on strength and load-deformation relationship could be determined.

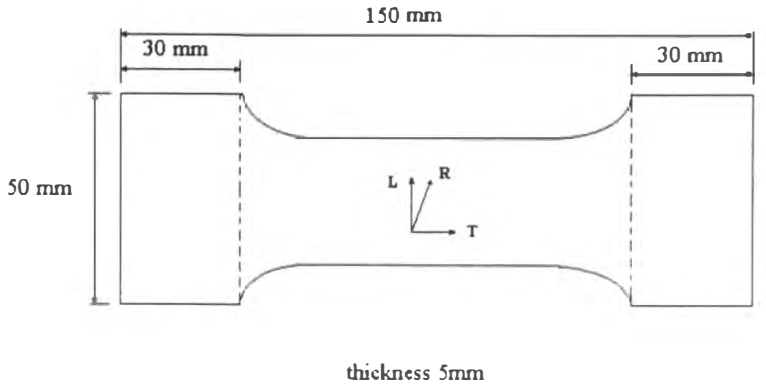

Fig. 6-1. Dimensions of tangential samples used in the tests.

§6.3 Measurement of elastic moduli of UTS in tangential and radial directions

Tangential specimens cut from boards

Three red beech boards wrapped and well-kept in the cool room were sawn and cut to give samples of the required size. As the samples came from narrow boards, only tangential samples could be prepared. These samples were used to obtain the load-deformation curve at different temperatures and moisture content levels. Some of the samples were also used for thermal strain tests, the results of which will be discussed later in this chapter.

Tangential and radial specimens cut from discs

Samples cut from two discs permitted both radial and tangential samples to be prepare.

Radial and tangential samples were tested using an Instron testing machine with an extensometer to verify the climate chamber tests; to confirm that the results were independent of the test procedures.

§6.4 Results

§6.4.1 Ultimate strength of *N fusca* at different temperature levels and moisture contents*:*

Stress-strain curves for tangentially aligned samples of the red beech samples at different moisture contents and temperatures were obtained using the climate chamber at three temperatures (Figs 6-2, 6-3), and the effect of hot-water soaking was examined (Figs 6-4).

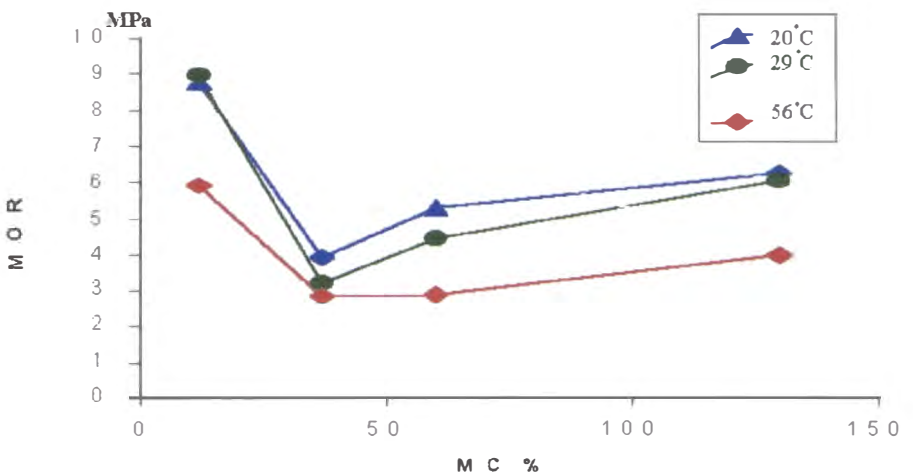

Fig 6-2 Moduli of rupture (MOR) of red beech at different moisture contents (MC) and temperatures

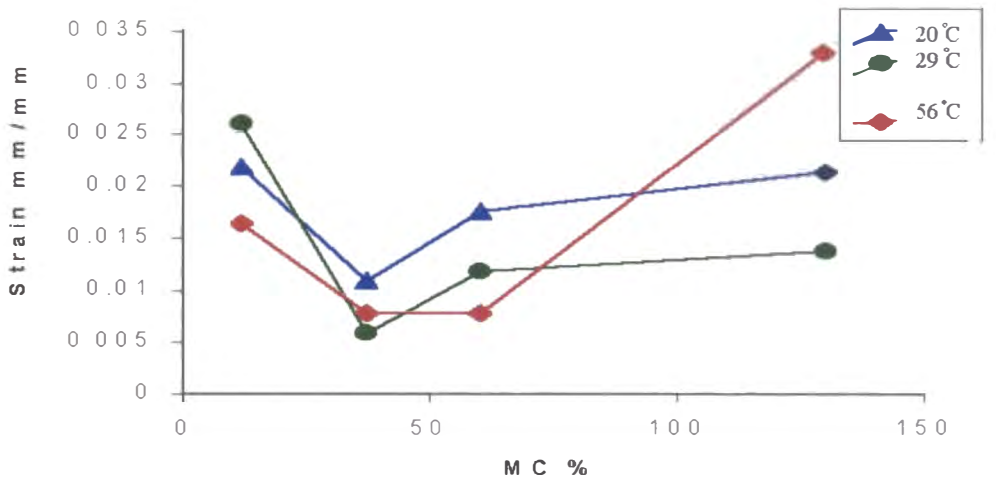

Fig 6-3 Ultimate strains of red beech under tension at different moisture contents and temperatures

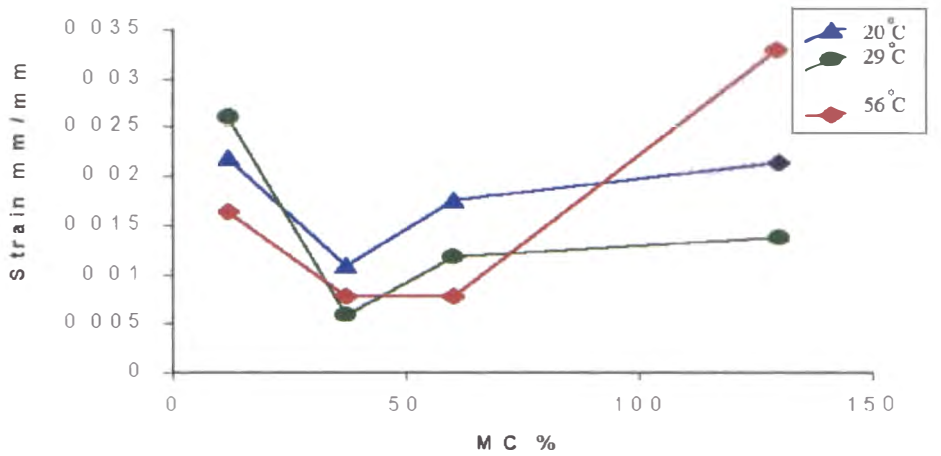

Fig 6-4 The ultimate or failure tensile strain for hot-water soaked samples at different moisture content (MC) and temperatures.

Hot-water soaking reduce the ultimate tensile strength of the samples by about 0.7 MPa (Fig. 6-5), while the ultimate strains may be slightly reduced.

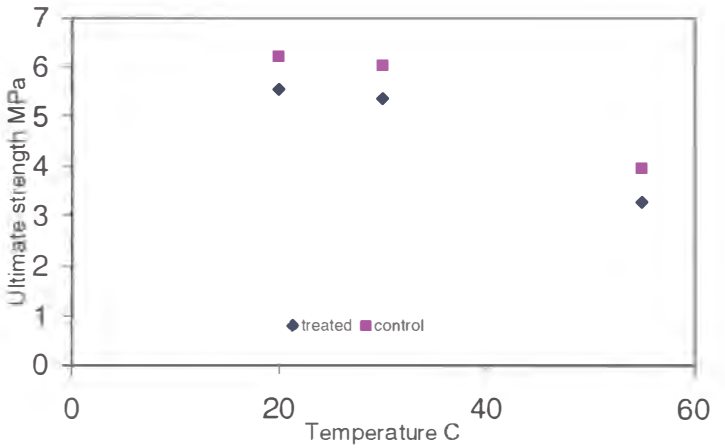

Figure 6-5. Comparison of ultimate tensile strength between treated and control samples of red beech.

The ultimate tensile strains in the hot water-soaked samples also changed as a result of the treatment. Figure 6-6 compares the treated sample and the control ones.

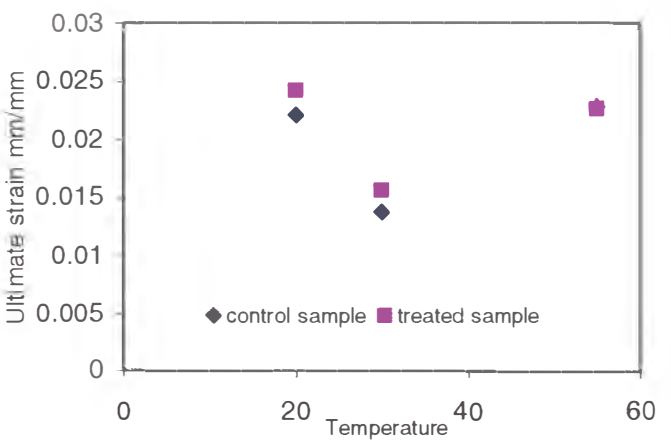

Fig 6-6 Comparison of ultimate strain between treated and control samples of red beech

§6. 4.1.4 The elastic proportional limit and modulus of elasticity in the load-deformation curves for the red beech samples

The stress-strain curves were analysed to determine the limits of elastic proportionality, so that the corresponding elastic strain could be found and Young's modulus calculated.

§6. 4.1.4.1 Untreated samples tested at three temperature (20, 29, 55 °C) and four moisture contents (140%, 37% and 12%)

Stress- strain curves for fresh red beech samples were obtained at three different temperature levels and four moisture content levels, data for tests at 140% mosure content are given in Fig 6-7 a, b, c.

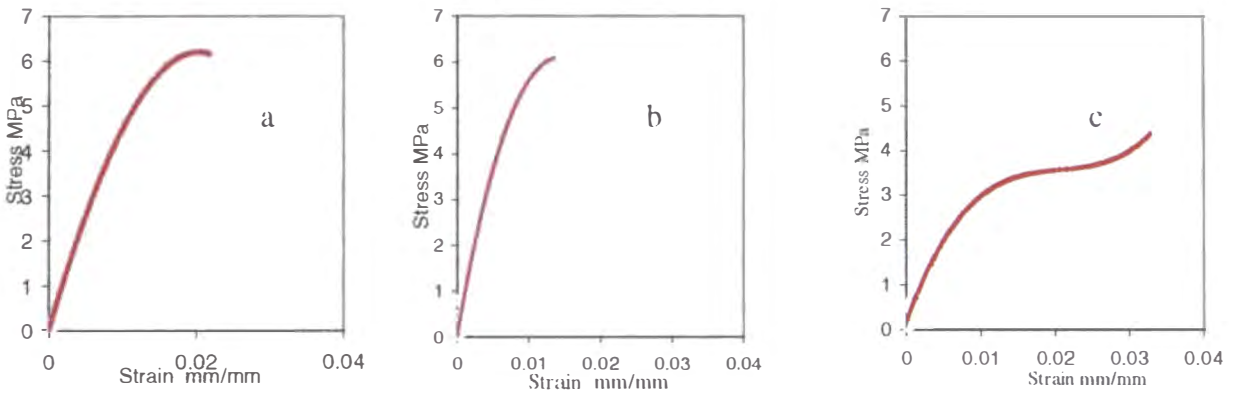

20 °C 29 °C 55 °C

Fig 6-7 a, b, c. Stress-strain curves of red beech samples of 140% MC and at 20°C, 29°C and 55°C respectively

Stress- strain curves for red beech with 60% moisture content samples at three different temperature levels are given in Figs 6-8 a, b, c.

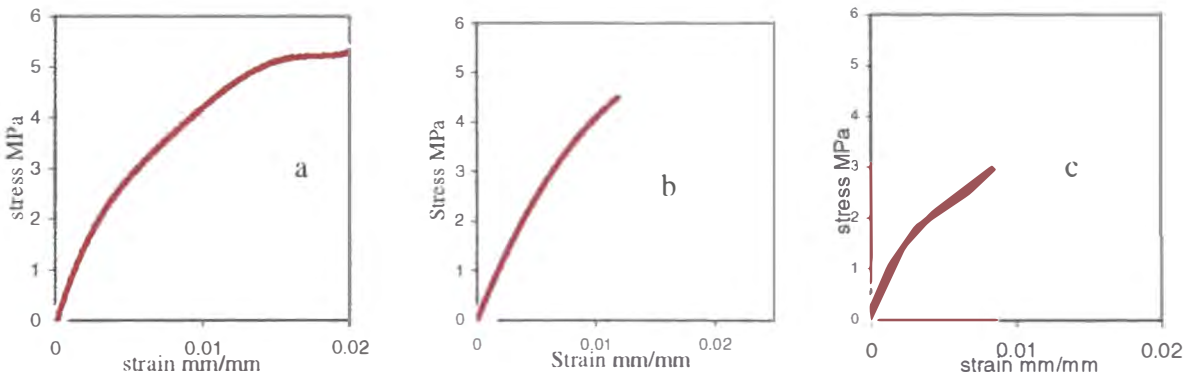

20 °C 29 °C 55 °C

Fig 6-8, a, b, c. Stress-strain curves of red beech samples of 60% MC and at 20°C, 29°C and55°C respectively

Stress- strain curves for red beech with 37% moisture content samples at three different temperature levels:

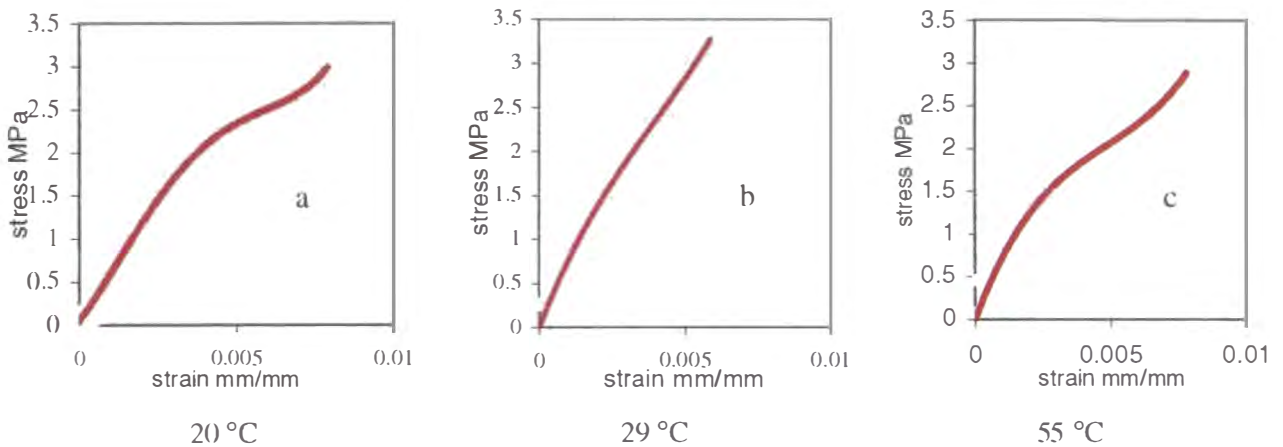

20 °C 29 °C 55 °C

Fig 6-9 a, b, c. Stress-strain curves of red beech samples of 37% MC and at 20°C, 29°C and 55°C respectively.

Stress- strain curves for red beech with 12% moisture content samples at three different temperature levels:

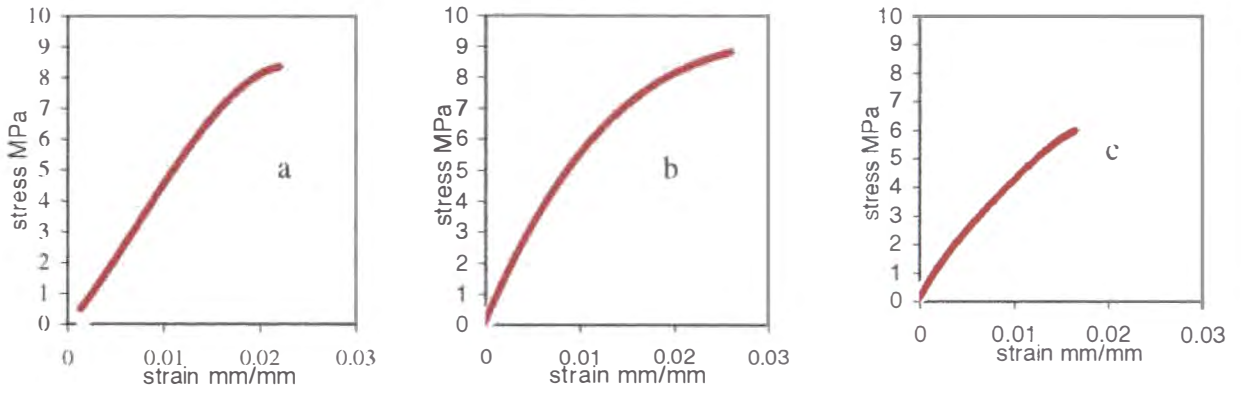

Fig 6-10 a, b, c. Stress-strain curves of red beech samples of 12% MC and at 20°C, 29°C and 55°C respectively.

§6. 4.1.4.2 Hot-water soaked samples tested at three temperature (20, 29, 55 °C) and four moisture contents (140%, 37% and 12%)

The hot water-soaked samples were tested using the same methods and procedures as the controls and the stress-strain curved compared to that of the untreated fresh samples in Figs 6-11 a, b, c.

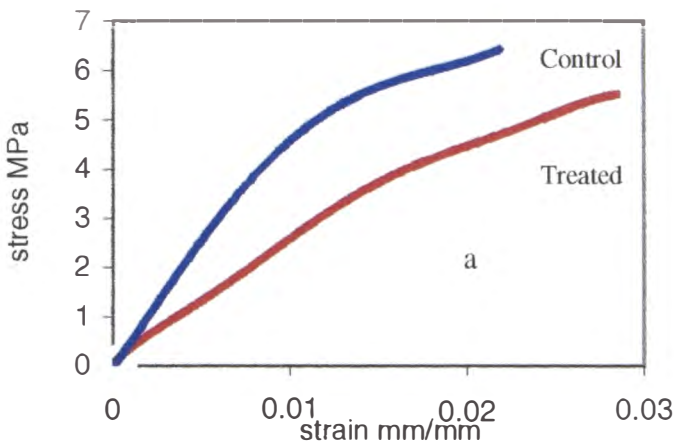

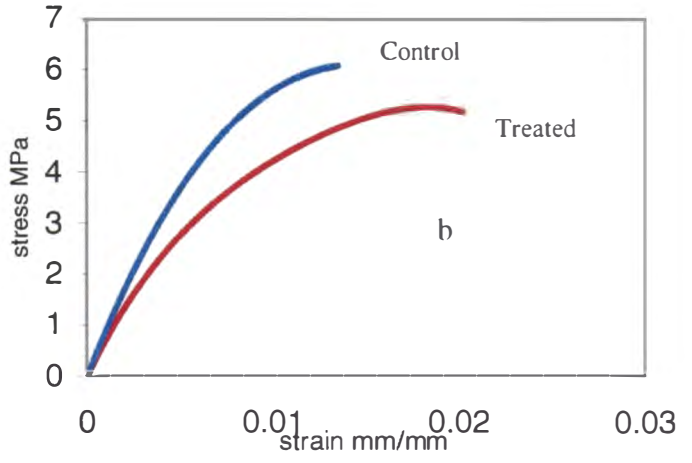

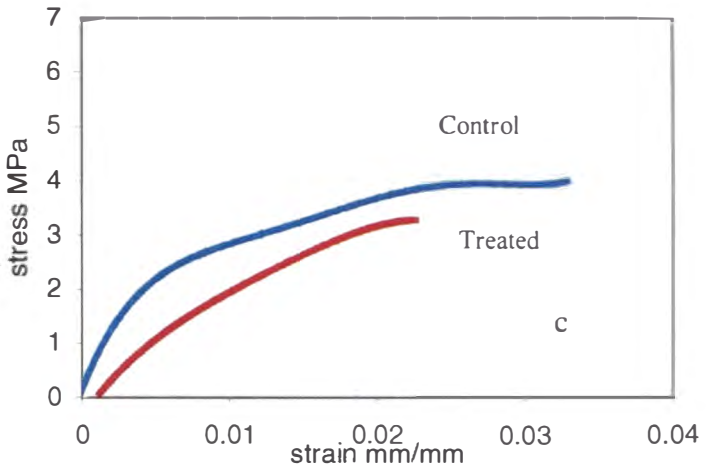

Fig 6-11 a, b, c. The comparison of stress-strain curves for hot water-soaked and untreated samples of red beech at 20°C, 29°C and 55°C respectively.

In evaluating the moduli of elasticity (MOE) from the stress-strain curve, it is crucial to define the methodology. One of the common ways is to determine the limit of the elastic proportionality by estimating the approximate end of linear slope of the stress-strain curve visually. The following diagram (Fig. 6-12) showed the relationship between the MOE derived in this way with moisture content and temperature:

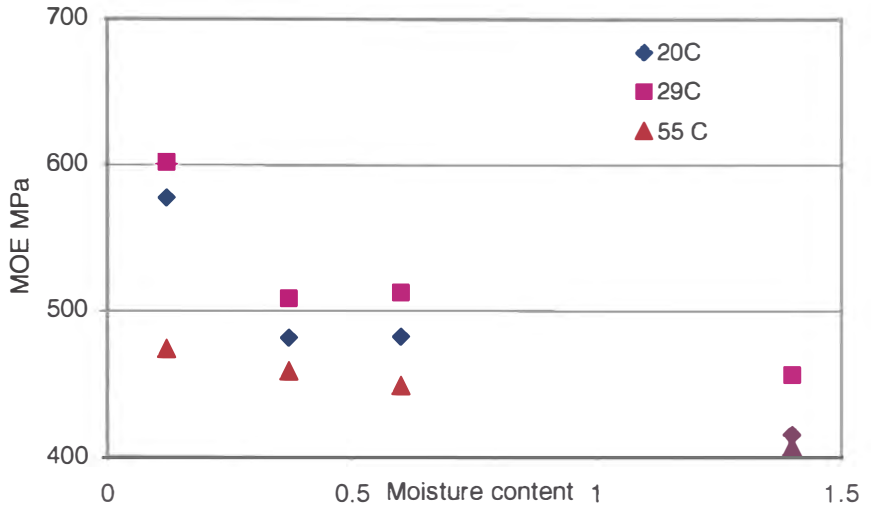

Fig 6-12 Moduli of elasticity (MOE) of red beech at different temperatures and moisture contents.

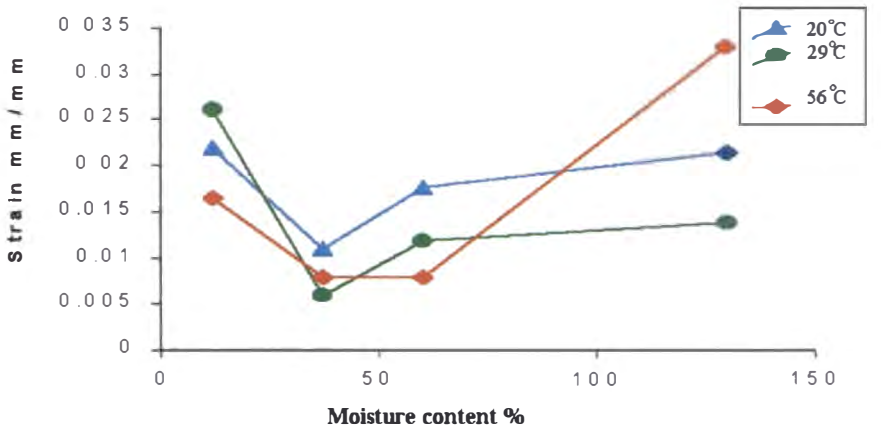

Fig 6-13 Ultimate strain of red beech at different temperatures and moisture contents

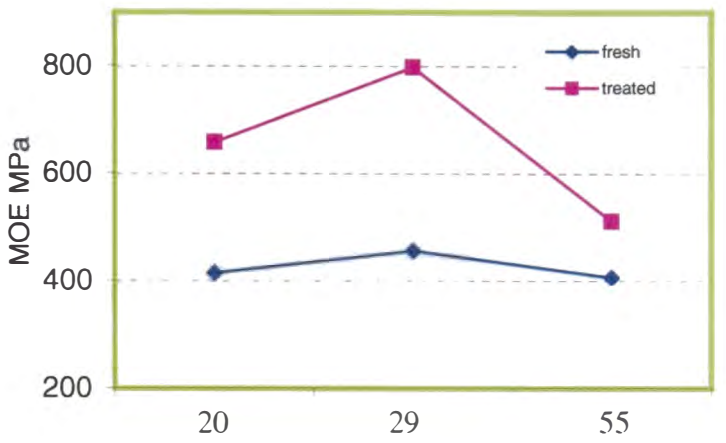

Fig 6-14 Moduli of elasticity of hot water-soaked and untreated red beech at different temperatures

The magnitude of the moduli of rupture, and the ultimate strain level were within a variation of ± 5% (Figs 6-9 to 6-11, 6-13). The calculated moduli of elasticity were within ±15% (fig 6-12, 6-14).

The tests used samples sawn from the three fresh red beech boards, from which only tangential samples could be swan. The use of the samples from two more red beech discs provided some validation of the earlier results, *ie* the mechanical properties in the tangential direction, as well measuring properties in the radial direction.

Radial samples were also tested for their mechanical properties. Fig 6-15 shows the comparison of stress-strain curves in radial and tangential directions for the fresh red beech at 20 °C.

Some difference could be found from figure 6-15, the tangential sample appears more elastic than the radial one. Since only limited 6 tests were carried out for this type of comparison, it is, therefore not intended to draw a clear different line for them here.

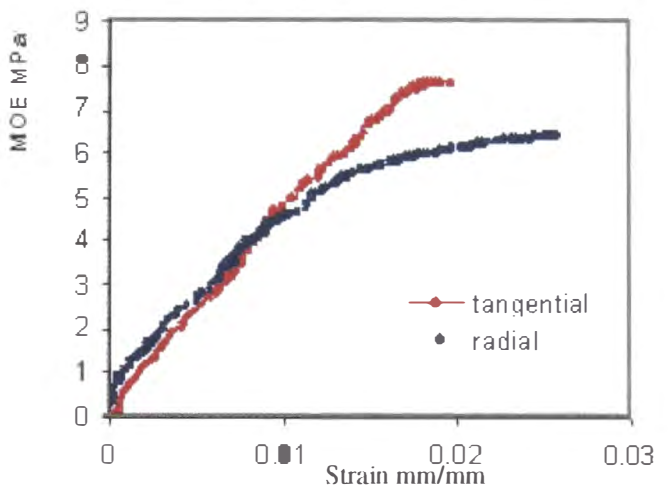

Fig 6-15 Comparison of the stress-strain curve between radial and tangential direction for fresh red beech at 20 °C

§6.4.3.1 *Verification of results*

Further tests were undertaken because of the concern that the measured stress-strain curves of the red beech samples were not as linearly elastic as might have been expected, and verification of the data on different equipment would eliminate the possibility of a system error.

The radial and tangential samples also came from the same two discs used earlier. The Instron unit with an extensometer measures deformation in the midspan of the tested sample more accurately than the LPSs used in the climate chamber.

The samples were rectangular (160mmx20mmx5mm) to fit the jaws of the testing machine and the surfaces dressed. The change introduced a problem; the trimming of the sample into a rectangular shape meant the ends of the sample were subject to extra forces in the test. Because of the concentration at grips, so failure could not be expected in the central tested area. However, the objective of these tests was to compare the elastic stress-strain curves from the two testing systems (climate chamber and Listron unit).

In Fig. 6-16, the stress-strain curves are superimposed for fresh red beech samples at ambient temperature using the two test systems.

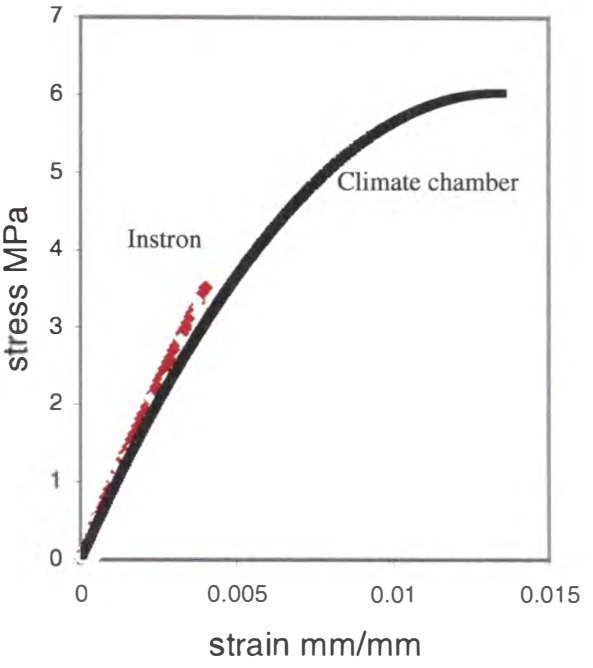

Fig 6.16. Comparison of the stress-strain curves for fresh red beech samples (80% MC) at ambient temperature.

The curves refer to the green samples (80.0 % MC). The Instron with the extensometer gives a smoother curve that the climate-chamber system. However, the climate chamber records a very similar stress-strain relationship. The stress-strain curve from recorded by the extensometer is not exactly linear. Because that system does not have the temperature control, the tests were only possible under room condition at 20 °C and 65% relative humidity. In the Instron test, the tangential to the slope, giving the MOE, decided for 1.082GPa at 0% strain and 0.958 GPa at 0.2% of strain and 0.906 GPa at 0.4% of strain.

§6.4.4 Creep strain in the tangential and radial directions for New Zealand red beech timber

Creep is a time-dependent deformation in timber. It is caused by the ability of wood fibre to deform plastically under stress, and is additional to the instantaneous compliance. There is little information on the time-dependent strain perpendicular to the grain for New Zealand beech timbers. In this project, the optimisation program for the drying schedule was initially based on the presumption that at temperature lower than 55 °C the creep strain of New Zealand beech timber is negligible.

Experimental Procedure

The samples used for testing the creep strain were of the same dimensions as those used in the other mechanical property tests, which have been described in the section 6.2.1. Samples were sawn in such a way that the direction of the application of stress onto the samples would be either radial or tangential.

Three samples were used for each of the tests. These creep strain tests were carried out over a range of temperature 23-55 °C. This temperature range covers the conditions for dehumidifying kilns. The moisture content ranged from oven-dry to green conditions. During the tests, the temperature and relative humidity were kept constant as was the stress applied to the sample, with the stress level ranging from 20% to 60% of the modulus of rupture for red beech under the same conditions, but for short-term loading (less than 30 seconds).

All the tests were carried out at a relative humidity of 100%. As the temperature is kept constant, it is presumed that no moisture change occurred in the sample, and therefore there will be no mechanosorptive (MS) strain: the MS strain is a time-dependent strain caused by a change of moisture contents under load.

The moduli of rupture for New Zealand red beech at different temperature levels obtained in the mechanical property tests in this project (see Fig. 6-9) are list in Table 6-1:

Table 6-1 The moduli of rupture for New Zealand red beech

Moisture content %	Temperature		
	20 °C	30 °C	55 °C
140	6.80	6.50	4.00
60	5.28	4.42	2.90
37	3.90	3.20	2.84
12	8.90	8.75	5.95

However, only green samples were used for the creep strain tests.

Test results

The purpose of this experiment is to determine the magnitude of the creep strain under different level of tensile stress, and at different temperatures.

Keep (1998) used the same apparatus measured the creep compliance for *P. radiata* timber previously.

The creep strain has been defined by Wu and Milota (1995) as

$$\varepsilon_C = \varepsilon_{total} - D_I \sigma \qquad (6\text{-}1)$$

where D_I is the instantaneous compliance:

$$D_I = \frac{\varepsilon(0.2)}{\sigma} \qquad (6\text{-}2)$$

where $\varepsilon(0.2)$ is the total strain at a time of 0.2 minutes, when it is assumed that creep development is negligible.

Initially the creep strain of New Zealand red beech at room temperature was measured when the stress was 60% of the ultimate tensile strength under short-term loading, this test result is shown in Fig 6-17.

Further experimental work was carried out at higher temperatures and different stress levels. The creep strains were evaluated from the total tensile strain observed in each of the tests, which is not necessarily the failure strain because of the test time is relatively short (maximum 700 minutes).

In this thesis, the instantaneous strain was defined slightly differently. The loading system in the climate chamber is controlled manually and it takes up to 7 seconds to apply the required load. The instantaneous $\varepsilon(0.2)$ is therefore defined as the strain at the time 0.2 minutes after the load is applied to the required level (i.e. approximately 17 seconds).

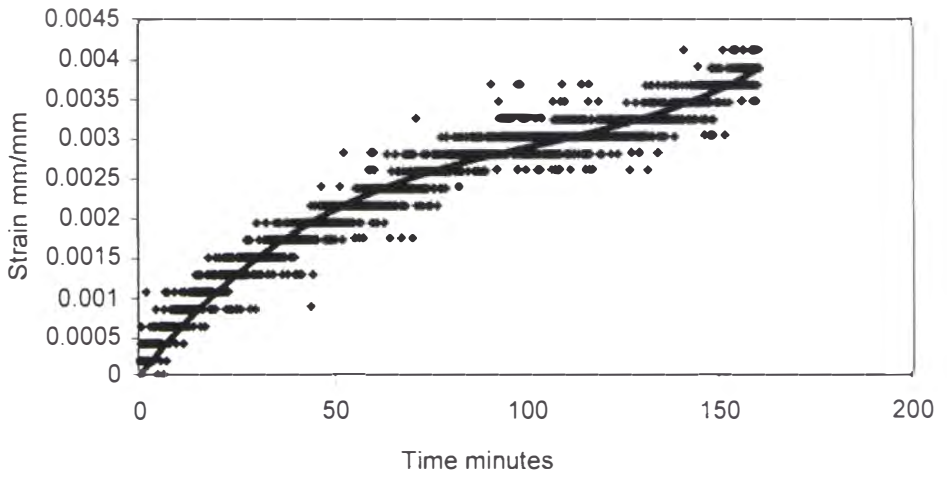

Fig .6-17 creep strain of red beech at 23 °C and 100% RH

Figure 6-17 shows some significant creep (0.4%) at 23 °C and 100% relative humidity prior to rupture. From the creep-strain curve, one can detect the onset of tertiary creep (accelerating creep) towards the end of the test, which lasted just under 3 hours.

An identical test under the same condition with a second sample sawn from the same position within the same board was carried out for a length of time over 500 minutes. The result show a similar magnitude of the creep strain, but fail to verify the rising creep rate after at about 150 hours as indicated in the earlier test.

Further tests were carried out at different temperatures and stresses, among which 50 °C temperature was used to with the same stress level:

The higher temperature condition seemed significantly increased the creep strain, but only after the stress had been maintained for about 150 minutes. This can be seen in the figure 6-19. This might be interpreted as the onset of tertiary creep, which would imply that the applied stress is in excess of 60% the short-term failure.

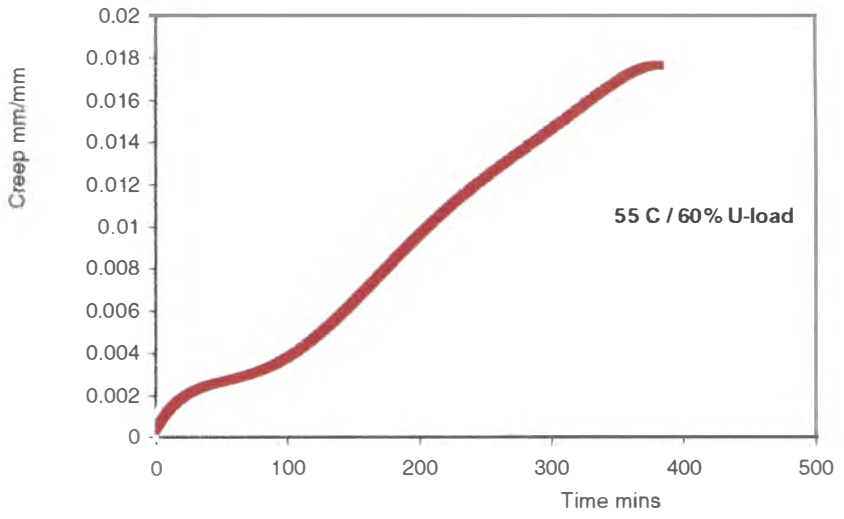

Figure 6-18 creep strain of red beech at 55 °C and under the load of 60% ultimate strength

The creep strain reaches to over 2% after 500 minutes of the test. This phenomenon can be explained by the start of the softening of timber major components like lignin at that temperature level.

Creep strains at different load levels were also compared and the curves super-imposed in one diagram as shown in Fig. 6-19.

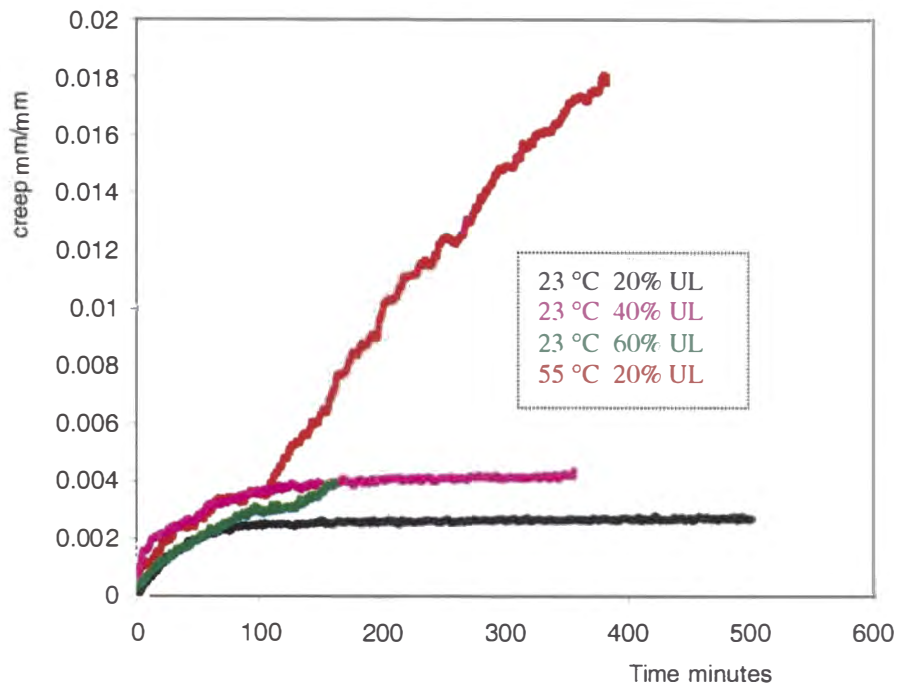

Figure 6-19 Comparison of creep strain for red beech at different load levels and temperatures

Some similarity of the time-creep strain relationship can be seen from the above figure. For the first 150 minutes or so, there is relatively not much difference between the tests at different temperature and load levels and shows a primary (decelerating) creep followed by secondary (steady-state) creep. The load level does not even affect the creep strain at the ambient conditions.

§6.5 References

Chen, G., 1997 Stress relief for sapwood *Pinus radiata* Boards by cooling and steam-conditioning processes, Holz als Roh- und Werkstoff, Vol **55** pp 351-360

Clifton, N. C., 1990 New Zealand timbers: The complete guide to exotic and indigenous woods, GP Books Wellington.

Desch, H. E. and Dinwoodie, J. M., 1981 Timber structure, properties, conversion and use 6th edition Food Products Press, London.

Desch, H. E. and Dinwoodie, J. M., 1996 Timber: Its structure, properties, conversion and use 7th edition, Food Products Press London.

Dimwoodie, J. M., 1989 Wood: Natures cellar, polymeric, fibre-composition, Institute of Metals, London.

Dimwoodie, J. M., 1981 Timber: Its nature and behaviour, Macmillan, London.

Grace, C., 1996 Drying characteristics of *Nothofagus truncata* heartwood, M.E. thesis, University of Canterbury.

Kininmonth, J.A., 1973. Timber drying in New Zealand. New Zealand Forest Service, Wellington.

Innes T. C., 1995 Collapse and internal checking in the latewood *of Eucalyptus regnans* F Mull. Wood Science and Technology **30** (1995) pp 373-383.

Innes T. C., 1996 Collapse during seasoning of *eucalypt* timbers, 5th IUFRO International wood drying conference, Quebec City, Canada.

Innes T. C., 1995 Stress model of a wood fibre in relation to collapse, Wood science and technology **29** (1995) pp 363-376.

Kass, A. J., 1969 Inelastic mechanical behaviour in wood stresses perpendiculat to the grain radially. Ph.d thesis, The University of Michigan, USA.

Keep, L-B., 1998 The Determination of time-dependent strain in *Pinus radiata* under kiln-drying conditions, M.E. thesis, Department of Chemical & Process Eng. Univ. of Canterbury.

Kininmonth, J.A., 1971. Effect of steaming on the fine structure of *Nothofagus fusca*. New Zealand Journal of Forestry Science, **1**(2) pp129-39.

Kininmonth, J.A., 1973. Timber drying in New Zealand. New Zealand Forest Service, Wellington.

Ministry of Forestry, 1996 Producing quality kiln-dried timber in New Zealand, Wellington.

Morlier, P., 1994 Creep in timber structures, E & FN Spon, London.

Morlier, P., 1997 Micro-mechanical aspects of oak drying, International conference of COST action E8, USA.

NZFS. 1974. Timber properties and uses of the New Zealand beeches. New Zealand Forest Service, Wellington.

Ranta-Maunus, A., 1989 Analysis of drying stresses in timber, Paper and Timber 10/1989 pp 1120-1122.

Wu, Q., 1995 Rheological behaviour of Douglas-fir perpendicular to the grain at elevated temperatures. Wood and Fibre Science, Vol. **27**(3), pp 285-295.

Chapter 7

The development of a strain-limited drying schedule

§7.1 Introduction

The stepwise drying schedules used in the initial drying tests succeeded in drying New Zealand red and hard beech timber boards that meet the quality requirements of New Zealand Standard 3631:1981. However, an energy-efficient drying schedule is a further constraint for hardwood timber drying, especially for Australia eucalyptus and New Zealand beech timbers because they are heat-sensitive, prone to defects and collapse, and so must be dried slowly. It is very important that the stepwise drying schedules be optimised so that these timbers can not only be dried without producing defects, but also with acceptable energy use and cost.

§7.2 Modelling of the drying behaviour

Modelling the drying process of timber usually consists of two parts: the modelling of the moisture movement and the related thermal dynamics; and the modelling of the stress-strain relationship.

Most of the drying models simplify the three-dimensional transport of the moisture movement into a single dimension with little loss of accuracy because of the way in which moisture is lost from stacked boads, which are much longer than they are thick.

Doe *et al.* (1994) believe that moisture transport within hardwood may be adequately described by Fickian diffusion model, which will be reviewed later in this chapter on the optimisation of the drying schedule Langrish *et al.* (1997) used this model to predict successfully the moisture profiles of Australian eucalyptus timber boards on kiln drying.

When wood is exposed to drying, the physical and mechanical behaviour change as the moisture is evaporated from the boards. The mechanical properties of wood are strongly affected by moisture and there is also a strong interaction between mechanical response and moisture change.

As the moisture content changes, the mechanical behaviour in the transverse direction dominates the stress-induced dimensional changes of the timber boards, while that in the grain direction is much smaller and may be regarded as negligible.

Martensson *et al.* (1997) developed a constitutive model describing the stress-strain relationship for woods, which has been verified for the behaviour perpendicular to the grain in test results on Scots pine timber. Later they derived a two-dimensional model to describe the stress-strain relationship, which was also verified in tests on several softwood species. That study also concluded that, if wood were an elastic material without mechano-sorptive behaviour, it would be impossible to dry timber without causing defects. Their study found that at 60 °C the mechano-sorptive effect was larger than at either 20 °C or 80 °C.

A dynamic model has been put forward by Carrington *et al.* (1999) for simulating the wood drying process in a dehumidifier kiln. The model solves the fundamental balance equations, for the dehumidifying drier system, which is comprised of the sub-systems of the timber stack, kiln circulation fans, kiln envelope, air heater, and the dehumidifier. The model can be used for analysing the influence of design and control variables on the performance of the system as a whole. This dynamic model can also be used to investigate conventional vented kilns by setting the dehumidifier capacity to zero.

§7.3 Optimisation of the drying schedule

The following is the theory of the optimisation techniques used by Langrish *et al.* (1997) to develop a strain-limited schedule:

§7.3.1 The drying model:

The moisture transport within the timber is assumed to be one-dimensional, and described by a simple Fickian diffusion model:

$$\frac{\partial X}{\partial t} = \frac{\partial}{\partial x}\left(D\frac{\partial X}{\partial x} \right) \qquad (7\text{-}1)$$

where X is the moisture content and x is the position within the timber board from the core, and D represents the temperature-dependent diffusion coefficient,

$$D = D_r e^{\frac{D_E}{T}} \qquad (7\text{-}2)$$

The heat transport within the timber is described by another partial differential equation:

$$\frac{\partial T}{\partial t} = \frac{\partial}{\partial x}\left(\frac{k}{\rho c_p}\frac{\partial T}{\partial x} \right) \qquad (7\text{-}3)$$

Since the thermal conductivity k, the density ρ, and the heat capacity c_p of timber are functions of moisture X, and moisture diffusivity D is a function of temperature T, Equation (7-1) and (7-3) must be solved simultaneously.

At the timber surface, the mass flux of water from board (j) is proportional to the difference between the gas humidity just above the timber surface Y_S and that in the bulk air stream Y_G:

$$j = \rho_{Air} k_m (Y_S - Y_G) \qquad (7\text{-}4)$$

In this equation, ρ_{Air} represents the density of air while k_m is a mass-transfer coefficient. While the humidity of the air Y_G can be calculated from dry and wet-bulb

temperatures (T_G, T_w) in the kiln, Y_S is a function of the moisture content at the timber surface X_S (Wu, 1989), and thus equation (7-4) forms a boundary condition to equation (7-1).

At the board surface, both convective heat transport, as well as the heat transfer associated with the evaporation of moisture must be considered to yield the net heat gain by the board:

$$Q = h_F(T_G - T_S) - (\lambda_W - \lambda_S)j \qquad (7\text{-}5)$$

In the above equation, h_F is the heat transfer coefficient, λ_w is the latent heat of vaporisation, λ_S is the heat sorption, and T_S the surface temperature. This equation forms a boundary condition for equation (7-4). An implicit assumption here, which is used to specify the heat flux to the board, is that moisture evaporates close to the board surface. If this were not the case, then the equation (7-5) would need to be modified to account for internal evaporation, a phenomenon which does occur during the drying of softwood, but less likely in the drying of hardwood.

If we assume that the same amount of heat and mass transport is occurring at the upper and lower surfaces of the board, then the temperature and moisture profiles will be symmetric about the centre of the timber board. Consequently, moisture and heat transport cannot occur across the centre, a fact which defines another two boundary conditions:

$$\frac{dX}{dx}\Big|_c = 0 \qquad (7\text{-}6)$$

$$\frac{dT}{dx}\Big|_c = 0 \qquad (7\text{-}7)$$

If the moisture and temperature gradients are approximated by finite differences (Wan and Langrish 1995), then the drying model reduces to a "stiff" system of ordinary differential equations applicable at the surface, within the timber and at the centre of the board respectively:

Surface:

$$\frac{dX_S}{dt} = \frac{1}{\Delta x_s}\left[\frac{D(X_1 - X_s)}{\Delta x_s} - j\right] \qquad (7\text{-}8)$$

$$\frac{dT_S}{dt} = \frac{1}{\Delta x_s \rho c_p}\left[\frac{k(X_1 - X_s)}{\Delta x_s} + Q\right] \qquad (7\text{-}9)$$

(Within board):

$$\frac{dX_i}{dt} = \frac{D}{\Delta x_s}\left[\frac{X_{i+1} - X_i}{\Delta x} - \frac{X_i - X_{i-1}}{\Delta x}\right] \qquad (7\text{-}10)$$

$$\frac{dT_i}{dt} = \frac{D}{\Delta x \rho c_p}\left[\frac{T_{i+1} - T_i}{\Delta x} - \frac{T_i - T_{i-1}}{\Delta x}\right] \qquad (7\text{-}11)$$

Centre (mid plane):

$$\frac{dXc}{dt} = \frac{1}{\Delta x_c}\left[\frac{D(X_c - X_{c-1})}{\Delta x_c} - j\right] \qquad (7\text{-}12)$$

$$\frac{dTc}{dt} = \frac{1}{\Delta xc \rho c_p}\left[\frac{k(Xc - X_{c-1})}{\Delta x_c}\right] \qquad (6713)$$

In the present case, the board was divided into 24 elements which led to a system of 34 differential equations (30 describing conditions within the board, and two each for the centre and the surface) which can be easily solved using an integrator suitable for a stiff system (Appendix 2).

§7.3.2 The stress/strain model

As timber dries out, it will begin to shrink as soon as the moisture content falls below the fibre saturation point X_{fsp}. Since a one-dimension drying model is used, it is assumed that the moisture content in every finite layer parallel to the surface is uniform and the stresses are planar. If any one layer *i* could move independently of all other layers, its shrinkage ζ_i can be approximated by the linear relation (Johnson, 1989),

$$\zeta_1 = \beta M_i \qquad (7\text{-}14)$$

where the moisture change is given by M_i = Max (X_i-X_{fsp}, 0), and β is the moisture swelling coefficient. The stress σ which was required to keep the layer at its original length can be calculated using Hook's law together with a temperature and moisture-dependent Young's modulus E:

$$\sigma = E_i \beta M_i \qquad (7\text{-}15)$$

However, none of the layers can move independently as any board will keep its general shape as shrinkage occurs. Therefore, the internal forces must be calculated in relation to the average shrinkage $\bar{\xi}$ of the whole board. The sum of these internal forces must be zero, a fact which can be expressed in terms of the finite elements as follows:

$$\sum E_i \left(\bar{\xi} - \beta M_i \right) \Delta x_i = 0 \qquad (7\text{-}16)$$

From (7-16), the average shrinkage of the timber is calculated to be:

$$\bar{\xi} = \frac{\sum E_i \beta M_i \Delta x_i}{\sum E_i \Delta x_i} \qquad (7\text{-}17)$$

Consequently, the strain (ε) which is imposed on each layer to keep it at the same length as the timber board as a whole may be approximated by:

$$\varepsilon_t = \bar{\xi} - \beta M_t \qquad (7\text{-}18)$$

Model predictive control (MPC) is a technique that allows process behaviour to be optimised, as described by Partwardhan *et al.* (1990). In this case, a one-step ahead prediction horizon was found to be adequate (Langrish, *at al.* 1997), as a result of slow moisture transport dynamics, with a four-hour time step. The aim in using MPC for timber drying is to optimise the process conditions, namely the dry and wet-bulb temperature as a function of moisture content, to obtain the best possible schedule *i.e.* one that combines acceptable checking and reasonable drying time.

There are at least two possible approaches for implementing MPC in timber drying. One is to minimise the overall drying time t_f using time-varying controller inputs *U(t)* (which represent the dry and wet-bulb temperature) that maintain the timber within all process constrains at all time. This may be expressed mathematically as follows:

To solve for *u(t)*, while minimising t_f for a set of wood properties *P*:

$$\begin{cases} \dfrac{dX}{dt} - f\left[X(t), T(t), u(t), P\right] = 0 \\ \dfrac{dT}{dt} - g\left[X(t), T(t), u(t), P\right] = 0 \end{cases}$$

Subject to

$$\begin{cases} \varepsilon_t(t) < \varepsilon \\ X_s \geq X_{s\min} \\ X(t_f) = \bar{X}_{req} \\ \max\left[X(t_f)\right] - \min\left[X(t_f)\right] \leq \Delta X_{req} \\ T_G \leq T_{G\max} \\ X(t=0) = X_0 \\ T(t=0) = T_0 \end{cases} \qquad (7\text{-}19)$$

In the above, p represents the properties of the timber and $X(t)$ and $T(t)$ are the temperature profiles of the moisture content and temperature within the timber as a function of time. This approach is computationally very expensive, and a simpler approach is to minimise the average moisture content (within all appropriate constraints) over successive time intervals which are small relative to the overall drying time, in the following way.

We minimise $\bar{X}(t_{i+1})$ for the controller limit $u(t_i)$

$$\begin{cases} \dfrac{dX}{dt} - f\left[X(t), T(t), u(t), p\right] = 0 \\ \dfrac{dT}{dt} - g\left[X(t\ ), T(t), u(t), p\right] = 0 \end{cases}$$

Subject to
$$\begin{cases} \varepsilon_i(t_{i+1}) \prec \varepsilon_{\max} \\ X_S(t_{i+1}) \geq X_{S\min} \\ T_G \leq T_{G\max} \\ X(t = t_i) = X_i \\ T(t = t_i) = T_i \end{cases} \qquad (7\text{-}20)$$

This approach is implemented within the Matlab programming software using moving-time horizons of 4 hours, which are small compared with overall drying time of over 100 hours. The process behaviour is optimised subject to a number of constraints; the most important of which is an upper limit on the strain. Doe *et al* (1994) suggested that a strain level of 0.02mm/mm will lead to failure of *Eucalyptus* timber. The minimum surface moisture content is set to 7% to avoid excessive surface checking, while the maximum temperature is also carefully chosen to avoid excessive collapse which is a phenomenon known to occur as the temperature is raised (Campbell, 1980).

§7.4 The strain-limited drying model

The optimisation program used in this work is based on a computer program which has been quite successful in predicting a satisfactory drying schedule for drying some of the Australian eucalyptus timbers like ironbark (Langrish *et al.* 1996, 1997, 1998). The purpose of using this program is to achieve similar results using parameters of New Zealand beech timbers particularly for red and hard beech.

The determination of the initial parameters was the first step in the application of this optimisation program. The initial parameters include:

Dmre - pre-exponential factor
DmpE - activation energy
Tstart - initial temperature of the timber
SurfX - initial surface moisture content of the timber
CentX - initial core moisture content of the timber
SkalF - the scaling factor used to determine the initial moisture content

Among those initial parameters, the reference diffusion coefficient and the activation energy are associated with the value of the diffusion coefficient in equation (7-2). To obtain values for the two initial parameters, the results of some previous work on New Zealand hard beech were compared (Table 7-1) as it was considered that the value for red beech would be similar.

Table 7-1 Diffusion coefficients (m^2/s) for hard beech (*Nothofugas truncata*)

source:	Ross (1986)	Barnes (1988)	Crawshaw (1988)	Grace (1996)
tangential	$6.9\pm0.8 \times 10^{-11}$	$3.3\pm0.8 \times 10^{-11}$		3.0×10^{-11}
radial:	$1.2\pm0.2 \times 10^{-10}$	$1.4\pm0.3 \times 10^{-10}$	$2.2\pm0.2 \times 10^{-10}$	
temperature:	45°C	35°C	36°C	20 °C

Grace (1996) also obtained a tangential diffusion coefficient for pre-treated (hot-water-soaked) hard beech of 5 x 10^{-11} (m^2/s).

A "characteristic" value for the diffusion coefficient of red beech was also evaluated in this project from drying tests using a stepwise drying schedule with an average temperature of about 45 °C. The values for the pre-treated (hot-water-soaked) and control samples are 4.45 x 10^{-10} m^2/s and 1.09 x 10^{-10} m^2/s, respectively.

As reported by Wu (1989) the activation energy is about 3800 K for eucalypts, and this should not vary greatly with species. The initial reference diffusion coefficient was then calculated from the equation (7-2), to agree with the values of the diffusion coefficients from previous work, when the effect of temperature is taken into consideration. This procedure yields the values of reference diffusivity of 1.54 x 10^{-5} m^2/s, for untreated, and 1.93 x 10^{-5} m^2/s for hot-water soaked timber, for activation energy of 3771 K.

§7.4.1 *Shrinkage of the New Zealand beech timber*

The shrinkage rates in the transverse directions of the board play a very important role in the strain-limited drying schedule optimisation program. New Zealand red beech and hard beech are among these species which have large overall shrinkage rates, and large changes in dimension. Total shrinkage includes both recoverable and unrecoverable dimensional changes.

Grace (1996) studied the shrinkage of New Zealand hard beech. By steaming the dried boards, and then air drying the boards back to their original moisture content he obtained the recoverable as well as the unrecoverable shrinkage (Fig 7-1).

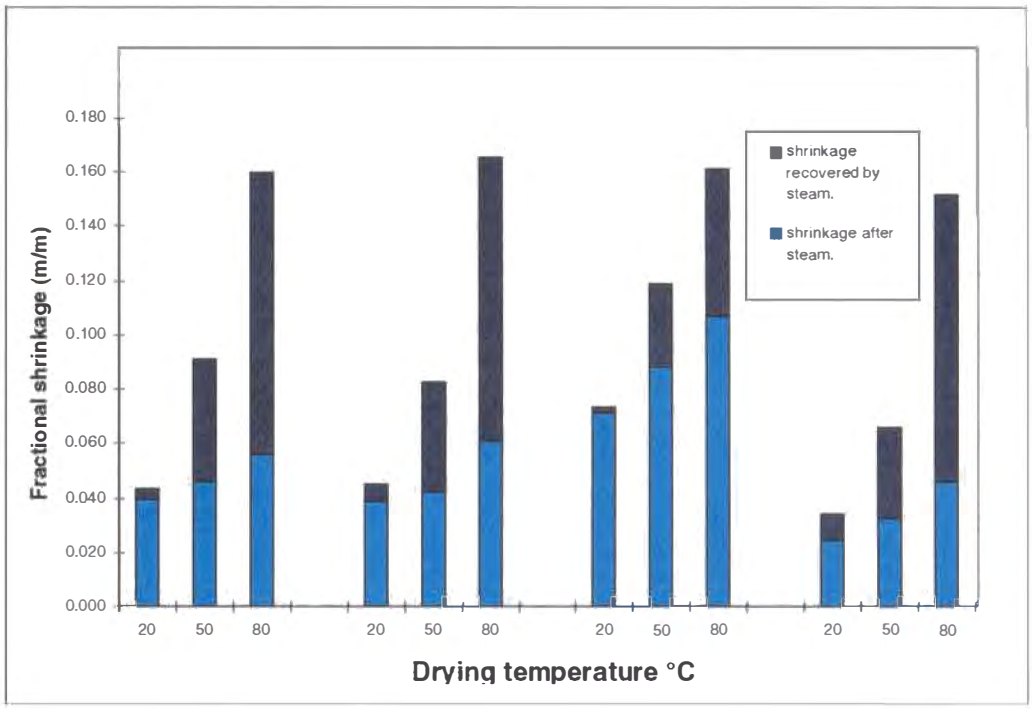

Figure 7-1 Total shrinkage of four samples dried at three temperature, divided into recovered and unrecovered proportion. After Grace (1996)

The dried boards were initially dried at different temperature between 20 to 80 °C and different shrinkages were observed, as shown in Fig 7-2:

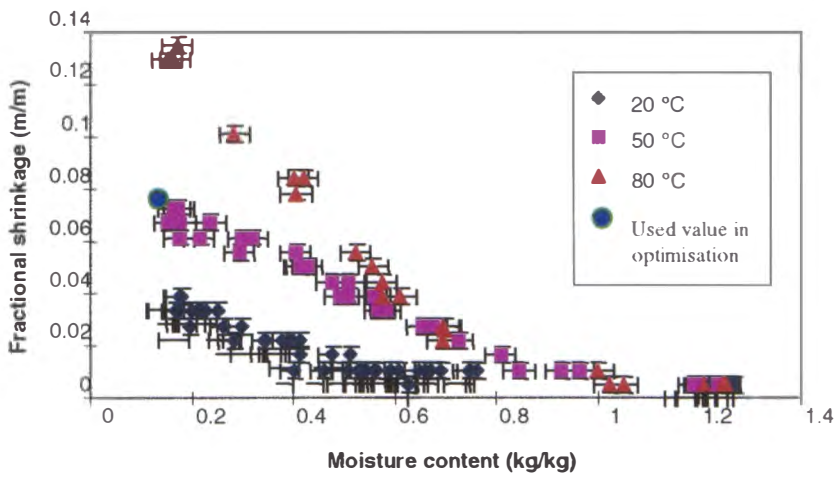

Figure. 7-2 The influence of drying temperature on fractional shrinkage, Adapted from Grace (1996)

Earlier tests showed that the total shrinkage in the transverse direction was 7.5%

The shrinkage used in the optimisation program was obtained from drying tests within the temperature range (20-45 °C) used in the schedule. The assumed shrinkage in both the tangential and radial directions was 7.5% to a final moisture content of 12%when the dry-bulb temperature ranged from 22-45 °C during drying (§5.2). This value may be compared with the total fractional shrinkage obtained by Grace (1996), and illustrated in Fig 7-2, for various fixed temperatures in the range from 20 °C to 80 °C. In the optimisation program, a uniform shrinkage value of 7.5% was assumed for both tangential and radial movement.

§7.4.2 The fibre-saturation point and other initial parameters

The fibre-saturation point is assumed to occur at 25% (0.25kg/kg). (The reason of making this assumption is discussed in section § 2.2.5. The other initial parameters were chosen either from the values used in actual drying tests, such as the initial average moisture content or with consideration of the dehumidifying system's operational range.

§7.5 The initial drying schedule predicted for red beech timber

To test if the initial values for these parameters could be used in the optimisation program, a stepwise drying schedule with observed average moisture-content chenges was fitted to the diffusion model by a least-squares procedure. Fig. 7-3 shows that the observed experimental curve and the curve predicted on the basis of the estimated parameters are very similar.

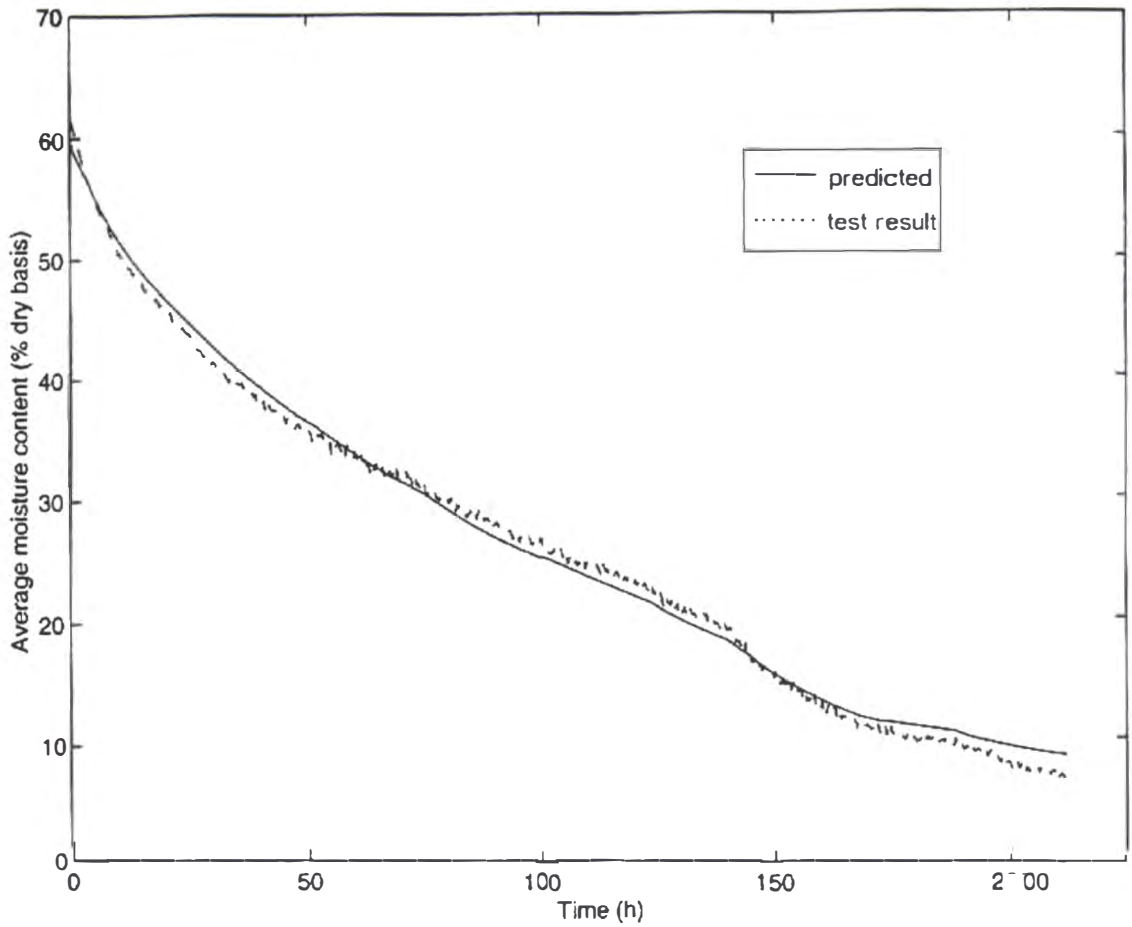

Figure 7-3. Comparison of actual drying curve with predicted curve from stepwise schedule using preliminary values for wood parameters.

The maximum allowed strain was initially set at 0.017 mm/mm, just under the recommended value of 0.02 mm/mm for Australian *Eucalyptus* timbers (Doe *et al.*1994). The lower limit was taken because it is thought that red beech timber is even easier to degrade. This value, together with other initial parameters, generated a drying schedule by the optimisation program.

The Fig. 7-4 shows the resultant optimised drying schedule with this maximum strain limit at 0.017 mm/mm:

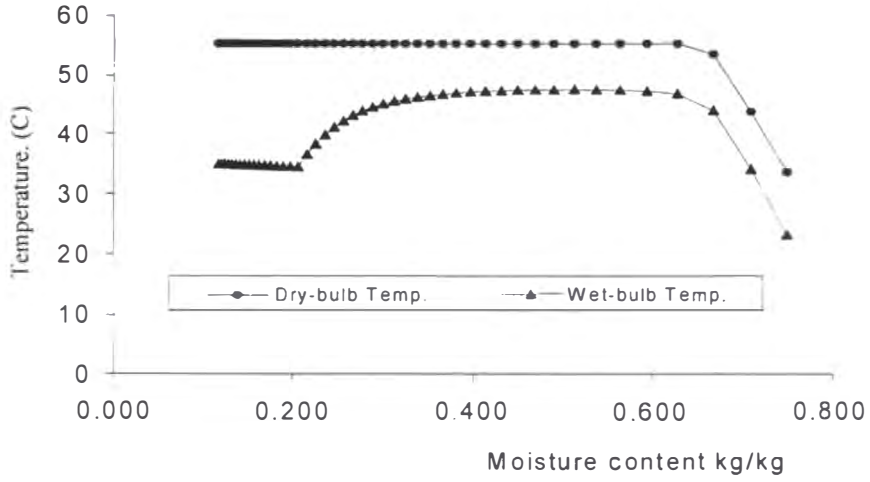

Fig. 7-4 The optimised drying schedule with the maximum strain limit at 0.017 mm/mm

The optimised drying schedule is different from the step-wise drying schedule in the following ways:

1. It predicts a very short drying time, much shorter than the actual length of the step-wise drying schedule (Compare Fig. 7-4 with Table 4-1,4-2).

2. The dry-bulb temperature has been raised to the maximum allowable drying temperature much earlier than the time when the timber reaches its fibre-saturation point (Fig. 7-4).

3. The initial wet-bulb depression is quite high, and that in the optimised schedule for the first step, it is 10 °C, whereas that of the stepwise schedule is only 2 °C (Compare Fig 7-4 with Table 4-1,4-2).

4. The impression of the overall drying schedule is "harsh", with relatively low relative humidity in the early stage of the drying schedule, when red beech timber is likely to have small cracks, which may eventually lead to further degradation of the board.

The optimised drying schedule needs to be verified in an actual drying test using the drying chamber with the modified control system, where both dry and wet-bulb temperatures can be ramped up according to the timber moisture content as required by the schedule.

§7.6 The first verifying trial results

The predicted drying schedule was then programmed into the computer, which monitors and controls the drying conditions in the testing small drying chamber. The recorded data was then compared with the that generated by the optimisation program (Fig. 7-5).

The drying results show that:

1. The drying period of the drying red beech sample board from 65% to 12% is very similar to the predicted time from the optimisation program, which is 2/3 of the drying time of that using the initial step-wise drying schedule (Fig 5-2).

2. About 5-6 cracks have been found in the sample boards dried using the optimised schedule, the cracks have up to 10mm in width and 25 mm in length when sliced for visual observation.
3. The predicted moisture profile does not match actual one when the moisture content is under fibre-saturation.

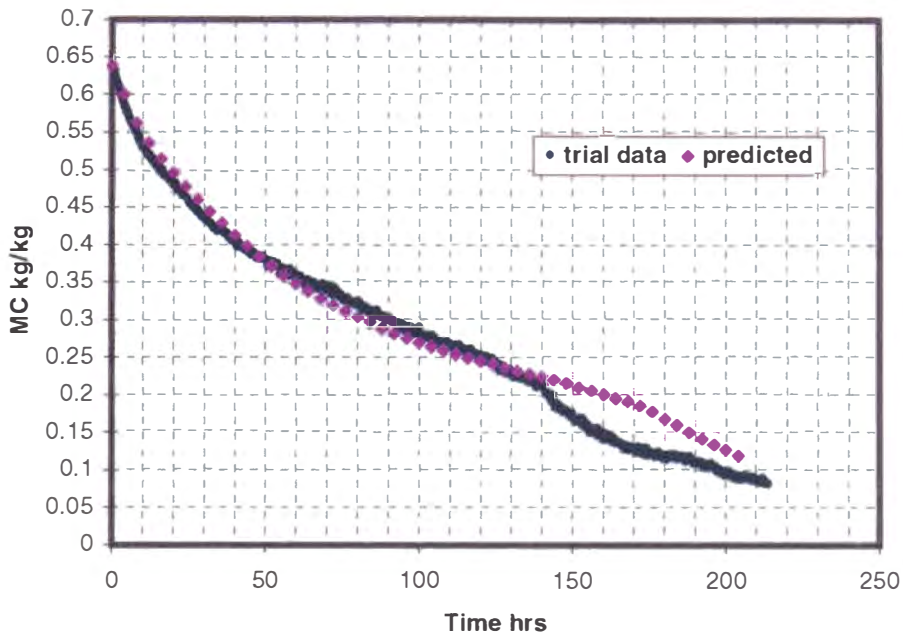

Fig 7-5 The comparison of moisture profile of 13mm red beech board observed from test trial and predicted from optimisation program with the drying schedule as given in Fig. 7-4 and a maximum strain of 0.017

The reasons for the results (Fig. 7-5) could be the following:

1. From the visual appearance of the dried sample boards, the maximum allowed strain value 0.02 mm/mm recommended from Australian experience (Doe *et al.*1994.) is still too high for New Zealand red and hard beech. Even though a less value of 0.017 was used for this program, it still appears too high for beech timbers from the degrade of the samples in the verification trial.

2. The other factor that may influence the optimised drying schedule is the modulus of elasticity, and its relationship with moisture content and temperature. The value of Young's modulus (MOE) at oven-dry moisture content and 20 °C for Australian ironbark timber (420 MPa) was used in optimisation program for was 420 MPa. Based on the temperature dependence of the Young's moduli (Pordage priv. comm.), the estimated MOE for drying between 25-55 °C, would be about 250-400 MPa. The Young's moduli of New Zealand red and hard beech in its transverse directions are not available and the borrowed properties may not be

applicable, so test were under way to determine the Young's modulus he found experimental vales were used in a further optimisation.

By changing the maximum allowed strain to a lower value, the program predicts a milder drying schedule. When it is reduced to 0.009 mm /mm, which is 40% of the recommended strain limit for *Eucalyptus* (Doe *et al.* 1994), the optimisation program gives a low dry-bulb temperature which slowly increases until the timber reaches the FSP. The initial depression is also much milder (1.5-3.5 °C) as against 10 °C used in the simulation, and only increases dramatically once the MC reaches FSP (Fig. 7-6). This predicted mild drying schedule is very similar to the previously used step-wise drying schedule (compare Fig. 7-6 and Table 5-1 and 5-2).

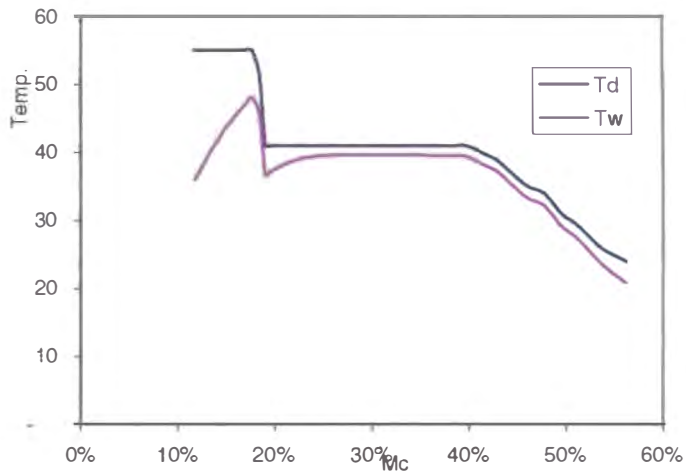

Fig. 7-6 The optimised drying schedule with the maximum strain limit at 0.009 mm/mm

§7.7 *Symbols*

c_p specific heat capacity of moisture wood
D temperature-dependent diffusion coefficient
D_E activation energy
D_r pre-exponential factor
E Young's modulus
j mass flux of water from the board
k_m mass-transfer coefficient
Mi change of moisture

Q total rate of heat transfer

t time

T temperature

T_g air temperature

T_s surface temperature

x distance of the evaporative plane from the surface

X moisture content

X_{fsp} fibre-saturation point

X_{start} initial temperature of timber

X_s moisture content at the timber surface

Y_G humidity in the bulk air stream

Y_s gas humidity above the timber surface

z distance from the surface

Creek

ε_c creep strain

ε_i instantaneous strain

ε_{MS} mecano-sorptive strain

ε_T thermal strain

ε_X free-shrinkage strain

λ_w latent heat of vaporisation

λ_s heat of sorption

ρ wood density

ρ_{air} air density

σ stress

ξ shrinkage

§7.8 Reference

1. Barnes, P.C.I., 1988. Moisture diffusion in Red and Hard Beech during drying. Bachelor of Engineering Report, Department of Chemical and Process Engineering, University of Canterbury

2. Campbell, G. S., 1980 Index of kiln drying schedules for timber dried in Australia, Commonwealth Scientific and Industrial Research Organisation Building Research Division.

3. Carrington, C. G., 1999 Dehumidifier dryers for hard-to-dry timbers, 20th IIR Congress, Sydney Australia.

4. Chawshaw, A.J., 1988. Pretreatments to hasten the drying of Hard Beech. Bachelor of Engineering Report, Department of Chemical and Process Engineering, University of Canterbury.

5. Doe, P. D., Oliver, A. R., Booker, J. D., 1994, A non-linear Strain and Moisture Content Model of Variable Hardwood Drying Schedules, 4th IUFRO International Wood Drying Conference, Rutorua, New Zealand pp. 203-210.

6. Grace, C., 1996 Drying characteristics of *Nothofagus truncata* heartwood, M.E. thesis, University of Canterbury.

7. Langrish, T. A. G., Brooke, A. S., Davis, C. L., Mush, H. E., Barton, G. W., 1997, An Improved Drying Schedule for Australian Ironbark Timber: Optimisation and Experimental Validation, Drying Technology **13** (1) pp. 47-70.

8. Musch, H. E., *et al*. 1996, Model predictive Control of Timber Drying, Accepted for publication at IFAC World Congress, San Francisco.

9. Nassif, N. M., 1983, Continuously Varying Schedules (CVS) – A New Technique in Wood drying, Wood Science and Technology **17** (2) pp. 139-144.

10. Partwardhan, A. A., Rawlings, J. B., Edgar, T. F., 1990, Non-linear Model Predictive Control, Chem. Eng. Comm., **87** pp.123-141.

11. Rensi, G., Weintraub, A., 1988, Using Dynamic Programming to Obtain Efficient Kiln-drying Schedules, Wood and Fiber Science, **20** (2) pp. 215-225.

12. Ross, D.A., 1986. Investigating the moisture movement of Hard Beech during drying. Bachelor of Engineering Report, Department of Chemical and Process Engineering, University of Canterbury.

13. Stanish, M. A., Schajer, G. S., Kayihan, F., 1986 A mathematical model of drying for hygroscopic porous media, AIChE Journal Vol. **32** No. 8.

14. Wu, Q., 1995 Rheological behaviour of Douglas-fir perpendicular to the grain at elevated temperatures. Wood and Fiber science, Vol. **27**(3) pp285-295.

15. Wu, Q., 1996 Mechano-sorptive deformation of Douglas-fir specimens under tensile stress during moisure adsrption, Wood and Fiber science, Vol. **28**(1) pp128-132.

Section D

Overview

Chapter 8 The optimised drying schedules and their validity

Chapter 9 The energy efficiency of the optimised drying schedule

Chapter 10 Discussion

Chapter 11 Conclusion and recommendation for future work

Chapter 8

The optimised drying schedules and their validity

§8.1 Introduction

The initial optimised drying schedules using the parameters taken from the corresponding values for Australian eucalyptus timbers like ironbark, have been used for the drying of 13mm and 26mm red beech boards. The results of these verification-drying trials showed that surface checking and internal cracks occurred. Clearly, these optimised schedules failed to achieve the desired results.

There are two major differences between the two types of drying schedules. Compared to the initial step-wise drying schedule the optimised drying schedules have the following features:

1) A large wet-bulb depression before the average moisture content of the board reaches its fibre-saturation point.
2) The dry–bulb temperature reaches its maximum allowed value before the board local moisture content drops below its FSP.

The wet-bulb depression is given a value over 10 °C at a very early stage of the drying schedule when the sample board moisture content is still large (above 75%). It comes down to around 5 °C shortly thereafter. The early large wet-bulb depression means a low relative humidity and hence would reduce moisture loss more quickly and cause a larger shrinkage-related stress on the sample board.

Regarded as a heat-sensitive species, red beech timber has been traditionally air-dried till its average moisture content is close to its FSP, before being kiln-dried to required moisture content of around 12% using mild kiln conditions in order to minimise degradation. However, the drying schedule initially predicted by optimisation program using the parameters taken from that for the Australian eucalyptus species

raises the dry-bulb temperature to its maximum allowed value defined by the program at the start of the schedule.

The two features of these drying schedules indicated that somehow the stress-related parameters used might not be appropriate as the actual drying trials using these schedules showed severe cracks in the sample boards. The only way to achieve a more useful drying schedule is to obtain the corresponding parameters for New Zealand beech timbers.

The mechanical tests were aimed to collect all the parameters needed for the optimisation program. The results can be found in an earlier chapter (Chapter 6).

§8.2 The optimised drying schedules with new parameters obtained from mechanical tests of red beech timber

With the observed mechanical properties of New Zealand red beech timber from the mechanical tests using the climate chamber, the optimisation program was re-run to generate drying schedules for red beech timber with different initial moisture contents and thickness. The optimisation program generated a short-span (the default value is 4 hours in the program) step-wise drying schedule, as well as the stress and moisture-content profiles of the sample board throughout the drying process.

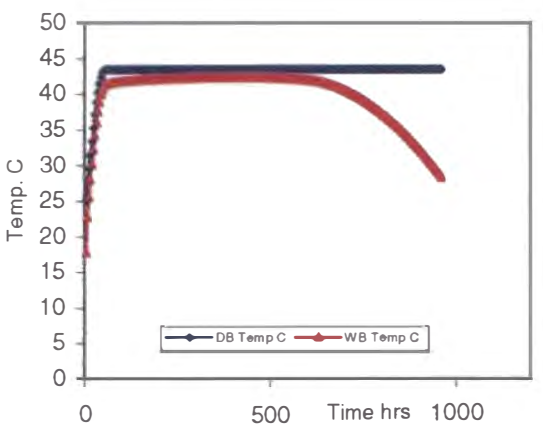

Fig.8-1a
Optimised drying schedule
(temperature vs time)

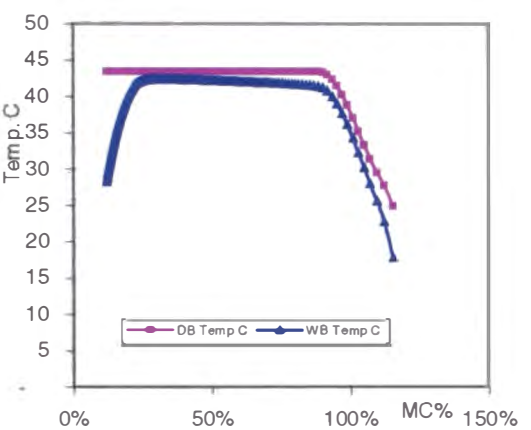

Fig 8-1b
Optimised drying schedule
(temperature vs moisture content)

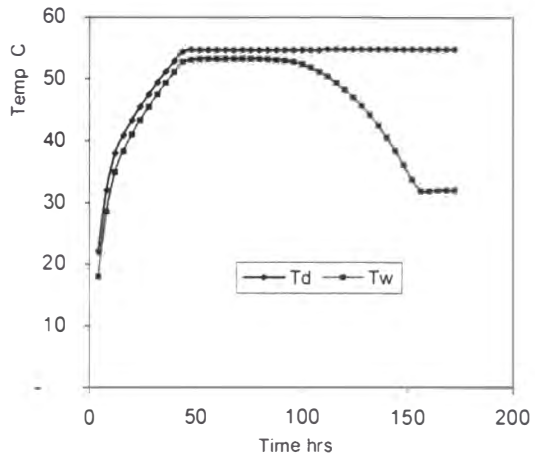

Fig.8-2a

Optimised drying schedule

(temperature vs time)

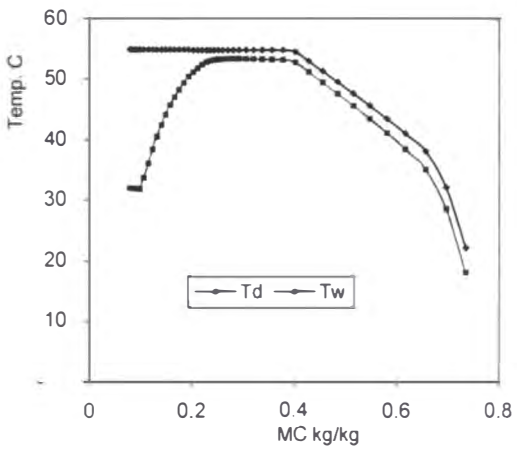

Fig 8-2b

Optimised drying schedule

(temperature vs moisture content)

Figures 8-1a and 8-1b show the optimised drying schedule for 26mm thick red beech timber boards with an initial moisture content of 120%. Figures 8-2a and 8-2b show the optimised drying schedule for 13mm thick red beech timber boards with initial moisture content of 80 %.

The moisture profile throughout the drying process was used when the validation of the drying schedule was assessed later in the drying trial.

The moisture profile is derived from the moisture contents calculated for each of the finite layers (in this study, 24) at each time step of the whole drying process. From the moisture-content profile, important information like the movement of the penetration front, and the characteristic drying curve and the drying stage when all local moisture content drops below fibre-saturation point could be obtained.

The moisture profile also gives the board-averaged moisture content profile, which can be compared with the actual average moisture content profile in the drying trial. The comparison was counted as one method to measure the validation of the optimisation program.

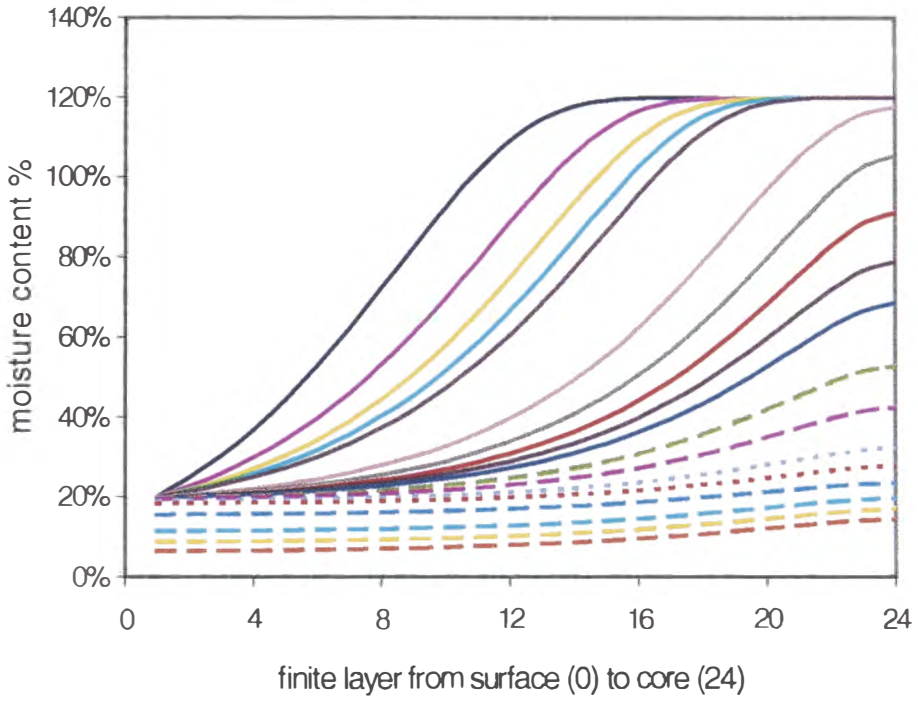

Fig 8-3 The predicted moisture profile of the whole course of drying a 26mm red beech board

The moisture profile was used to calculate the relative moisture content rate for the characteristic drying curve, which was discussed in previous in §5.4.

§8.3 The actual drying results using the optimised drying schedules

The optimised drying schedules have been used to define the drying conditions of drying 13mm and 26mm red beech board samples in the small drying chamber. The drying schedule, including dry-bulb temperature, wet-bulb temperature, and the correlation of the moisture content with the temperature and relative humidity was programmed with a software named Genis used in the control system of the drying apparatus. The control program sets the drying conditions of dry-bulb temperature, wet-bulb temperature and relative humidity according to the moisture content and the thickness of the timber board.

The drying trial which used the optimised drying schedule aimed to verify the validity of the optimisation program and its predictions for the drying schedules. The verification was based on the observation (or the lack thereof) of the deformation of the dried timber board, namely internal cracks, surface checking and collapse and shrinkage rate, as well as the difference between the predicted drying time and that of the drying trial.

Because the initial board conditions of the timber board may be different in any given case, the optimisation program would predict a different drying schedule for that board. As a result, the control program had to be modified each time to suit the timber board conditions, or some limiting condition taken to meet the range of moisture contents expected. The initial average moisture content was obtained by measuring the moisture content of sample from similar position from the large board which the drying sample was sawn from. The sample board was usually dried to an average MC of 12% as the final moisture content in the optimisation program is set at 12%.

The drying curve of the actual drying trial was compared to that which was predicted by the optimisation program.

The actual drying cure was obtained from a drying trial once the drying schedule predicted by the optimisation program had been implemented and programmed into the control system, in which both dry-bulb temperature and wet bulb temperature can be controlled within ± 0.5 °C and changed according to the monitored moisture content of the sample board. The sides of the sample board were sealed with Altex Devoe paint, as in the previous drying trials.

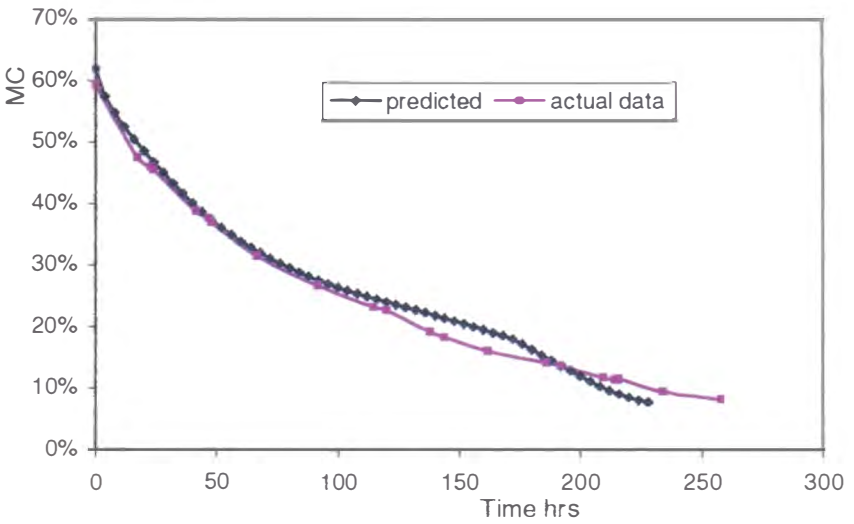

Fig. 8-4 Comparison of drying curves between gram-predicted and actual drying trial

From Fig. 8-4, it can be observed that the predicted drying curve matches the actual drying curve when the average moisture content of the sample board is above the fibre-saturation point. However, when the average moisture content drops below FSP, the drying curve is flatter than the predicted one, which slightly prolongs the last-stage drying time.

§8.4 The deformation of the dried samples with the optimised schedules

The aim of the optimisation program is to shorten effectively the drying period of the previously devised step-wise drying schedule without causing unacceptable degradation of the timber boards. The following features were examined on the dried sample board with the optimised schedules:

- Shrinkage and shrinkage-related warping

Shrinkage, which occurred in the dried sample board, causes its major dimensional change. Warping was also found due to the possible effect of the differential shrinkage rates in the radial and tangential directions of the grain.

The shrinkages of the dried samples were measured without any further conditioning procedure. Therefore theoretically the measured values should be higher than the values used in the optimisation program, because other types of deformation like collapse and time-dependent deformation were considered not to occur under such mild drying conditions. The shrinkage values used in the optimisation program were for purely irrecoverable shrinkage.

The samples used in this trial were chosen randomly from the samples available, which means they were either approximately quarter-sawn or flat-sawn. The shrinkage observed was 6.50 ± 0.25 % in the transverse direction (Chapter 5). It is higher than the value of the 4.5% (Grace 1996), which is believed to be the irrecoverable shrinkage of the red beech timber.

Slight warping was found from the dried sample boards under optimised drying schedules. Since the samples used in the verification drying trials were chosen regardless of their growth-ring orientation, the curvature of the sample boards varied slightly as well.

The following feature were noted:

- Collapse

No visually visible collapse was observed in the sample boards with the thicknesses of either 13 mm or 26 mm dried under the optimised drying schedules.

- Surface and internal cracks

The sample boards dried under the optimised drying conditions were examined visually for possible surface checking and the method of slicing the boards was used to examine internal cracks, but no such cracks were found, and

§8.5 The energy efficiency of the optimised drying schedules

The optimised drying schedules for different thicknesses that are to be used in the dehumidifying drying kilns, their energy efficiencies will be discussed in the next chapter which involves the comparison of the energy efficiency of the conventional kiln and dehumidifying kiln.

§8.6 References

Carrington, C. G. Sun, Z-F., 1999 Dehumidifier dryers for hard-to-dry timbers, 19th IIR Congress, Sydney, Australia.

Sun, Z-F., Carrington, C. G., 1994 Determination and application of characteristic drying-rate curves in dehumidifier wood drying, 5th IUFRO Conference Rotorua New Zealand.

Chapter 9

The energy efficiency of the optimised drying schedule

§9.1 Introduction

Drying of wood products is an energy-intensive process, particularly in use of thermal energy. This study aims to generate drying schedules which might be used in a dehumidifying kiln, which utilises the latent heat from the water vapour evaporated from the timber boards and therefore theoretically needs less thermal energy to maintain the kiln conditions than in a conventional unit.

§9.2 The evaluation of the energy efficiency for drying 40mm red beech timber

Carrington *et al.* (1999) assessed aspects of the design for a dehumidifier kiln drying 40 mm green red beech (*N. fusca*) timber boards using a dynamic process model. The results show that the drying period can be extended to 100-200 days without incurring high energy costs, while the on-site energy use is small relative to a conventional heat-and-vent kiln. By using the drying schedule supplied by this thesis as well as the principal parameters of a dehumidifying system, the model predicts the drying time of 40mm thick red beech boards from initial average moisture content of 100% to final moisture content of 12% to be 99 days (Carrington *et al.* 1999), which well matches the 100-day drying time from the strain-limited model used in this thesis.

Carrington *et al.* (1998) also compared the energy efficiencies of different system configurations, including heat-and-vent kiln and dehumidifier kiln with different reference capacities.

Table 9-1 shows a summary of performance data for the four different kiln configurations:

Table 9-1 performance data for the four different kiln configurations (Carrington *et al.* 1999)

configurations	*Time (days)*	*Total energy Input (kWh)*	*Direct electric Heat (kWh)*	*Kiln fan (kWh)*	*SMER (kg/kWh)*
(a) heat &vent	**85**	**54324**	**49248**	**5076**	**0 .61**
(b) reference dehumidifier	**99**	**15650**	**3728**	**5803**	**2 .13**
(c) 80% reference dehumidifier	**107**	**11593**	**1325**	**1868**	**2.88**
(d) 40% reference dehumidifier	**201**	**13207**	**1699**	**3518**	**2.52**

The results of these workers indicate that well-designed dehumidifying kilns provide an opportunity to kiln-dry *N. fusca* under controlled conditions with significant saving in process costs. Even though there are factors that would influence the energy efficiency of the dehumidifier kiln, compared with the heat-and-vent kiln, the key index of the energy efficiency of the system (SMER) shows that the dehumidifier kiln is far more energy-efficient.

§9.3 The evaluation of the energy efficiency of the optimised drying schedules

The energy efficiency of the optimised drying schedules for red beech timber also has been assessed by means of the dynamic model developed by Sun *et al.* (1998). for drying green untreated 26mm thick red beech board (from 77% to 12 % moisture content). By controlling the dehumidifier, the supplementary heating and venting, good compliance has been obtained with the optimised drying schedule. The stack velocity was 1.5 m/s, supplementary heating was 0.6 GJ/m^3 timber, costing approximately \$16/m^3. Carrington *et al.* (1998) concluded that "it indicates it is feasible to kiln-dry red beech and other hard-to-dry species from green under a very slow schedule without incurring high energy costs" and "by comparison with uncontrolled air-drying followed by kiln-drying, this application of dehumidifier driers is promising in terns of drying time, cost, and product quality."

§9.4 References

Carrington, C. G., Sun., Z-F., 1999 Dehumidifier dryers for hard-to-dry timbers, 19th IIR Congress.

Keey, R. B., 1992 Drying of loose and particulate materials, HPC.

Keey, R. B., Langrish, T. A. G., Walker, J. C. F., 2000 Kiln-drying of lumber, Springer-Verlag, Berlin , pp315.

Sun, Z. Carrington, C. G., 1996 Determination and application of characteristic drying-rate curves in dehumidifier wood drying, 5th IUFRO Conference.

Chapter 10

Discussion

In this study, hot-water soaked and untreated red beech boards were used in initial drying trials, which were designed to verify the feasibility of drying New Zealand red beech from green conditions. Then, the selected drying schedules were optimised by the strain-limited optimisation program and the tests for its mechanical properties were carried out and the test results were used in this optimisation process to ensure the reliability of the optimised drying schedules. Finally the optimised drying schedules were put into actual tests for verification and for assessment of energy efficiency in the dehumidifier drying system.

§10.1 Initial drying trials

The initial drying trials were developed for drying schedules with a review to dry New Zealand red and hard beech from fresh conditions with acceptable degrade and energy efficiency. The selected drying schedules were chosen from the existing drying schedules for deformation-prone and temperature-sensitive timbers (NZFS. 1974, Rice and Gatchell 1983). The quality of the dried beech timber using these drying schedules meets the New Zealand NZS3631: 1981 with respect of degrade. (See Appendices 1)

Instead of air-drying, which is thought to be a mild way of reducing the initial moisture of the board and produce less stress to avoid severe degradation, the initial step-wise drying schedules adapted high relative humidties and lower wet and dry-bulb temperatures to reproduce similar effect. The degree of mildness of the drying schedule will affect the effectiveness of removing the initial moisture, the drying rate and will eventually affect the energy efficiency of the drying schedule. The initial drying schedules were optimised by using the optimisation program.

The objective of minimising degrade preceded studies of energy efficiency and cost effectiveness. The project requires that the method be suitable for a dehumidifying-kiln system, which is considered to be energy-efficient when drying hard-to-dry timbers above the FSP and which could be useful as the beech timbers are required to be dried from green conditions.

§10.1.1 Selected drying schedules and their effectiveness

Reducing possible degradation by using mild drying conditions, can be observed visually. However, the effectiveness of the drying schedule can only be reflected from the drying curves recorded during the drying trials.

The drying curves of drying hot-water treated and untreated red beech samples have shown that the pre-treatment enhances drying rate significantly (Figs 3-2, &3-3).

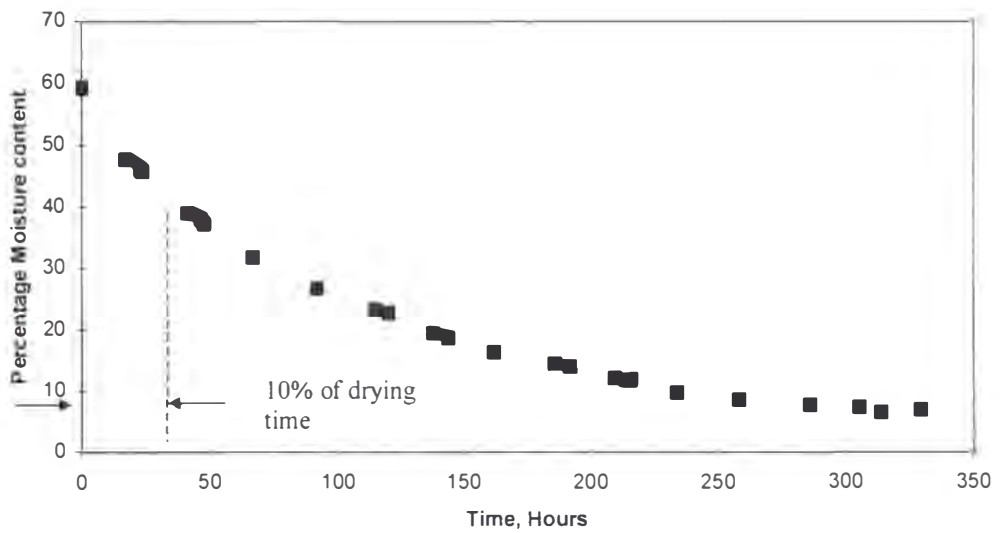

Fig 3-2 Moisture-loss curve for red beech timber dried with moisture-content control schedule

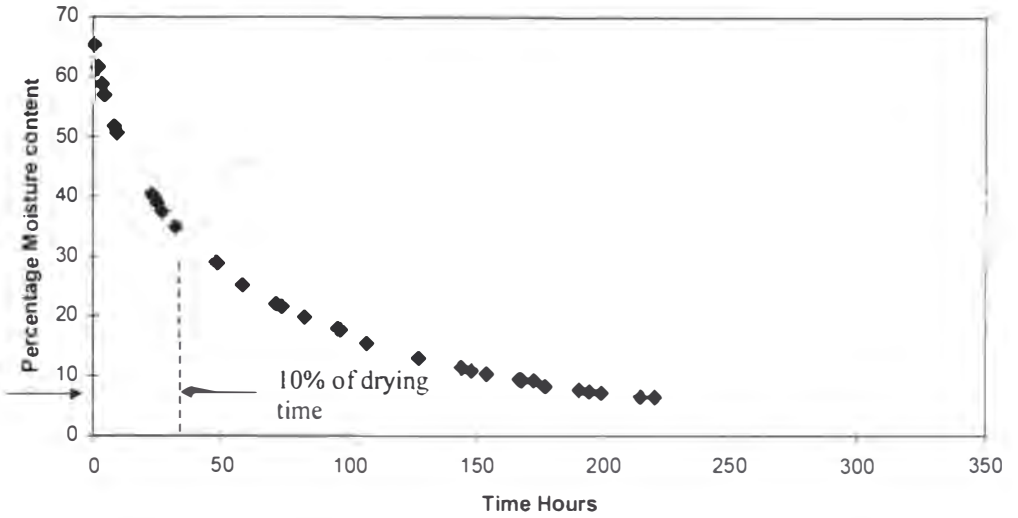

Fig. 3-3. Moisture loss for hot water-soaked red beech timber dried with moisture-content control schedule

With the moisture-content control schedule after 10% of the drying time the moisture content of the dried samples had fallen by over one-third for the control samples (from 62% to 40 %) and nearly 50% for the hot-water soaked samples. The time taken to dry both hot-water soaked and control sample to their fibre-saturation point (about 25%) took less than one-third of the time to dry the samples to 10% moisture content (Fig 3-2, 3-3).

A comparison of Figs 3-2, 3-3 shows that reduction of the drying length of time for 13-mm thick red beech board occurred mainly in the initial drying stages when the average moisture content of the board is above fibre-saturation point.

It takes about 100 hours to dry a untreated 13-mm thick board from about 62% of moisture content to 25%, while it takes only 55 hours for the hot-water soaked sample. However, there is little difference in the time in drying treated and untreated samples from 25% to final 12% average moisture content. Although hot-water soaking enhances the permeability in the early stage of the drying, there is no significant impact in the later stages when the drying rates are inherently low and thus the benefit is negligible.

The drying schedule used in the trials required the drying temperature early in the schedule to be lower than 30 °C while the moisture content of the entire sample boards is above the fibre-saturation point. This is a feature of both the traditional air-drying and conventional kiln drying. It has proved effective in reducing deformation in drying New Zealand red and hard beech timbers. This practice was adopted in the subsequent continuous drying schedule development.

The deformation of the dried boards derives from the dimensional shrinkage. The major form of the deformation is warping caused by the differential shrinkage in the axial and transverse directions. Small surface checks could occur in the early stage of the drying process, when the surfaces start to dry and the initial surface stresses cause this phenomenon. They even occur while the control sample was air-dried (Chapter 4). All the surface cracking closed again after stress-reversal, a phenomenon induced by the difference in shrinkage across the depth of the dried board.

The mild stepwise drying schedules not only included low temperatures but also high relative humidity. The drying schedules also have limited the airflow rate to 1.5 ms^{-1}, as the external convection is not rate-determining. The high relative humidity prevented the board from surface checking early in the schedule, which happened to two of the twelve control samples air-dried (Chapter 4). The slow drying schedule used made the recession of the wet-line slow and a virtually flat moisture content profile was found as a result (Fig. 5-5). The almost flat moisture content profile in turn reflected the smaller shrinkage stresses caused by the difference of the moisture content of different depths in the timber board. Visible deformation therefore should be also less.

Neither internal nor surface checking was found for all the dried samples, since this mild drying schedule had little or no impact on the quality of the drying product. It can be concluded that New Zealand red and hard beech timber can be dried from green conditions in a low-temperature kiln.

§10.2 Pre-treatment

Of several methods of pre-treatments, only hot-water soaking process has been widely used as an effective way to shorten the drying of New Zealand red and hard beech timbers and with little evidence of further deformation.

The experiment showed that hot-water soaking can reduce the ultimate tensile strength and modify some of the mechanical properties such as modulus of elasticity and ultimate tensile strain.

Mechanical tests show that if the hot-water soaking lasts as long as 8 hours at a temperature of 80 °C, the ultimate strength of the red beech boards decreases by about 12.5% (Figure 6-5). The duration of treatment and the temperature play a very important part in affecting the mechanical properties of the heated timber boards. Principally, the higher the temperature and longer the treating period, the severer the deformation and shorter the subsequent drying process (Haslett and Kininmonth 1986).

Hot-water soaking enhance the drying rate, which has been explained by the increase of the permeability due to the extraction or rearrangement of the extractives (Kininmonth 1974). There may be further reasons, since it has been shown that the diffusion coefficients of the timbers are increased by hot-water soaking.

The increase of the diffusion coefficient of New Zealand red beech timber as a result of hot-water soaking has been reported, (Ross 1986, Barnes 1988, Crawshaw 1988) but in most cases, it was only described in terms of decreased drying time. It has been reported that the drying time can be reduced by as much as 50%. The methods of hot-water soaking were differently in these studies (Grace 1996, Choong *et al.*1996), and deformations to some degree have also been reported in drying of these hot-water soaked sample boards.

The diffusion coefficient evaluated from the same drying experiments also increased by 28% over the control value, but as the values from the two coefficients were evaluated from a temperature-changing drying schedule, the values of the diffusion coefficients should only be considered indicative (Chapter 7).

Hot-waterer soaking causes discolouration of the boards. This is the result of certain kinds of chemical reactions of the extractives. Oxidation is believed to be the major chemical reaction to cause this change of colour. A simple test proves the important role of oxygen: a sample board dried at 100 °C in a space filled with air has a much darker shade comparing to that of the board soaked in 100°C for the same length of time.

However, the discolouration caused by hot-water-soaking would not be a concern for the commercial kiln operators if the colour of the timber is consistent (Clarke, Belfast Timber Kilns, pers. comm.).

§10.3 Characteristic drying curves

The characteristic drying curves both hot-water socked and untreated red beech boards are needed for evaluation of the energy efficiency of the optimised drying schedules developed for red beech timber (Chapter 9).

Two ways were used to obtain the characteristic drying curves for New Zealand beech timbers: one is from drying trials, the other is from the moisture profiles predicted by the optimisation program. Comparisons can be made between the two methods, and that could be another method to assess the validation of the optimisation program by looking into the differences between the curves from the two methods.

The characteristic curves obtained from the above methods have similarities, in particular both the curves showed an irregularity near the fibre-saturation point. The moisture content profiles also reveal that the penetration front reaches the mid-plane at the same time in the drying process (Chapter 8).

§10.3.1 Penetration front / wet line

When a timber board is dried from the green fresh condition, the surface of the board starts to dry out, and there will be a moment when the moisture at the surface reaches the fibre saturation. It is quite difficult to determine the movement of the wet line as drying progress. However, the optimisation program makes it possible to predict the movement of the wet line as the board dries. The detailed moisture-content profile makes it possible to calculate the position of the front and reveal this phenomenon.

There are some other characters of the predicted drying curve which yet to be explained, some of which seem to be echoed by the experimental drying curves. When the average moisture content of the board drops to around its FSP, the normalised drying rate has a sudden rise before falling again as expected. This actually cannot be explained by the theory of the characteristic drying curve.

§10.3.2 Characteristic drying curves observed from simulation of the drying process of Nothofagus fusca in the optimisation program

The optimisation program is an elastic model of wood behaviour, it utilises the information of drying conditions and the timber properties and predicts the moisture profiles throughout the drying process. The moisture profiles are consisted of different moisture contents at each of the infinite layers from the surface to the core of the timber board, which are defined by the program at the beginning of the program. The moisture profiles can be verified by use of the fitting program to a very good accuracy (See Chapter 7).

This normalisation of the drying rate based on moisture content profiles predicted by the optimised drying schedule, which is a 4-hour stepwise drying schedule, predicted by the optimisation program according to the initial condition of the boards as well as the species properties.

The features of the characteristic curve for the optimised drying schedule are:

- An unusual feature close to $\Phi=1$ which is an artefact of the strain-limited schedule program.

- The end of the penetration period, when the core moisture content starts to fall, occurs at $\Phi \approx 0.82$.

- For much of the subsequent drying, the kinetics are described by a first-order process (rate ≈ moisture difference). This starts when wet-bulb temperature has reached its maximum value.

- There is a small irregularity when the core moisture content reaches 30%, a little higher than the fibre saturation point (25%) assumed. The reason for the irregularity is not known.

§10.4 The strain-limited optimisation program and optimised drying schedules

This optimisation program has been used successfully in producing improved drying schedules for Australian eucalyptus timbers like ironbark and yellow stringybark and spotted gum that are difficult to dry (Langrish *et al.* 1997, 1998).

The program assumes that under mild drying conditions, the boards will behave elastically when stressed by the shrinkage-related internal forces. It also assumes that under these drying conditions the time-dependent strains are negligible.

The first part of the program utilises experimental drying data to obtain some of the needed parameters of the program like scaling factors. This part of the program is called the fitting program, because the purpose is to show the accuracy of the drying model in predicting the moisture profile at each step of the drying process. The fitting results (figure. 7-7) in previous chapter (7) showed that the diffusion model is capable of describing the moisture movement of New Zealand beech timber under low-temperature drying. The predicted moisture profile fits to the actual test results

particularly well when the average moisture content is above fibre-saturation point before it reaches the final drying stage.

The optimisation program requires some information on physical and mechanical properties, including basic density, FSP moisture content and sample surface and average moisture contents. It also needs further information which was not available until the mechanical properties of the red beech timber had been tested during this thesis. Some of the parameters like diffusion coefficient in the tangential / radial direction, modulus of elasticity perpendicular to the grain and relationship of MOE with temperature and moisture contents were taken from the corresponding values of the eucalyptus species (Langrish *et al.* 1997 1998), while others were chosen from previous studies on New Zealand beech timber (Grace 1996).

The tangential shrinkage coefficient is usually regarded as the largest among coefficients in the three dimensions, and was used in the program. The value of 4.5% was chosen for the shrinkage from green to 12% moisture content, the initial shrinkage value input to the optimisation program, and was based on the study of Grace (1996) on irrecoverable shrinkage of hard beech boards. Because this optimisation program uses an elastic model, which excludes other type of deformation such as collapse, the value for the shrinkage should only be the irrecoverable shrinkage.

The diffusion coefficient used in the optimisation program is taken from previous studies on beech timbers. (Ross 1986, Barnes 1988, Crawshaw 1988, Grace 1996). Average values were chosen the control samples and for the hot-water soaked samples.

The results from running the optimisation program using these parameters show some unreasonable features:

The optimised drying schedule has a low starting dry-bulb temperature, however, it also allows an unexpectedly large wet-bulb depression, as may be seen in Fig 10-4.

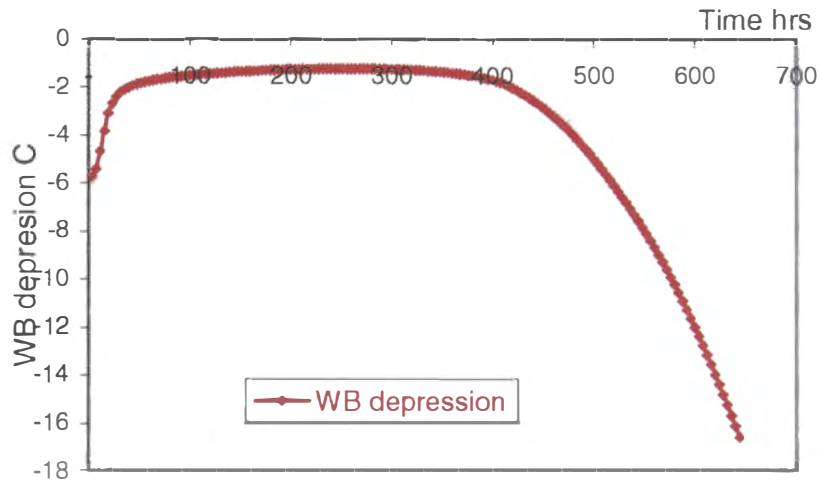

Figure 10-4 Wet-bulb depression in the optimised drying schedule.

Some of the parameters, can be set to a slighter lower (like the maximum allowed strain) or higher value (like the final surface moisture content) to eliminate the possible degrade. By slightly changing the parameters, the optimisation generate drying schedules with slightly milder conditions two drying schedules were obtained from running the optimisation program, which were used for verifying tests. The tests showed that all the samples have visible surface checks or internal cracks (Fig. 10-5), which suggests the " optimised" schedules were still too severe, unlike the early tests under mild conditions.

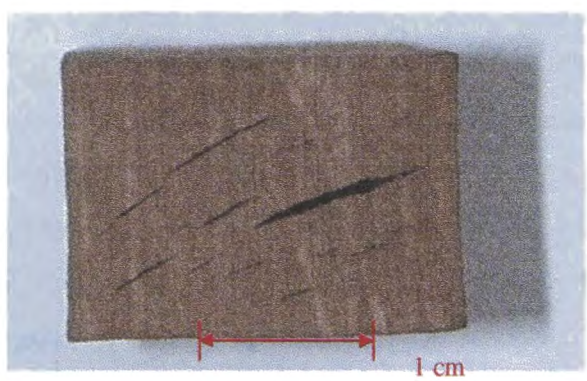

Figure 10-5 Checks found in the red beech samples using drying schedule in Figure 10-4.

The deformation appears as large cracks up to 20mm long within a growth ring between earlywood and latewood.

Factors that may affect the validity of the optimised schedules include:

- The strain-limited model used in the optimisation program allows the boards to be subjected to a maximum strain that has been defined in the program. Languish *et al.* (1997) used the 2% value as the maximum strain in predicting drying schedules for some Australian eucalyptus timbers and its value was used in the optimisation program for New Zealand beech timbers (chapter 7). However as the specific value for New Zealand beech has yet to be found. A 2% strain almost certainly exceeded the appropriate value for New Zealand beeches.

- The fibre-saturation point for red and hard beech. The original default value for the FSP moisture content was 30%. However, according to Shubin (1990) it may vary with the basic density of the wood (Shubin 1990). *Nothofagus fusca* (red beech) from Murchison and Reefton area has a basic density of 505±25 kgm^{-3} while being 555±25 kgm^{-3} from elsewhere. The red beech boards used in this project were in the latter category. The fibre-saturation point for some hardwoods seem to be slightly less than the mean value for softwoods of 30% (Shubin1990). Since the European beech (*Fagus sp*) are closely related to the Southern beeches (*Nothofagus spp*), a figure of 25% appears to be the appropriate value for the FSP of red beech. This figure was subsequently used in the optimisation program.

- The modulus of elasticity in the transverse direction used in the optimisation program is 420 MPa at oven-dry conditions, this value is that taken for the Eucalyptus timber by Langrish *et al.* (1997). The program also defines the Young's modulus-temperature/moisture content relationship using empirical equations which may need verification and modification for New Zealand beech timbers (Langrish *et al.* 1997).

- The degradation of the dried boards may be cause by incorrectly defining the schedule through the inaccuracy of these parameters used in the optimisation program, but there are also other factors that should be considered:

- Tension / compression wood frequently occurs in New Zealand beech timber, the appearance of these tissue would likely to effect the physical and mechanical properties of the boards.

- Growth stresses are also likely to influence the drying process, as the existence of growth stresses would reduce the resistance of the shrinkage-related stresses during the drying process.

§10.5 Mechanical properties and drying behaviours of New Zealand beech timbers:

To supply the required parameters for the optimisation program is the main purpose of measuring the mechanical properties of red beech timber in this study. The mechanical properties measured include the ultimate tensile strength (MOR), ultimate tensile strain, Young's modulus (MOE) in the radial and tangential directions at different moisture contents and temperature level. The mechanical properties of both hot-water soaked and untreated red beech samples so that drying schedules developed for the two types of red beech boards can be optimised.

§10.5.1 Proportionality in the transverse direction:

Timber is not a perfectly linear elastic solid up to the proportional limit. The microstructure of wood is quite different from that of a homogeneous body like metal. These differences may be reflected in the load-deformation curves seen in the mechanical property tests (Figs 6-7 to 6-21).

The improved the resolution of the data recording, provided a better chance to examine the load-deformation relationship of red beech timber under tensile stress in

its transverse direction (Figs 6-7 to 6-21). When loading the specimen in the longitudinal direction, the stiffness remains constant with increasing stress until the elastic limit is reached. Thereafter, with further loading, the material behaves plastically, the stiffness become less as the material becomes plastic as the fibres slide pass each other. On the other hand, when loading the specimen in the cross-grain direction, wood deforms as a nonlinear-elastic body in the elastic region, but the gradient varies abruptly at an apparent elastic limit.

If the sample is hot-water soaked beforehand, the transition from a non-linear is less marked, with a reduction in gradient over the tested loading range. Hot-water soaking for instance, provides a way to reduce the initial high modulus (so less possibility to check), but not without a cost. According to Grace (1996), the strength of the timber decreases as a result of the treatment, which also means an increase in the chance of degradation if severe drying conditions are applied.

The moduli of elasticity taken from the oven-dry eucalyptus species which was used in the optimisation program is 420 MPa (Langrish *et al.* 1997), and using this in the empirical equations, one could calculate the value of the Young's moduli of these samples at different moisture contents and temperature. Comparison showed that the Young's moduli of red beech were much higher than those of the Eucalyptus species (Langrish *et al.* 1997, Musch 1996). Using these empirical equation which are part of the optimisation program to express the relationship between temperature, moisture content with Young's modulus, the Young's moduli of Eucalptus timbers are calculated to be about 250 MPa for sample with moisture content above fibre-saturation point. The test results showed that the Young's modulus of the red beech timber is considerably higher than suggested by the work with eucalyptus (Figure 6-22). Tests showed that the Young's modulus for New Zealand red beech timber was higher than 450 MPa.

Red beech samples with different moisture contents were tested under tensile stress. Nearly all the test results showed some degree of non-linear elasticity at the very early stage of the loading, which is usually considered to be the elastic period with a linear correlation between the stress and the strain. The tests that used the accurate extensometer had also showed similar pattern, which excludes possible system errors.

These results may be explained to a certain degree by the non-linear elasticity of the wood.

The non-elasticity might be explained by its microstructure, which seen from the transverse directions especially in hardwood species, shows much greater difference to the common solid structure of an elastic material than that in the grain direction. This type of microstructure, as well as the complicated cell wall which is fabricated by cellulose, hemicellulose and lignin polymers may cause some significant creep, even when the stress applied is relatively low, to distort the elasticity of the samples.

The results also agreed with the practical experience in drying red and hard beech timbers that not only lower temperature but also high relative humidities are required when these timbers are dried from green conditions.

§10.5.2 Tensile strength-moisture content relationship

The relationship of moisture content and strength has been expressed in some textbooks (Dinwoodie 1989) indicating that the fibre saturation point will be that position which divides the range where the strength of the wood start to rise when the MC is lower than that of FSP and where there is no change when the MC is higher than that of FSP.

It has also been reported that the relationship of moisture content to the longitudinal modulus of elasticity also has similar pattern as the MC-compression strength relationship (Dinwoodie 1989 Keey *et al.* 2000). Fig. 2-3 shows that if the compressive stress applied is relatively small, the value of MOE is independent of moisture content when it is above 50%. But Fig. 2-3 also suggests that the effect of increasing moisture content above FSP on the modulus of elasticity and rigidity is to give high values.

The data for the modulus of rupture of *Pinus radiata* at 20 °C in the cross-grain direction are consistent with a minimum value at about the fibre-saturation point, and rising above FSP. (Keep 1997)

The test results of the tensile failure strain showed similar pattern as that of strength, i.e. FSP is the condition where the tensile failure strain has a minimum value (figure 6-4).

§10.5.3 Tensile strength-temperature relationship

Test results in Chapter 6 showed a trend of a minimum strength value of red beech at temperature about 29 °C at different moisture content levels. There is not yet a good explanation for the minimum value of tensile strength and strain at the temperature close to 29 °C in the low-temperature range (20 to 55°C). One assumption is that the increasing rate of polymerisation of some of the polyphenolic compounds will increase the stiffness, but as the temperature reaches about 30 °C or over the softening of the extractives like fatty acids and waxy material will help to decrease the stiffness. When the temperature over 55 °C, the tensile strength of red beech timber starts to decrease dramatically due to the reason that some of the constituent polymers of timber like lignin start to soften.

§10.5.4 The influence of pre-treatment on NZ beech timbers

Hot-water-soaking the red beech samples affects not only the tensile strength in the transverse directions Figure (6-5); it also affects the value of corresponding strain Figure (6-6). The possible changes caused by the treatment are rearrangement of the extractives, hydrolysis of the constituent polymers of the wood tissue, excessive thermal stress causing irrecoverable thermal strain.

Dinwoodie (1989) shows that thermal expansion of wood in the radial and tangential directions is usually 8 to 10 times higher than that of the grain. The softening of wood polymers like lignin at certain temperature level could add to a higher value of the timber thermal expansion rate beyond the thermal expansion of the wood substance. There could be a possibility when the thermal strain is raised above the value of the plastic limit, and some types of deformations like collapse and cleavage of the fibre cell, occur before the timber moisture content falls below the fibre-saturation point.

§10.6 Energy efficiency of the optimised drying schedules in a dehumidifier kiln

Dehumidifier drying presents a unique opportunity to improve the energy efficiency of product drying by recycling the latent and sensible heat requirements of the process (Carrington and Bains, 1988). However, dehumidifier technology has had only limited acceptance in the wood industry largely because of operational difficulties, such as erratic and often poor performance, mechanical failure, and lack appropriate drying schedules (Bannister *et al.* 1994).

Using the optimised drying schedule in this study, Carrington *et al.* (1998) dried green untreated 40 mm red beech boards from 77% to 12% moisture content within 35 days. The energy used by the fans, dehumidifier and supplementary heating was 0.6 GJ/m^3, costing approximately \$16/m^3. This indicates it is feasible to kiln dry red beech and other hard to dry species from green under a very slow schedule without incurring high energy cost (Garrington *et al.* 1998).

In a practical dehumidifier wood drying kiln, the drying process in side the wood stack and the process in the dehumidifier can not be considered independently, since the wood stack and the dehumidifier are closely linked with each other. Moreover, other operating and design factors such as other control strategy, the drying schedule, the load-to capacity ratio, the fan and air flow design, the air pre-heater design, the kiln insulation and venting etc..., have influence on the drying process as well. The energy efficiency of the drying system, therefore, will also be affected by those factors. The assessment of the energy efficiency of a drying schedule is only comparable in each individual dehumidifying drying unit.

§10.7 References

Barnes, P.C.I., 1988. Moisture diffusion in Red and Hard Beech during drying. Bachelor of Engineering Report, Department of Chemical and Process Engineering, University of Canterbury.

Carrington, C. G., Bains, P. G., 1988 Second law limits in convective heat pump drier. Int. J. Energy Res., 12 pp 481-494.

Carrington, C. G., Sun, Z-F., Bannister, P., Chen, G., 1998 Dehumidifier drier – what to expect and pitfalls to avoid, WTRC workshop, Christchurch.

Chawshaw, A.J., 1988. Pretreatments to hasten the drying of Hard Beech. Bachelor of Engineering Report, Department of Chemical and Process Engineering, University of Canterbury.

Choong, *et al.*, 1996 Effect of steaming and hot-water soaking on movement of moisture in hardwood during drying, 5th IUFRO International wood drying conference.

Clarke, N., 1996 Personal Communication, Belfast Timber Kilns Ltd.

Dimwoodie, J. M., 1989 Wood: Natures cellar, polymeric, fibre-composition, Institute of metals London.

Grace, C., 1996 Drying characteristics of *Nothofagus truncata* heartwood, M.E. thesis, University of Canterbury.

Gunzerodt, H., Walker, J.C.F., Whybrew, K., 1986. Compression rolling and hot-water soaking: effects on the drying and treatability of *Nothofagus fusca* heartwood. New Zealand Journal of Forestry Science, 16(2) pp223-36.

Haslett, A.N., Kininmonth, J.A., 1986. Pretreatments to hasten the drying of *Nothofagus fusca*. New Zealand Journal of Forestry Science, 16(2) pp237-46.

Keep, L-B., 1998 The Determination of time-dependent strain in *Pinus radiata* under kiln-drying conditions, M.E. thesis, Department of Chemical & Process Eng. Univ. of Canterbury.

Keey, R. B., Langrish, T. A. G., Walker, J. C. F., 2000 Kiln-drying of lumber, Springer-Verlag, Berlin , pp315.

Kininmonth, J.A., 1971. Effect of steaming on the fine structure of *Nothofagus fusca*. New Zealand Journal of Forestry Science, 1(2) pp129-39.

Langrish, T. A. G., Brooke, A. S., Davis, C. L., Mush, H. E., Barton, G. W., 1997, An Improved Drying Schedule for Australian Ironbark Timber: Optimisation and Experimental Validation, Drying Technology **13** (1) pp. 47-70.

Musch, H. E., Langrish, T. A. G. Brooke, A., 1996, Model predictive Control of Timber Drying, Accepted for publication at IFAC World Congress, San Francisco.

Ross, D.A., 1986. Investigating the moisture movement of Hard Beech during drying. Bachelor of Engineering Report, Department of Chemical and Process Engineering, University of Canterbury. ,

Chapter 11

Conclusions and recommendations for further work

§11.1 Conclusions

From the results and studies presented in this thesis, some conclusions can be drawn:

1. The stepwise drying schedule (Table 5-2), which has a low temperature and high relative humidity at the beginning of the drying stage, and relatively higher temperature and low relative humidity at the later stage, is able to dry New Zealand red and hard beech timbers from the green condition. The dried sample boards using this schedule only have slight warping caused by the differential shrinkage in the three directions. The comparison with the air-dried sample (open air, office environment), which had surface checking at an early stage which later disappeared because of the stress reversal. This difference shows the importance of early low temperatures and high relative humidities to the quality of red and hard beech boards.

2. The stepwise drying schedule can also dry red and hard beech boards, which have been hot-water soaked at 80 °C for 4-8 hours, without significant deformation.

3. Using a hot-water soaking pre-treatment, the drying time of both 26mm and 13mm red and hard beech boards were shortened by approximately 1/3 of that of the control samples. The 4-8 hour hot-water treatment deepens the colour of the timber boards, but the colour change is superficial and could be removed by dressing the boards.

4. Hot-water soaking treatment at 80 °C for 8 hours increases the diffusion coefficient of the red beech timber by an average of 27.5 % in value. The red beech boards hot-water soaked for 8 hours were weakened by this thermal

treatment. The ultimate strength of the red beech board was reduced by 12.5% in its transverse direction (Chapter 6).

5. The optimisation program using reference parameters from Australian eucalyptus species like ironbark predicts drying schedules that were too harsh for red beech timber. Internal cracks occurred in the drying trial aimed to verify the validity of the program-predicted schedules. The results indicate that most of the parameters from corresponding *Eucalyptus* timber are not suitable to be used to describe New Zealand beech timbers. It is necessary to measure the mechanical properties of New Zealand beech timbers and use them in the optimisation program. Hot-water soaking treatment also affects the ultimate strain, which increases marginally as the result of the thermal treatment.

6. An optimisation program predicts a moisture-content profile close to the measured one from the verifying drying trials, especially when its average moisture content is above its fibre-saturation point. The diffusion-type model used in the program requires an accurate diffusion coefficient, so only a diffusion coefficient measured for a particular species can provide the accuracy of the moisture profile-the drying coefficient of Langrish *at al.* (1997,1998) for ironbark is not applicable to New Zealand beech.

7. The ultimate strength of green red beech timber in tangential and radial directions the is 7.75±0.25 MPa at room temperature (Chapter 6). Temperature and moisture content of the boards will affect the value as follows:

   - An increase of temperature generally reduces the ultimate strength of the red beech timber. The reduction rate increases significantly when temperature reaches 55 °C or over. There are also signs that there is a minimum value for ultimate strength at a temperature around 29 °C (Fig. 6-2, 6-4).

   - The ultimate strength of red beech is also moisture-content dependent. The fibre-saturation point is like to be a dividing point where the ultimate strength starts to increase as the moisture content drops below the FSP. The test results

also show that, as the moisture content of the timber is increased, the ultimate strength keeps steady till the moisture content reaches about 50% or over, when the strength has a tendency to increase (Fig. 6-2, 6-3).

8. The ultimate strain of *N. fusca* is also dependent on temperature and moisture content. When sample moisture content drops below the FSP, the sample becomes more brittle and the value of ultimate strain decreases, whereas when the moisture content is above the FSP the value of the ultimate strain does not change greatly (figure 6-3).

9. The Young's modulus of green *N. fusca* at room temperature (20 °C) is 7.50 ± 0.25MPa in the transverse planes, with little difference between the radial and the tangential directions. The stiffness value in the transverse direction only varies significantly with the moisture content when it is below the fibre-saturation point, is relatively stable when the moisture content is above FSP. The Young's modulus of red beech timber is also temperature-dependent. Generally speaking, the Young's modulus decreases greatly when the temperature is above 55 °C (Figs. 6-18 and 6-19).

10. Fresh red beech samples at room temperature under a stress of 20%-60% of the short-term ultimate strength induce a creep strain from 0.25 to 0.45%. Most of this strain is viscoelastic creep strain (Figs 6-16 and 6-17).

11. The creep strain increases to more than 2% within 600 minutes after the loading, when the temperature is raised to above 55 °C, but this increase in this study does not start till the primary creep strain occurs at about 150 minutes after the loading.

12. The optimisation program using the mechanical properties obtained from the experimental tests predicts drying schedules which are much milder than those using the mechanical properties of Australian *eucalypts*. This indicates that *N. fusca* is relatively harder to dry and easier to degrade. The optimised drying schedules for different thicknesses and initial conditions used in the verification drying trials have proved to be capable of drying red beech timber from green

conditions to 12% moisture content or less without causing severe deformation like collapse, end splitting, surface and internal cracks, with only slight warping.

13. The optimised drying schedules shorten the drying time by over 30% for untreated 13mm (from 253 hours to 176 hours when drying samples from 72% to 12 % moisture content), and 26mm thick red beech boards (from 1253 hours to 964 hours when drying samples from 120% to 12 % moisture content), comparing to the drying process using the initial stepwise drying schedule, which will effectively reduce the energy cost and overall cost of the drying process (Chapter 3, and Chapter 5,Chapter 8).

14. The optimised drying schedules can be adapted in dehumidifying drying kilns according to the study of Carrington *et al.* (1999) of Otago University.

15. The drying schedules for red beech timber suggested by this study were used in dehumidifying kiln drying system by Carrington *at al.* (1999) and proved to be energy-efficient and feasible in commercial operation (Chapter 9).

§11.2 Recommendations for further work

New Zealand beech timbers are among the hard-to-dry species, which are heat-sensitive and are prone to degrade. This study uses the optimisation program based on an elastic model of stress behaviour, which does not take in to account some of the behaviour of the beech timber like collapse and creep. The assumption that, under low temperatures and small wet-bulb depressions, the collapse is negligible needs to be verified by further experimental study.

The load-deformation curves obtained from the mechanical tests on red beech show certain degree of curvature. More precise data on using instruments like extensometers, could improve the stress-strain relationship to be used in the optimisation program.

The mechanical property tests show that ultimate strength and strain of red beech timber seem to have their lowest values at around 29 °C in the temperature range of 20-55 °C, which may indicate that some rather complex effect reduces the strength of the timber at that particular temperature point. Because the low strength and strain value could increase the risk of degradation of the timber in the early stage of the drying, an understanding of the phenomenon is very important in drying New Zealand beech timbers from fresh conditions.

Tests also show that the time-dependent strain of red beech timber under stress, creep strain for instance, increases significantly at temperatures around 55 °C, and could have significant effect on the drying behaviour of the timber boards at high temperatures, further investigations are needed for a better simulation of the drying process.

This study was carried out in relatively small drying systems and sample sizes used were small compared to the commercial operation. Therefore, the suggested optimisation program needs to be confirmed in á small-scale dehumidifier kiln trial.

Appendices

1

Hardwood Grades: permitted defects: NZS 3631:1981

Appearance:

Clears	-minimal defects, graded both sides. Suitable for cabinet and furniture where both face are visible.
Premium	-slight defects allowed (warp, 3 surface checks, 2 pin knots). Graded best face and one edge.
Dressing	-many defects allowed (blackheart, pinhole, pin knots, woolly or raised grain).

Structural:

Engineering	-Cross section of a knot or a hole must not be more than one quarter of the cross sectional area of the whole. This applies to all four faces of the board. Sloping grain less tat 1 in 10.
Building	visual and structural qualities, suitable for exposed beams.

Cuttings:

No.1 cuttings	- each piece must be capable of yielding cuttings of 1 meter or longer and totalling more than 2 metres cutting must be of high appearance grade.
No.2 cuttings	- each piece must be capable of yielding cuttings of .6 meter or longer and totalling more than 1.8 metres cutting must be of high appearance grade.

2

Optimisation Program

The following is an explanation of the flow chart of the current optimisation program called "optimise.m" with the relevant parameter specified. The flow chart function is italicised with an in depth explanation of what the function performs underneath.

Specify Timber Type

Currently there are three timber types to choose from. The variable is "ttype" and it can have a value of 1 - yellow stringy bark, 2 - spotted gum, or 3 - ironbark.

Specify Initial and Final Conditions and Constraints

These are:	Variable	Current Value	Description
	Xstarti	0.277	Initial moisture content of timber
	Tstart	293	Initial temperature of timber
	SurfX	0.061	Surface moisture content of timber
	CentX	0.277	Centre moisture content of timber
	SkalF	0.020	Scaling factor
	deltaT	4.0*3600	Time step in seconds
	Tg	293	Initial dry bulb air temperature
	Tw	-1	Initial wet bulb depression
	fin_avX	0.12	Final average moisture content
	min_Xsurf	0.07	Minimum surface moisture content
	max_dX	0.03	Maximum moisture difference
	max_eavX	0.0001	Maximum error in average moisture
	max_strain	0.018	Maximum strain
	Tg_max	353	Maximum air temperature

Specify Drying Model

Currently there are two types of drying models to choose from. These are an elastic strain model or a visco-elastic and mechano-sorptive model.

Load Parameter File

The parameter file is called "p_file.m" and specifies the board thickness, density of dry timber and the constant values in the equations of specific heat capacity of timber, thermal conductivity, moisture diffusivity, latent heat of vaporisation of free water, heat of sorption of water, vapour pressure just above the timber surface, relative humidity, vapour pressure just above the liquid surface, air density, specific heat capacity of dry air, specific heat capacity of water vapour, viscosity of vapour, viscosity of dry air, diffusivity of moisture, weighting factor for vapour, weighting factor for dry air, thermal conductivity of vapour, thermal conductivity of dry air, bulk air humidity, surface heat transfer, board thickness, and the parameters for the chemical potential model.

Calculate Thickness of Timber Slices

There are three variables used here, "deltax", "xpos", and "xvec". "deltax" is the actual thickness of each slice of timber (units in metres), "xpos" is the summation of the slices as they progress through to the centre of the board (units in metres), and "xvec" is the same as "xpos" but has units of millimetres instead of metres.

Calculate Initial MC & T Profiles

The variable "Xstart" is the moisture content profile through the board and "x0" is a vector that contains both the temperature the moisture content profiles through the board, alternatively.

Specify Flattening Phase & Horizon, Drying Phase & Horizon

This section of the code the users specifies whether the drying phase and/or flattening phase is included in the calculation of the optimised drying schedule. The horizon is the number of time steps the optimisation process is looking ahead.

Calculate X_{av}, X & T after 1 second of drying

This section uses the gear method which is built-in to Matlab to solve a set of ordinary differential equations. The command used is [T,X,Y]=gear(model,1,x0,1e-7). The various components of this are: T is the integration time points, X is the output trajectories, Y is the state trajectories, model is the file that contains ode's, 1 is the time step of 1 second, x0 is the vector of inputs, and 1e-7 is the error. "Xlin" and "Ylin" are then obtained from "X" and "Y". X_{av} is then calculated using the variable "avX". This is a summation since that each slice of timber is a different thickness.

avXok = 0 & skipdryph = 0 ?

This is a while loop, it will keep iterating until either "avXok" or "skipdryph" are not equal to zero.

Specify Options for Drying

The parameters are:

- options(1) - Display parameter (Default:0). 1 displays some results
- options(2) - Termination tolerance for X.(Default: 1e-4).
- options(3) - Termination tolerance on F.(Default: 1e-4).
- options(4) - Termination criterion on constraint violation.(Default: 1e-6)
- options(5) - Algorithm: Strategy: Not always used.
- options(6) - Algorithm: Optimiser: Not always used.
- options(7) - Algorithm: Line Search Algorithm. (Default 0)
- options(8) - Function value. (Lambda in goal attainment.)
- options(9) - Set to 1 if you want to check user-supplied gradients
- options(10) - Number of Function and Constraint Evaluations.
- options(11) - Number of Function Gradient Evaluations.
- options(12) - Number of Constraint Evaluations
- options(13) - Number of equality constraints.
- options(14) - Maximum number of iterations. (Default 100*no. of variables)

options(15) - Used in goal attainment for special objectives.

options(16) - Minimum change in variables for finite difference gradients.

options(17) - Maximum change in variables for finite difference gradients.

options(18) - Step length. (Default 1 or less).

Calculate upper & lower bounds of T_w & T_g

The minimum and maximum of the wet and dry bulb temperatures are specified step in the iteration. T_w (min) is -30, T_w (max) is -1, Tg_min is 30°C and Tg_max is 80°C. Tg for time step i + 1 can be either ±10°C from Tglast or the constraints.

Calculate T_w & T_g - optimised

The built-in Matlab optimising function "constr" is called. The output is Tg and Tw for the next time step.

Calculate X_{av}, X & T after 4 hrs of drying

Using the new Tg and Tw, the gear function is called and the timber undergoes four hours of drying. The average moisture content of the board, and the moisture content and temperature profiles through the board are determined.

Calculate avXok & skipdryph

An if statement is included in case the optimisation cannot converge on an average moisture content of 12%. The average moisture content is also compared with the constraints and if it exceeds these, the iterative process is terminated.

Skipdryph = ?

If the variable "skipdryph" has a value of zero, the drying schedule is saved to a file. This includes the average moisture content, the dry bulb temperature, and the wet

bulb depression at every time step. If instead the value is one, a file is loaded that contains a drying schedule and the flattening phase is performed on the schedule.

Flatphase = ?

If the variable "flatphase" has a value of zero, the flattening phase is skipped and the program proceeds to plotting the data. If the value is one, the flattening phase is performed. The purpose of this phase is to flatten the moisture content profile. This is achieved by decreasing the wet bulb depression, thus the moisture content at the surface is higher than a quarter distance into the board. As a result, the strain profile is also flatter, therefore reducing the maximum strain and stress levels within the board

Plot data from drying schedule

The first figure plotted is the moisture content profile. The second figure contains plots of average moisture content versus maximum strain, dry bulb temperature, and wet bulb depression, as well as the final drying time. The third figure contains plots of the drying time versus the dry bulb temperature, the wet bulb depression, and the average moisture content. The fourth figure contains plots of various parameter profiles through the timber board, such as the moisture content, the board temperature, and the strain. The fifth, sixth and seventh figures are only plotted when the mechano-sorptive and visco-elastic model is selected. These are surface plots through the board against the drying time of the total strain, the mechano-sorptive strain and the visco-elastic strain.

Flow Chart of the Original Optimisation Program

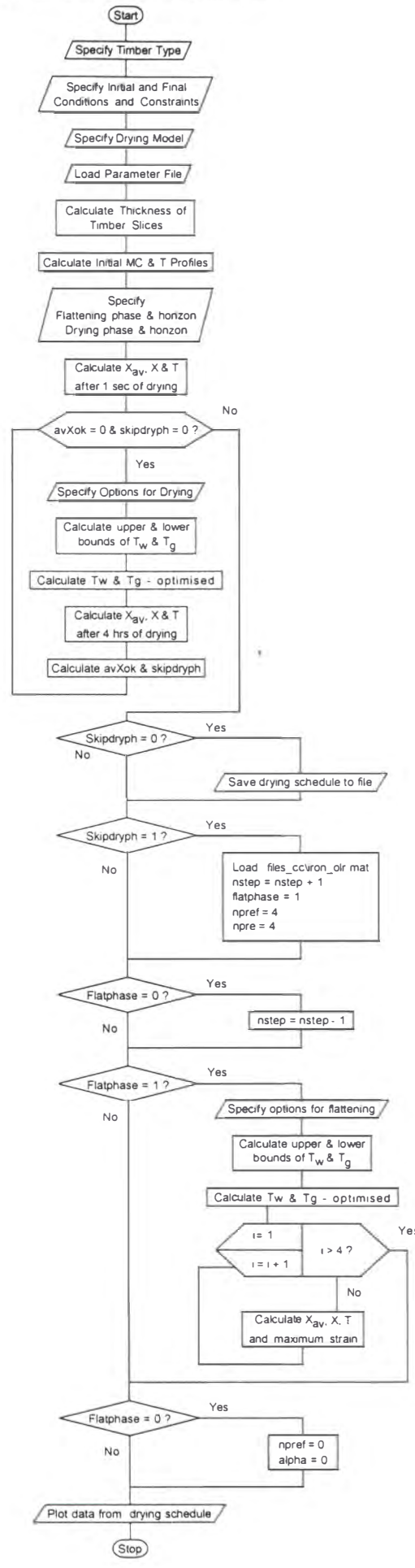

Appendices

3

Optimised drying schedules for red beech boards

The following schedules are based on approximating the optimised profiles in a stepwise manner and use parameters based on limited experimental data. In any given case, these schedules should be used with caution.

Schedule 1

Optimised drying schedule for mm red beech boards at 40% moisture content

TIME(hrs)	DB(°C)	WB(°C)
4	24	22
8	27	26
16	28	27
20	30	29
24	32	31
28	34	33
32	36	35
36	38	37
40	40	39
44	41	40
48	43	42
52	44	43
56	45	44
88	45	43
104	45	42
112	45	41
120	45	40
124	55	49
128	55	48
132	55	47
136	55	45
140	55	44
144	55	42
148	55	40
152	55	38

Schedule 2

Optimised drying schedule for 25 mm red beech boards at 40% moisture content

TIME(hrs)	DB(°C)	WB(°C)
4	23	21
8	23	22
16	24	23
20	25	24
24	26	25
28	27	26
32	28	27
36	30	29
40	31	30
44	32	31
48	33	32
52	34	33
56	35	34
60	36	35
64	37	36
68	38	37
72	39	38
76	40	39
80	41	40
84	42	41
92	43	42
96	44	43
104	45	44
108	46	45
116	47	46
124	48	47
136	49	48
152	50	49
248	50	48
316	50	47
352	50	46
380	50	45
404	50	44
428	50	43
448	50	42
464	50	41
480	50	40
492	50	39
504	50	38
516	50	37
528	50	36
544	50	35

Schedule 3

Optimised drying schedule for 40 mm red beech boards at 40% moisture content

TIME(hrs)	DB(°C)	WB(°C)
0	22	21
24	23	22
28	24	23
36	25	24
48	27	26
60	29	28
72	31	30
88	33	32
104	35	34
116	37	36
132	39	38
144	40	39
168	42	41
180	43	42
212	44	43
232	45	44
272	47	46
824	47	44
912	47	43
980	47	42
1,040	47	41
1,096	47	40
1,144	47	39
1,188	47	38
1,260	47	37
1,296	47	36
1,328	47	35
1,392	47	33

Schedule 4

Optimised drying schedule for 12mm red beech boards at 60% moisture content

TIME(hrs)	DB(°C)	WB(°C)
4	22	19
8	27	25
12	29	27
16	30	28
20	31	30
24	33	31
28	33	32
52	34	33
60	36	35
64	37	36
68	39	38
72	40	39
76	42	41
80	44	43
84	46	45
88	47	46
92	49	48
96	50	49
120	50	48
132	50	47
140	50	46
148	50	45
152	52	47
156	55	48
160	55	47
164	55	46
168	55	45
172	55	43
176	55	41
180	55	39

Schedule 5

Optimised drying schedule for 25mm red beech boards at 60% moisture content

TIME(hrs)	DB(°C)	WB(°C)
4	22	19
8	26	24
12	29	27
16	29	28
136	30	29
164	31	30
188	32	31
216	33	32
240	34	33
276	35	34
592	35	33
668	35	32
720	35	31
760	35	30
800	35	29
832	35	28
864	35	27
892	35	26
916	35	25
940	35	24
980	35	23

Schedule 6

Optimised drying schedule for 40mm red beech boards at 60% moisture content

TIME(hrs)	DB(°C)	WB(°C)
4	22	19
8	25	22
12	25	23
20	25	24
100	26	25
120	27	26
140	28	27
160	29	28
180	30	29
200	31	30
220	32	31
244	33	32
268	34	33
296	35	34
328	36	35
364	37	36
408	38	37
460	39	38
528	40	39
1,280	40	38
1,420	40	37
1,524	40	36
1,608	40	35
1,680	40	34
1,748	40	33
1,864	40	31
1,912	40	30
1,960	40	29
2,004	40	28
2,084	40	27

Schedule 7

Optimised drying schedule for 12 mm red beech boards at 90% moisture content

TIME(hrs)	DB(°C)	WB(°C)
4	22	17
8	22	19
12	22	20
32	22	21
176	23	22
204	24	23
228	25	24
252	26	25
276	27	26
300	28	27
324	29	28
352	30	29
380	31	30
408	32	31
436	33	32
464	34	33
496	35	34
528	36	35
560	37	36
592	38	37
624	39	38
656	40	39
688	41	40
720	42	41
752	43	42
788	44	43
824	45	44
860	46	45
904	47	46
956	48	47
1448	48	46
1564	48	45
1648	48	44
1712	48	43
1768	48	42
1820	48	41
1868	48	40
1908	48	39
1948	48	38
1984	48	37
2016	48	36
2048	48	35
2076	48	34
2112	48	33

Schedule 8

Optimised drying schedule for 25 mm red beech boards at 90% moisture content

TIME(hrs)	DB(°C)	WB(°C)
4	24	19
8	34	29
12	43	39
16	43	40
20	44	41
24	44	42
56	44	43
472	44	42
524	44	41
560	44	40
588	44	39
612	44	38
636	44	37
656	44	36
672	44	35
688	44	34
704	44	33
720	44	32
732	44	31
748	44	30
760	44	29

Schedule 10

Optimised drying schedule for 12 mm red beech boards at 120% moisture content

TIME(hrs)	DB(°C)	WB(°C)
4	25	18
8	34	29
12	38	34
16	43	40
20	47	44
24	50	47
28	53	50
32	55	53
56	55	54
100	55	53
112	55	52
120	55	51
124	55	50
128	55	49
132	55	48
136	55	47
140	55	46
144	55	44
148	55	43
152	55	41
156	55	39

Schedule 9

Optimised drying schedule for 40 mm red beech boards at 90% moisture content

TIME(hrs)	DB(°C)	WB(°C)
4	22	17
8	22	19
12	22	20
32	22	21
176	23	22
204	24	23
228	25	24
252	26	25
276	27	26
300	28	27
324	29	28
376	30	29
380	31	30
408	32	31
436	33	32
464	34	33
496	35	34
528	36	35
560	37	36
592	38	37
624	39	38
656	40	39
688	41	40
720	42	41
752	43	42
788	44	43
824	45	44
860	46	45
904	47	46
956	48	47
1,448	48	46
1,564	48	45
1,648	48	44
1,712	48	43
1,768	48	42
1,820	48	41
1,868	48	40
1,908	48	39
1,948	48	38
1,984	48	37
2,016	48	36
2,048	48	35
2,076	48	34
2,112	48	33

Schedule 11

Optimised drying schedule for 25 mm red beech boards at 120% moisture content

TIME(hrs)	DB(°C)	WB(°C)
4	22	16
8	27	22
12	31	27
16	35	31
20	39	36
24	43	39
28	45	42
32	47	45
36	48	46
40	49	47
96	49	48
300	50	49
332	51	50
440	51	49
504	51	48
540	51	47
568	51	46
572	51	46
592	51	45
612	51	44
628	51	43
644	51	42
660	51	41
672	51	40
688	51	39
700	51	38
708	51	37
724	51	36

Schedule 12

Optimised drying schedule for 40 mm red beech boards at 120% moisture content

TIME(hrs)	DB(°C)	WB(°C)
4	26	19
8	26	22
12	30	26
16	30	27
20	31	28
24	32	29
44	32	30
352	32	31
552	33	32
636	35	34
672	36	35
708	37	36
744	38	37
776	39	38
812	40	39
844	41	40
876	42	41
908	43	42
944	44	43
980	45	44
1016	46	45
1060	47	46
1112	48	47
1608	48	46
1724	48	45
1804	48	44
1868	48	43
1928	48	42
1980	48	41
2024	48	40
2068	48	39
2104	48	38
2140	48	37
2172	48	36
2204	48	35
2232	48	34
2268	48	33